

High-Energy Collisions with ALICE at the LHC

3. Jets in e^+e^- and $p+p(\text{pbar})$ Collisions

Graduate Days

of the Graduate School of Fundamental Physics

Heidelberg, 5. - 9. October 2009

PD Dr. Klaus Reygers

Physikalisches Institut

Universität Heidelberg

1 Introduction

1.1 Heavy-Ion Physics and the Quark-Gluon Plasma

1.2 Kinematic Variables

2 The Alice Experiment

2.1 Overview: Experimental methods

2.2 Inner Tracking System (ITS)

2.3 Time Projection Chamber (TPC)

2.4 Transition Radiation Detector (TRD)

2.5 Calorimeters and more

3 Jets in e^+e^- , and $p+p(\bar{p}p)$ Collisions

3.1 Jets in e^+e^- -Collisions

3.2 Hard Scattering and Particle Yields at High- p_T in $p+p(\bar{p}p)$ Collisions

3.3 Jets in $p+p(\bar{p}p)$ Collisions

3.4 Direct Photons

4 Jets in Nucleus-Nucleus Collisions

4.1 Parton Energy Loss

4.2 Point-like Scaling

4.3 Particle Yields at Direct Photons at High- p_T

4.4 Further Tests of Parton Energy Loss

4.5 Two-Particle Correlations

4.6 Jets in Pb+Pb Collisions at the LHC

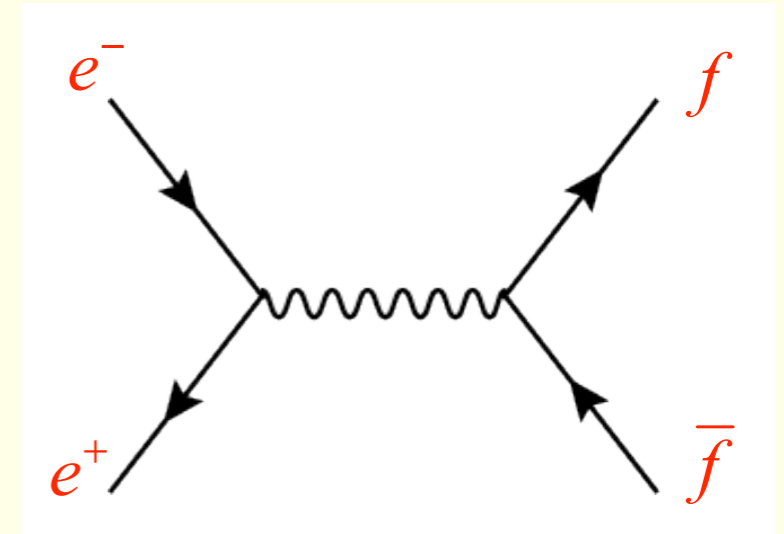
3.1 Jets in e^+e^- -Collisions

Experimental Evidence for Color Charge (I)

Total cross section for the production of a fermion-antifermion pair (to order $O(\alpha_s^0)$):

$$\sigma(e^+e^- \rightarrow f\bar{f}) = \frac{4\pi}{3} (\hbar c)^2 \cdot \frac{Q_f^2 \alpha^2}{s}$$

charge



f : Muon (μ) or quark with certain color (q_{color})

Total cross section for the production of a $u\bar{u}$ - pair:

$$Q_f = \frac{2}{3}, \text{ 3 colors} \Rightarrow \text{factor 3}$$

$$\sigma(e^+e^- \rightarrow u\bar{u}) = 3 \cdot \sigma(e^+e^- \rightarrow u_{\text{color}} \bar{u}_{\text{anti-color}}) = \frac{16\pi}{9} (\hbar c)^2 \cdot \frac{\alpha^2}{s}$$

Experimental Evidence for Color Charge (II)

$$\begin{aligned}
 R &= \frac{\sigma(e^+e^- \rightarrow \text{hadrons})}{\sigma(e^+e^- \rightarrow \mu^+\mu^-)} \\
 &= \frac{\sigma(e^+e^- \rightarrow \text{all } q, \bar{q})}{\sigma(e^+e^- \rightarrow \mu^+\mu^-)} \\
 &= 3 \cdot \sum_q Q_q^2
 \end{aligned}$$

Sum over all quark flavors whose production is energetically allowed

u, d, s:

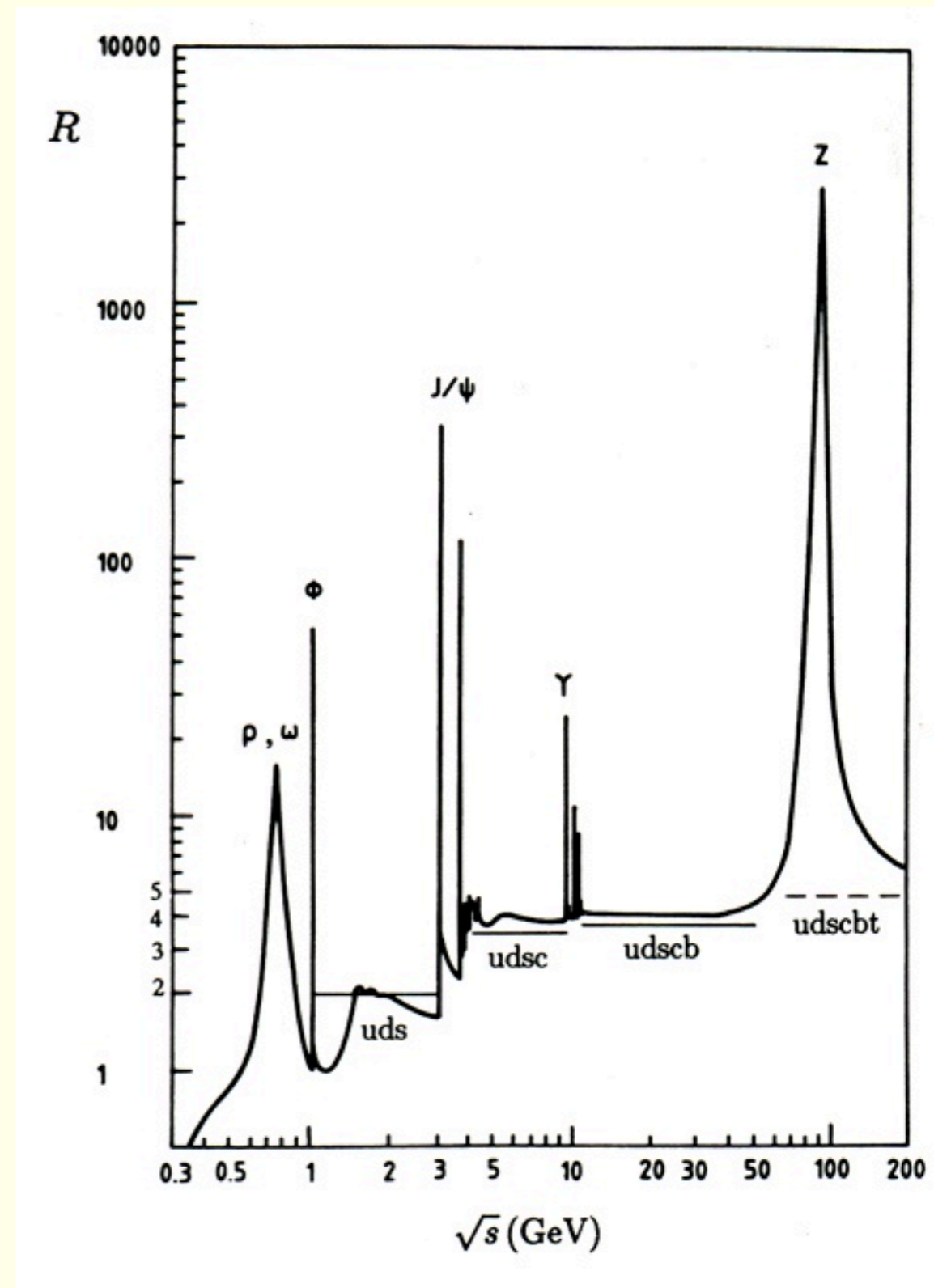
$$R = 3 \left[\left(\frac{2}{3}\right)^2 + \left(\frac{1}{3}\right)^2 + \left(\frac{1}{3}\right)^2 \right] = 2$$

u, d, s, c:

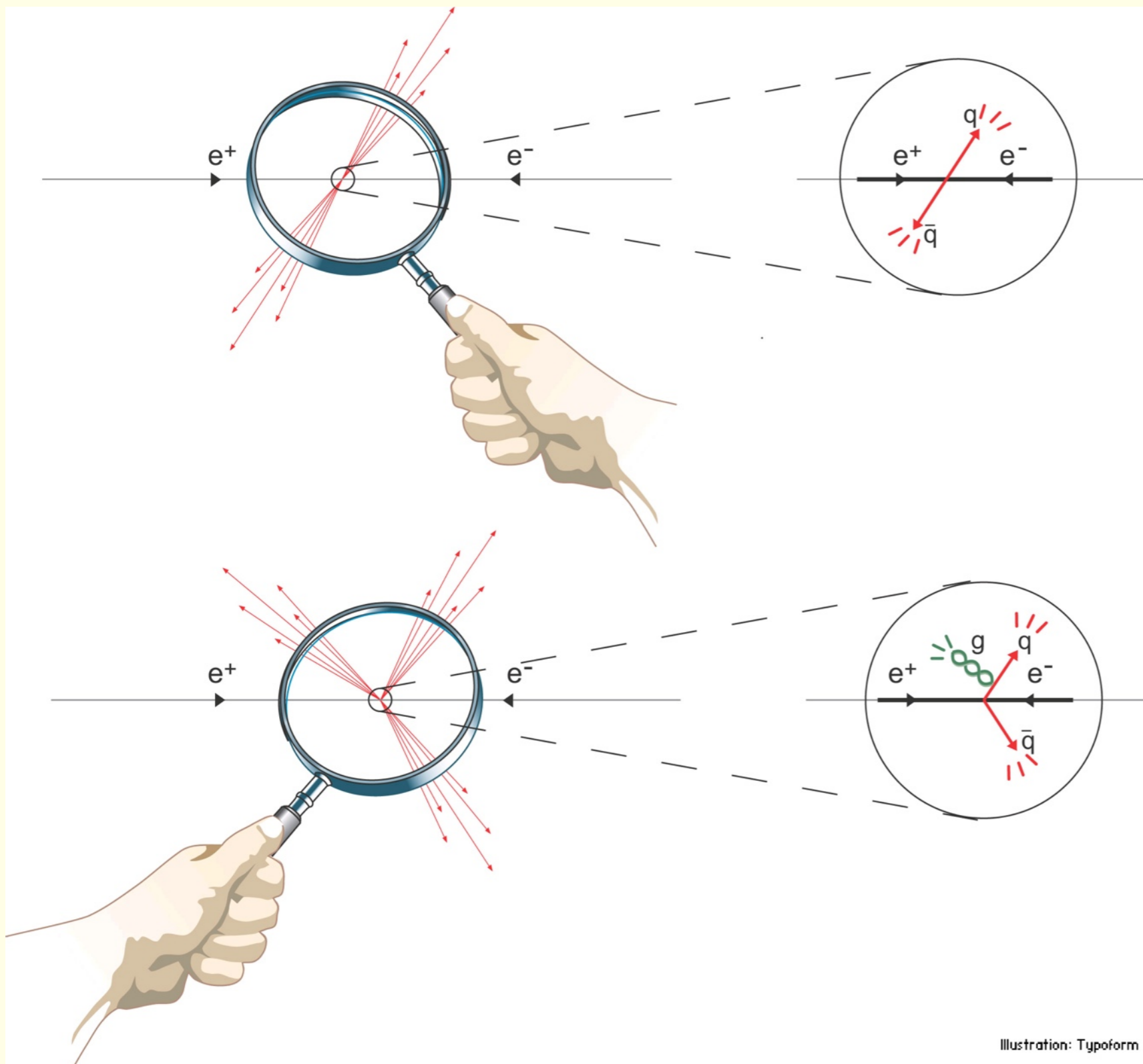
$$R = 2 + 3 \left(\frac{2}{3}\right)^2 = \frac{10}{3}$$

u, d, s, c, b:

$$R = \frac{10}{3} + 3 \left(\frac{1}{3}\right)^2 = \frac{11}{3}$$



Two- and Three-Jet Events in e^+e^-

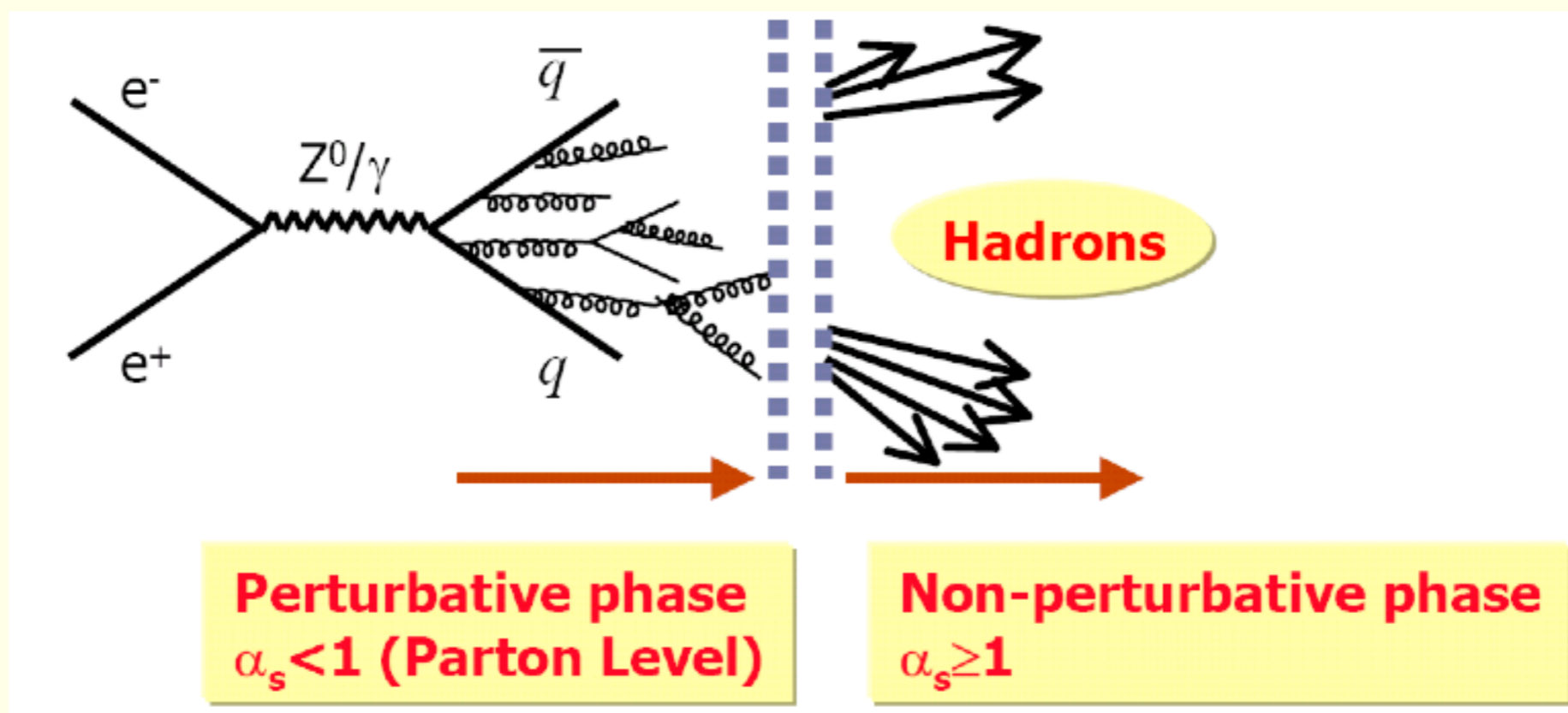
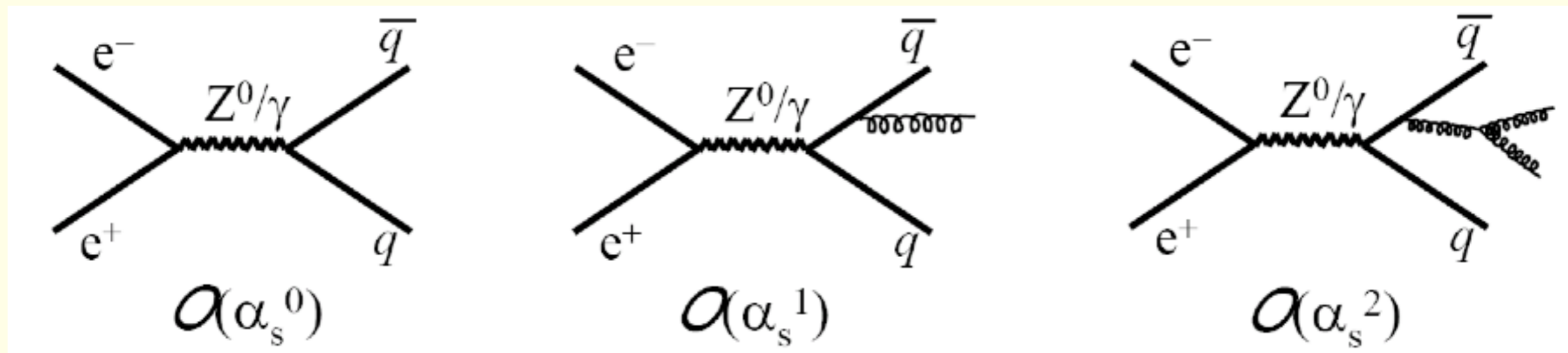


The two jets reflect the direction and the energy of the primordial quark-antiquark pair

**3-Jet event
Direct experimental evidence for gluons**

Illustration: Typoform

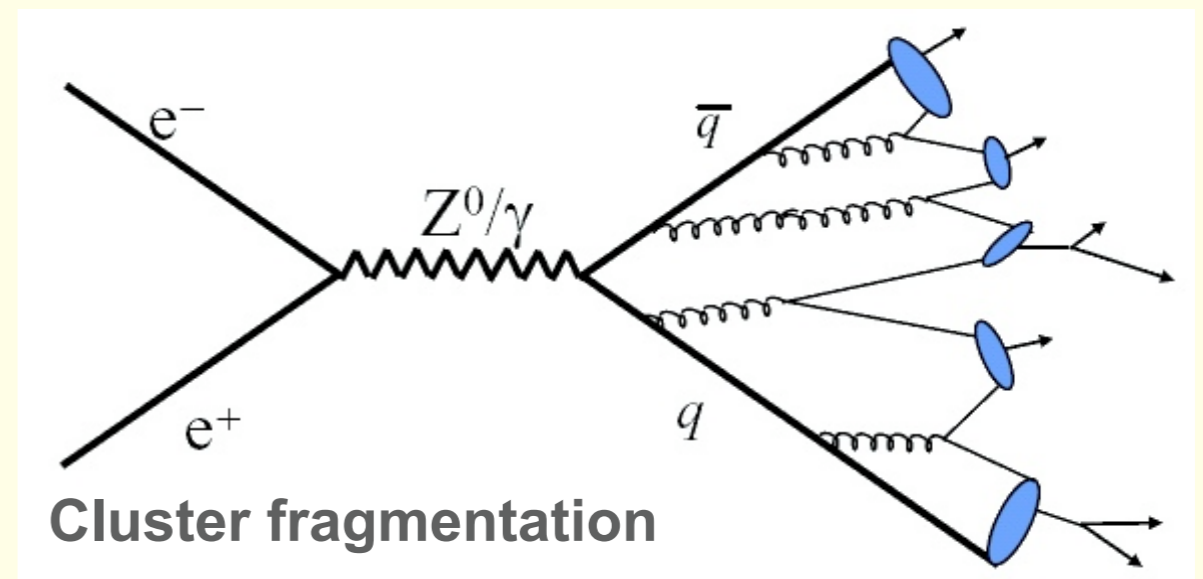
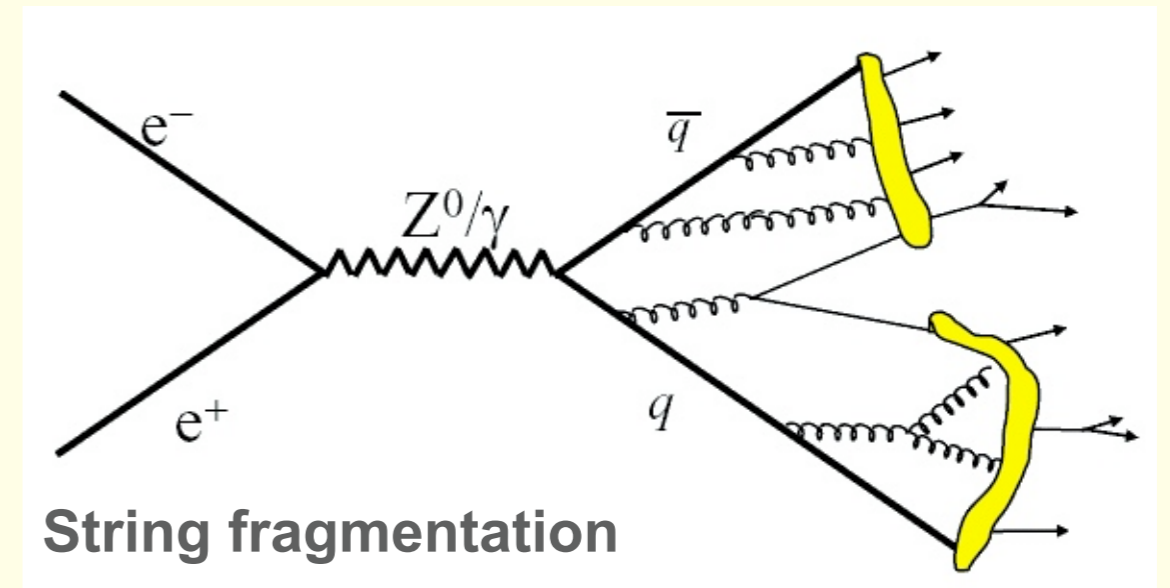
Feynman Diagrams: Higher Order Corrections



Digression: Models for Jet Hadronization

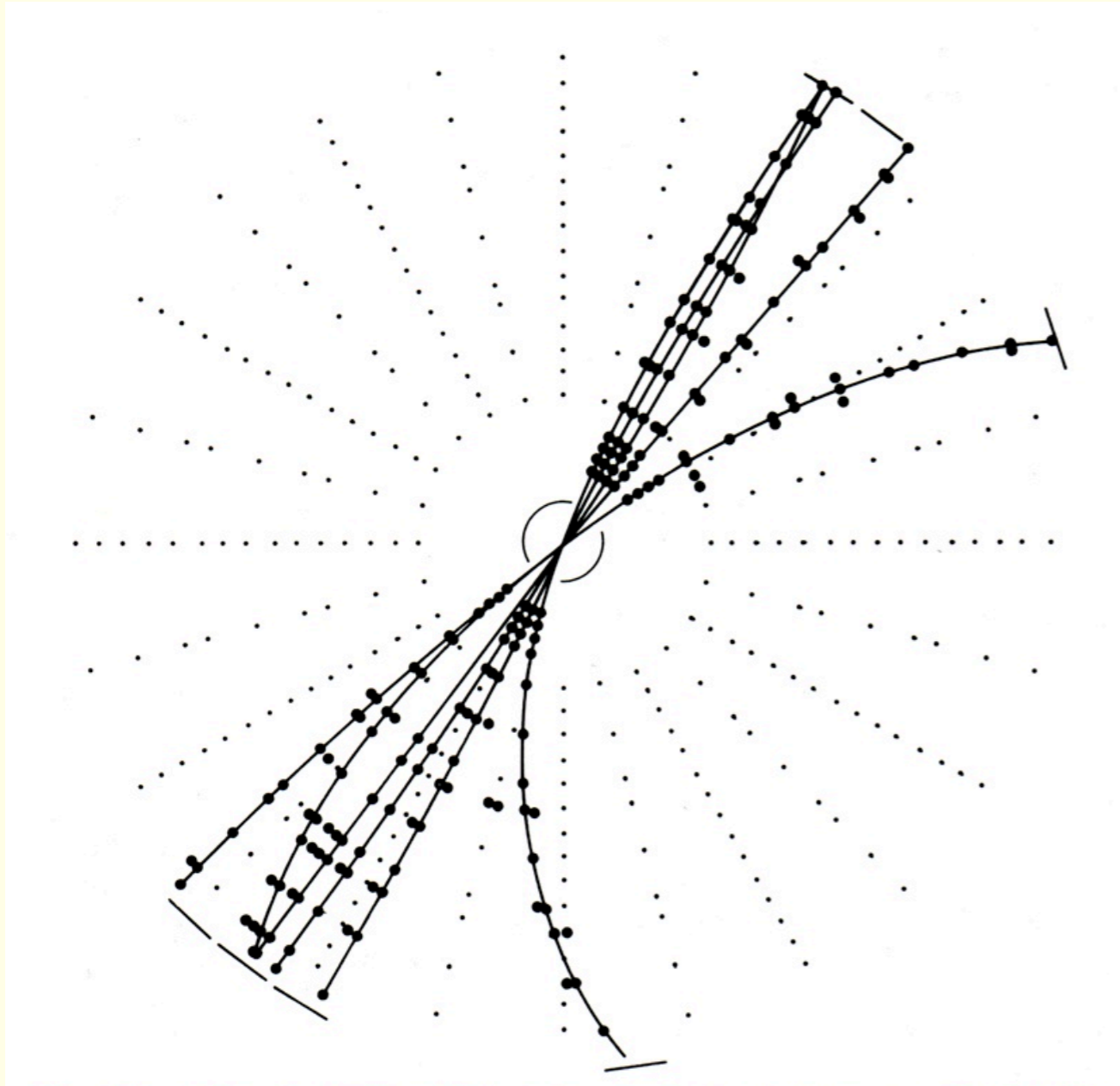
Nicos Varelas, CTEQ summer school

- **Independent fragmentation**
 - ▶ Each parton fragments independently
- **String fragmentation**
 - ▶ Separating partons connected by color string
 - ▶ Used in Pythia/Jetset
- **Cluster fragmentation**
 - ▶ Pairs of neighboring partons combine to color singlets
 - ▶ Then apply recipe for cluster decay, e.g., isotropic decay in rest frame into hadrons

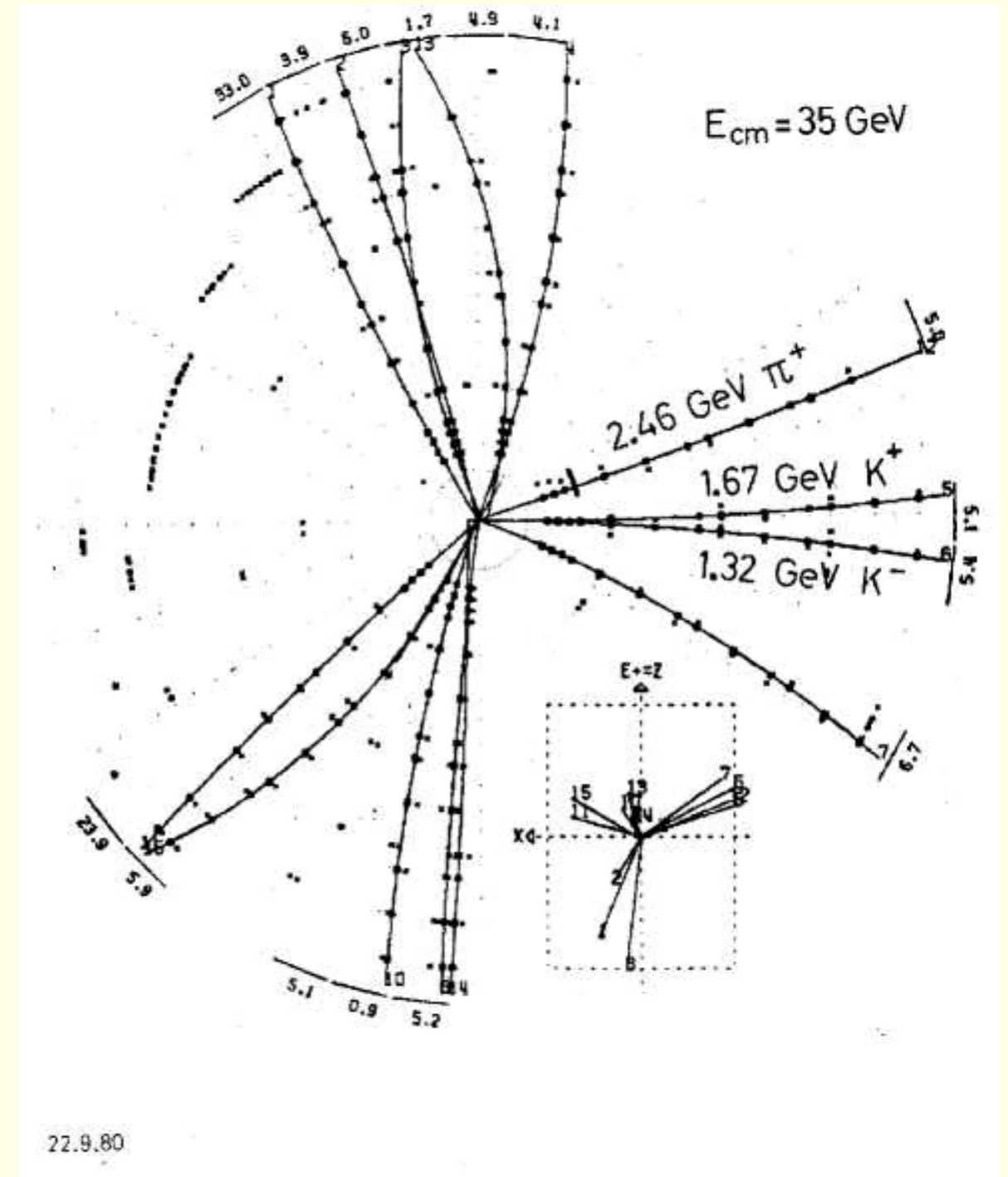


Experimental Evidence for Gluons from Three-Jet Events

e^+e^- - collision at PETRA storage ring at DESY (ca. 1980):



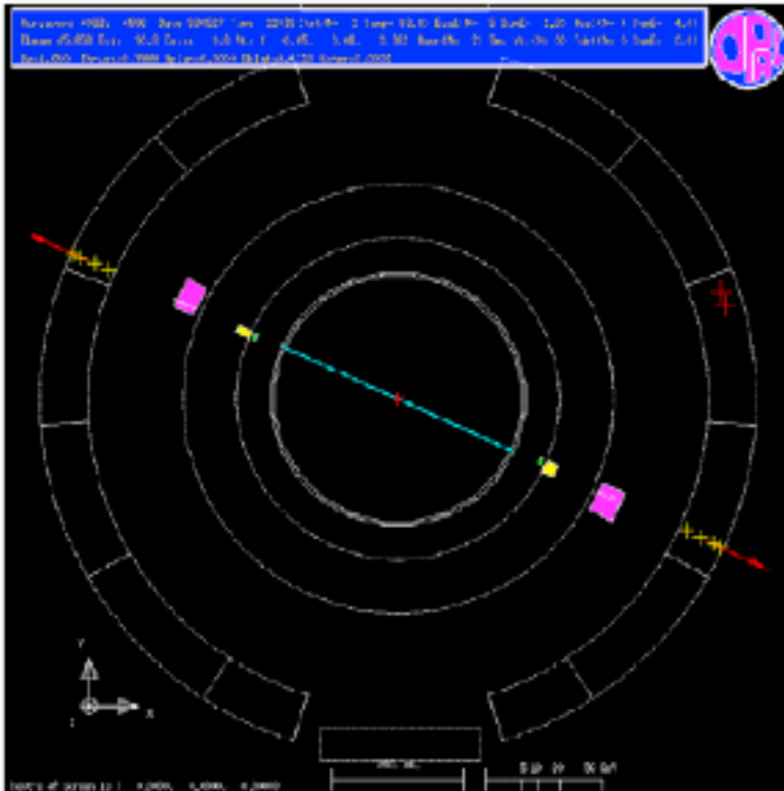
2-jet event



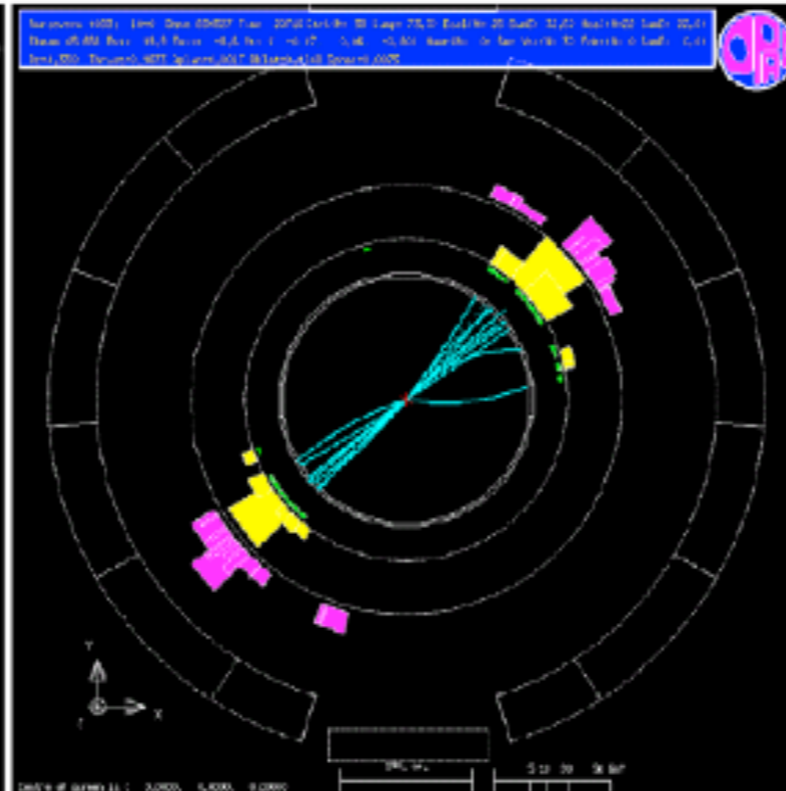
3-jet event

Jets at LEP (OPAL Experiment)

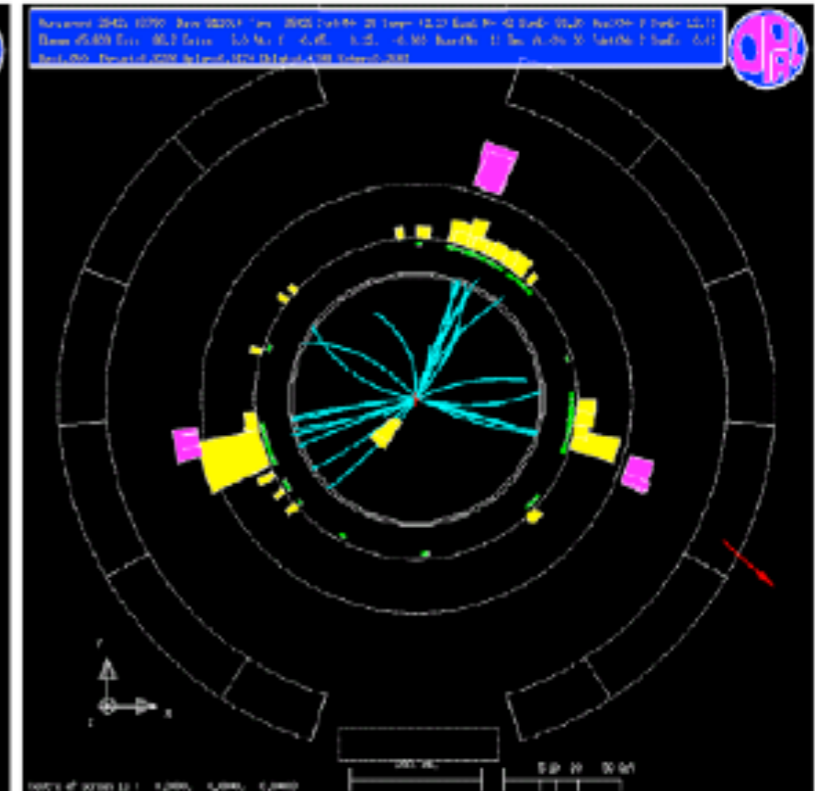
$$e^+e^- \rightarrow \mu^+\mu^-$$



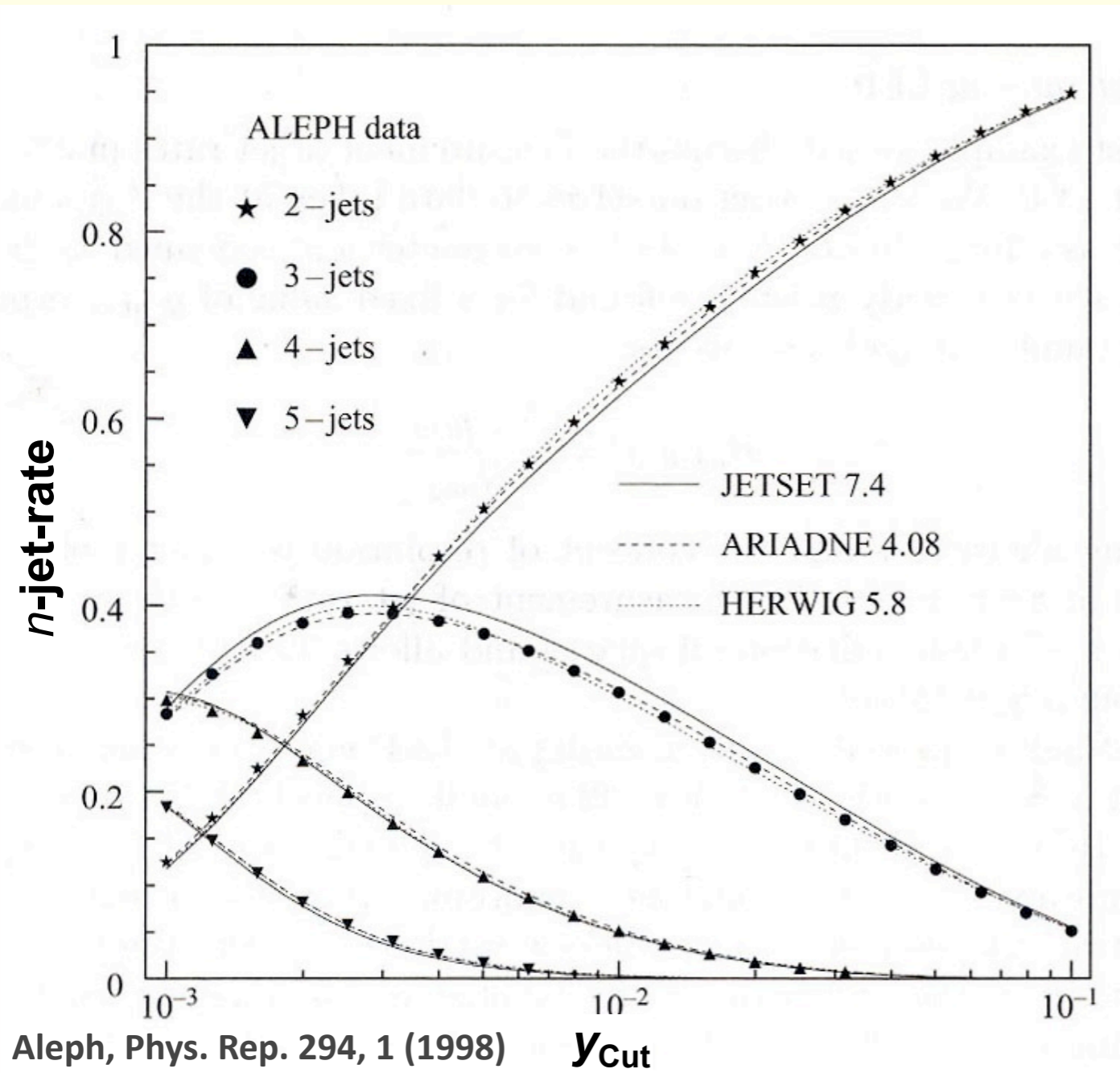
$$e^+e^- \rightarrow \bar{q}q$$



$$e^+e^- \rightarrow \bar{q}qq$$



What a Jet is Depends on the Jet Reconstruction: Rate of n -jet Events



$$R_3(y_{\text{Cut}}, \sqrt{s}) = \frac{\sigma_{3\text{-Jet}}}{\sum_n \sigma_{n\text{-Jet}}}$$

$$= C_{3,1}(y_{\text{Cut}}) \frac{\alpha_s(\sqrt{s})}{2\pi}$$

$$\approx 0,1 \quad \text{for large } y_{\text{Cut}}$$

y_{Cut} : Threshold in jet reconstruction algorithm
(Durham or k_T algorithm, will be discussed later)

Example of a Jet Variable: Thrust

Denoting the particle momenta in an event as \vec{p}_i and given a unit vector \vec{n} one can calculate

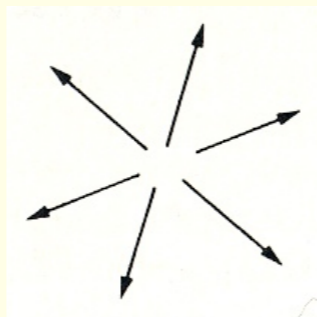
$$t(\vec{n}) = \frac{\sum_i |\vec{p}_i \cdot \vec{n}|}{\sum_i |\vec{p}_i|}$$

The vector \vec{n} that maximizes $\sum_i |\vec{p}_i \cdot \vec{n}|$ is called the thrust axis.

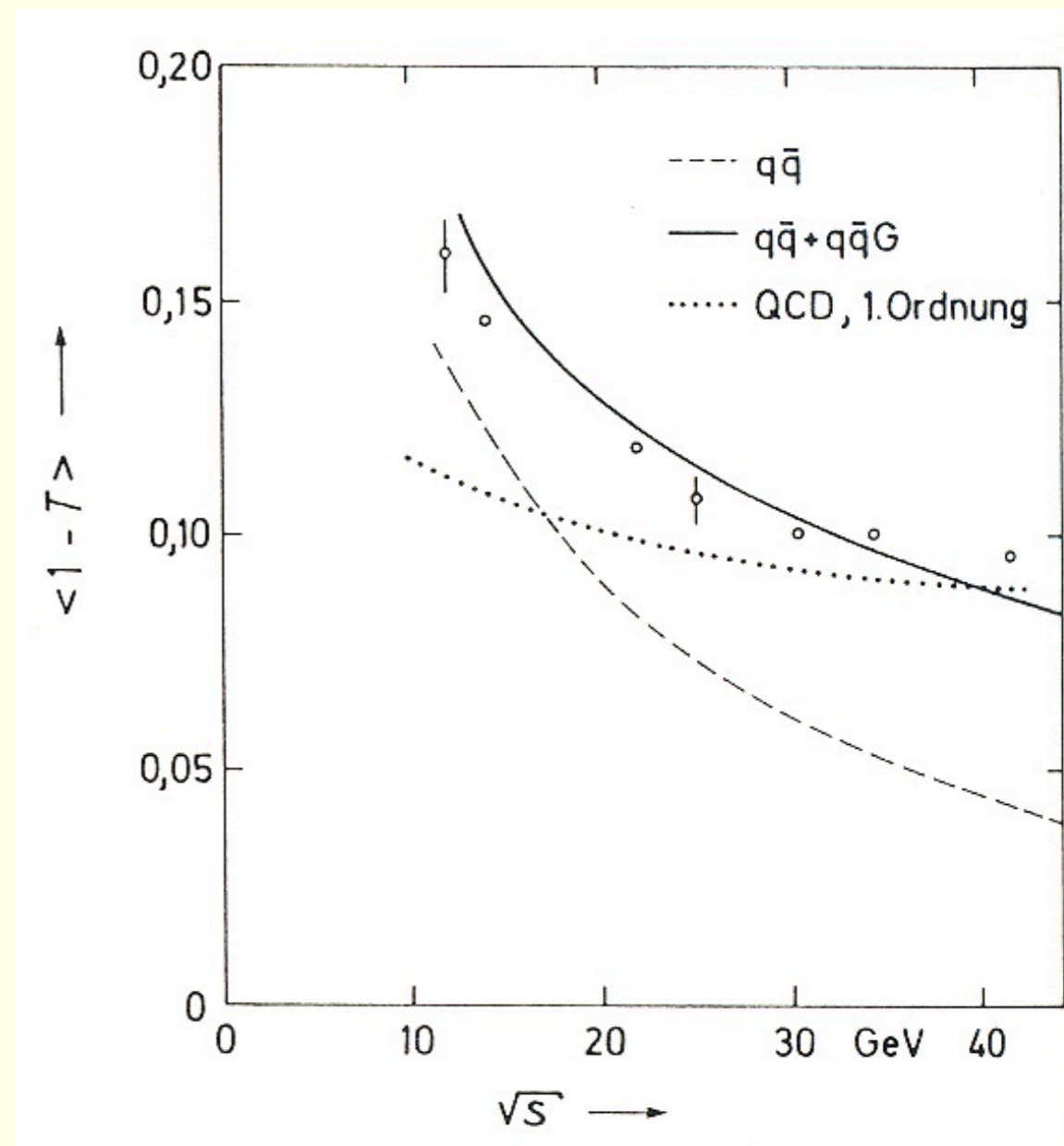
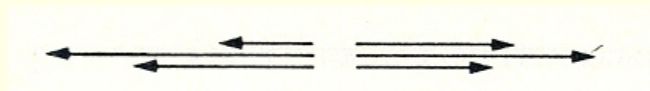
The thrust variable is defined as

$$T = \max t(\vec{n}) \quad (0.5 \leq T \leq 1)$$

Isotropic event: $T = \frac{1}{2}$

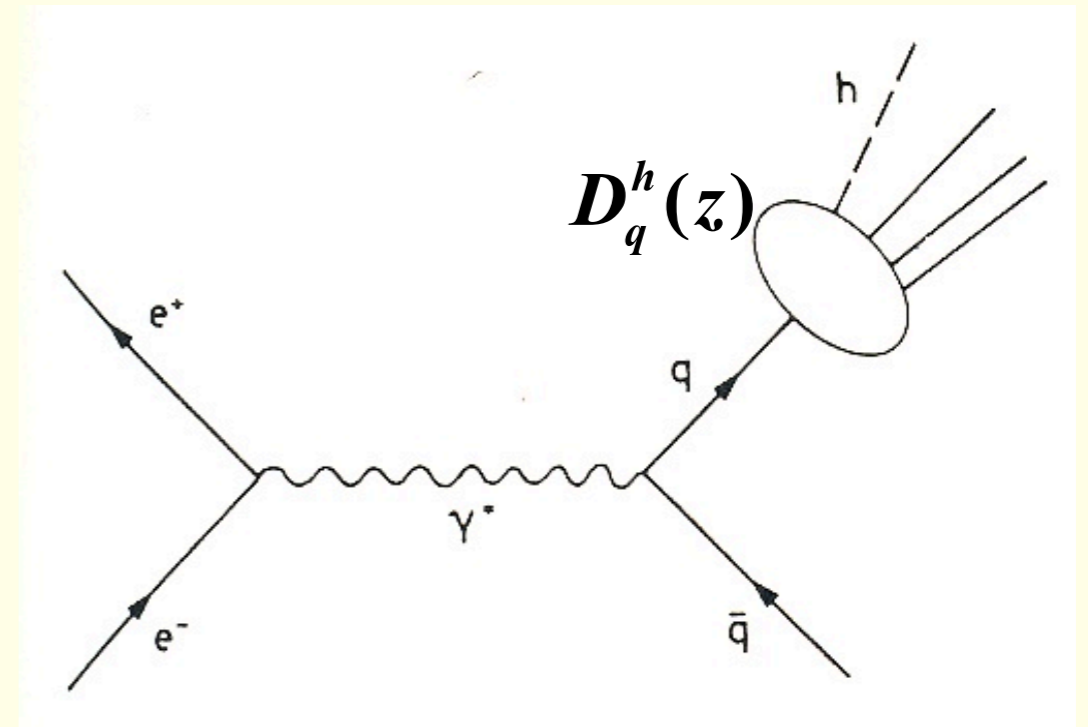


Ideal jet event: $T = 1$



Jet Fragmentation (I)

- Jet fragmentation is independent of the creation process of the mother parton
- Hadron transverse momentum p_T with respect to parton direction independent of parton momentum ($p_T < 300 \text{ MeV}/c$)
- Distribution of longitudinal hadron momenta depends only on the fraction z of the parton momentum (scaling)



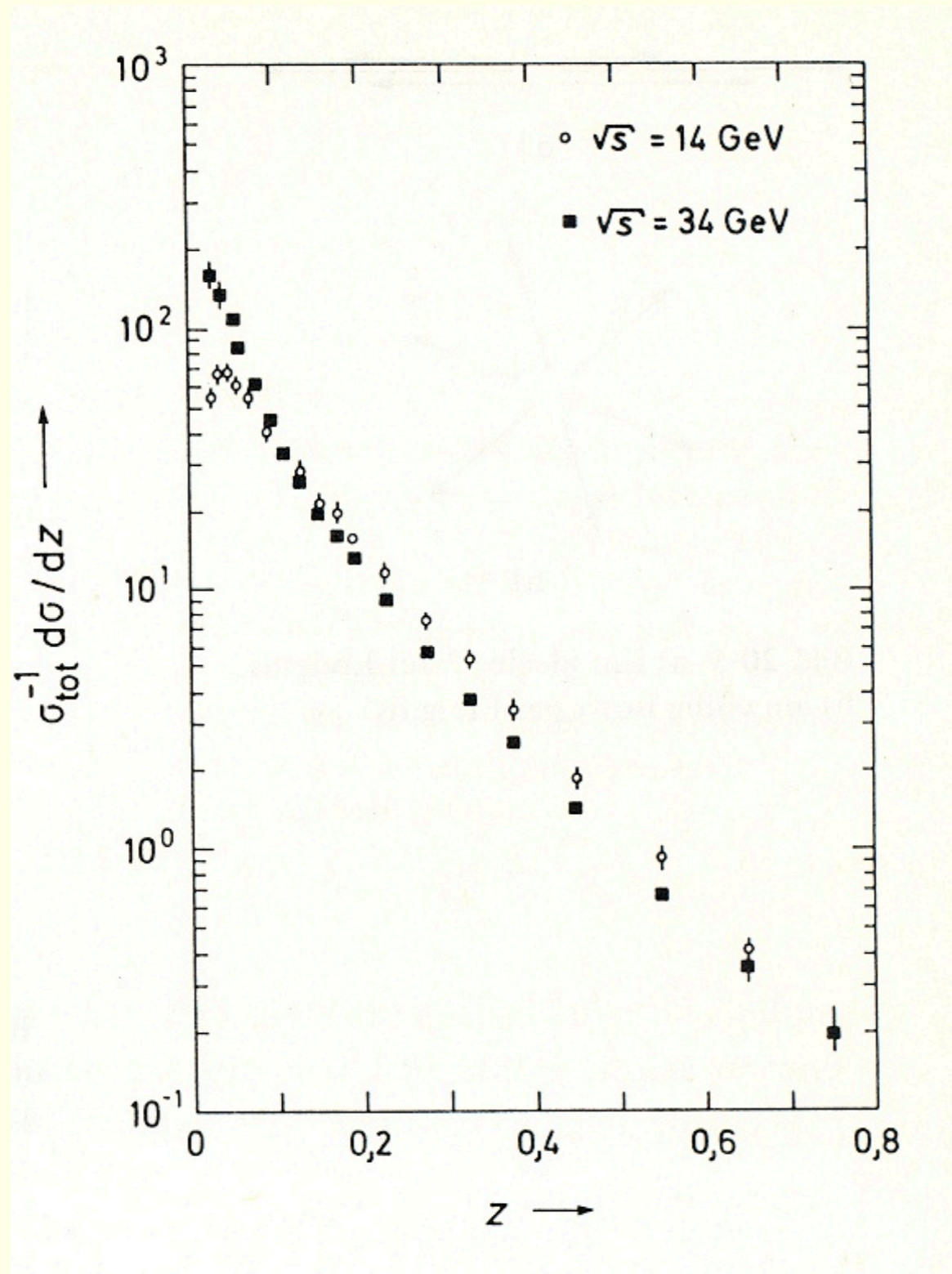
$$\frac{d\sigma}{dz}(e^- + e^- \rightarrow h + X) = \sum_q \sigma(e^- + e^- \rightarrow q + \bar{q}) \left[D_q^h(z) + D_{\bar{q}}^h(z) \right]$$

$$z = \frac{E_h}{E_q} = \frac{E_h}{E_{beam}} = \frac{2E_h}{\sqrt{s}}$$

Fragmentation function:

$D_q^h(z) dz$: number of hadrons of type h with momentum fraction between $z \dots z + dz$

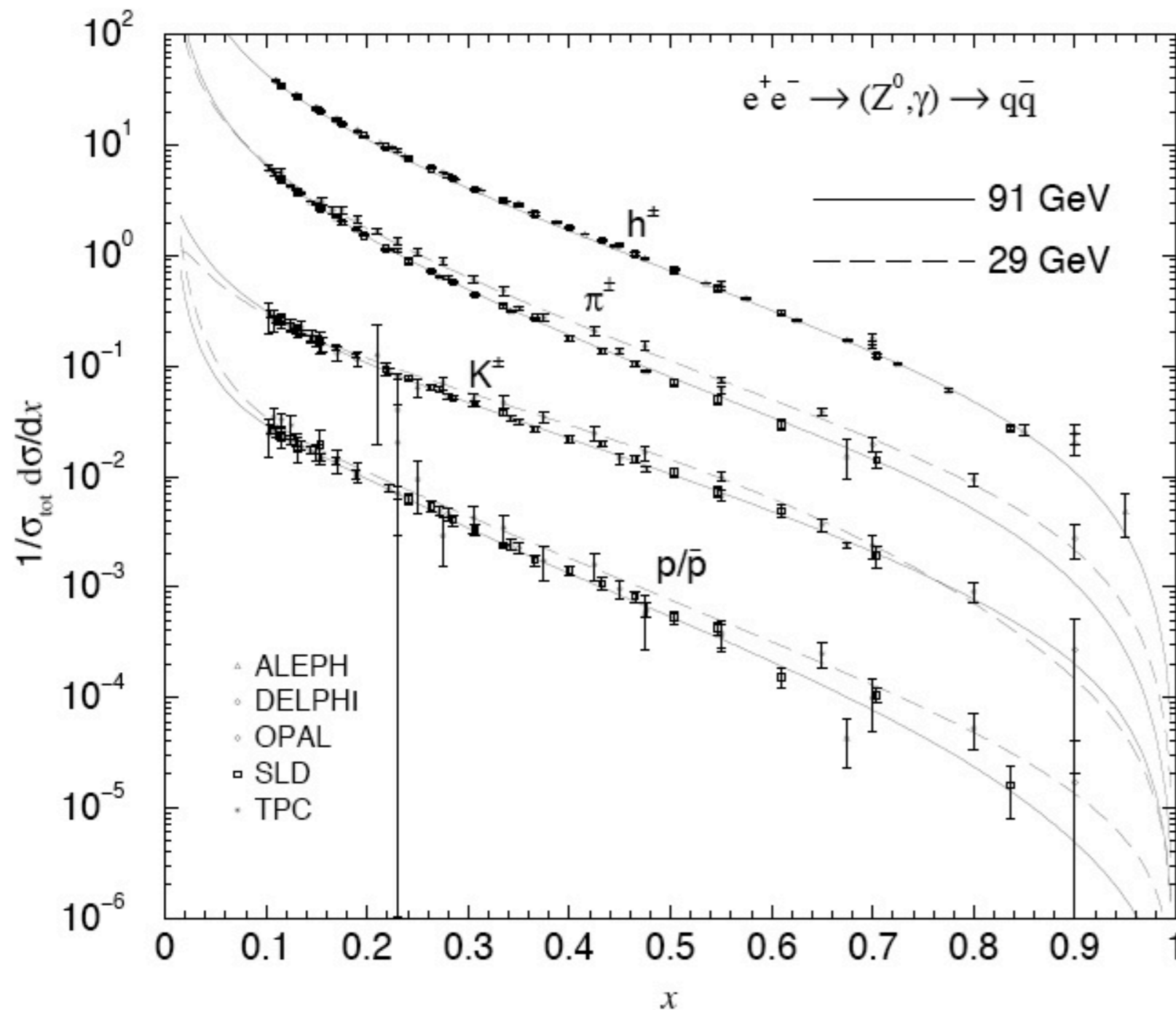
Jet Fragmentation (II)



$$\frac{1}{\sigma_{tot}} \frac{d\sigma}{dz} (e^- + e^- \rightarrow h + X) = \frac{\sum_q Q_q^2 [D_q^h(z) + D_{\bar{q}}^h(z)]}{\sum_q Q_q^2} \equiv f(z)$$

The expected scaling behavior is indeed approximately observed experimentally

Fragmentation Functions (FF) from e+e- Data



- Usual ansatz for functional form of the fragmentation function:

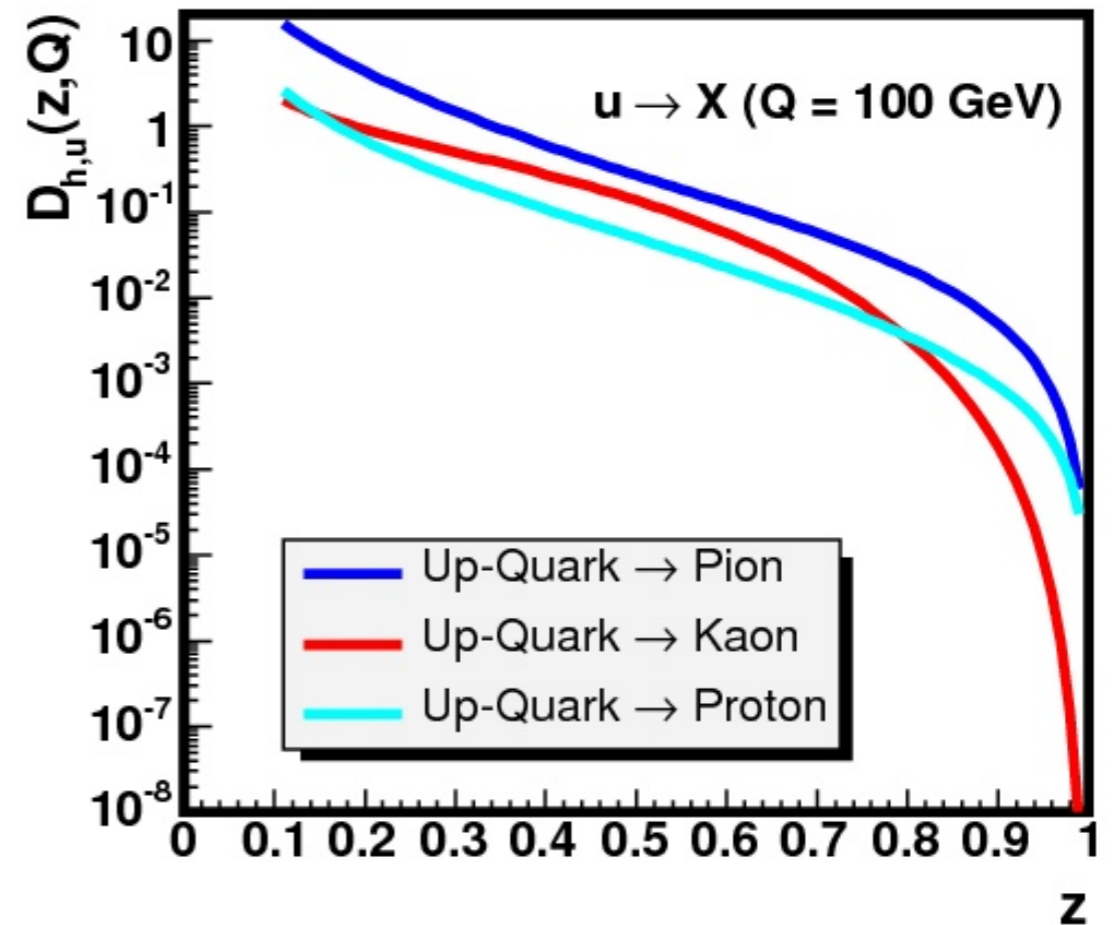
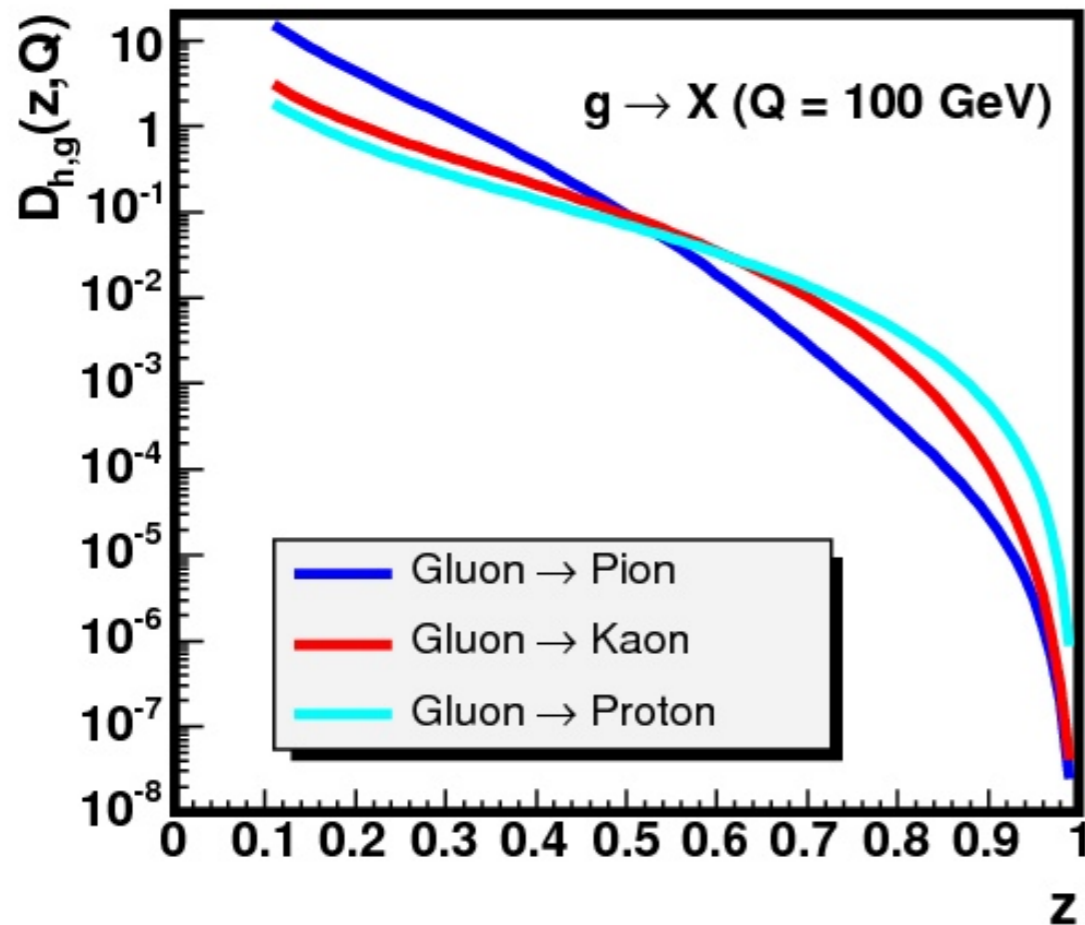
$$D_a^h(x, M_0^2) = N x^\alpha (1 - x)^\beta$$

- Small differences between FF's can be seen („scaling violation“)

NLO fragmentation functions from Albino, Kniehl und Kramer (hep-ph/0502188v2)

Example: Gluon and u-Quark Fragmentation Functions

Albino, Kniehl, Kramer, Nucl. Phys. B 725 (2005), 181



$$z = \frac{p_{\text{Hadron}}}{p_{\text{Parton}}}$$

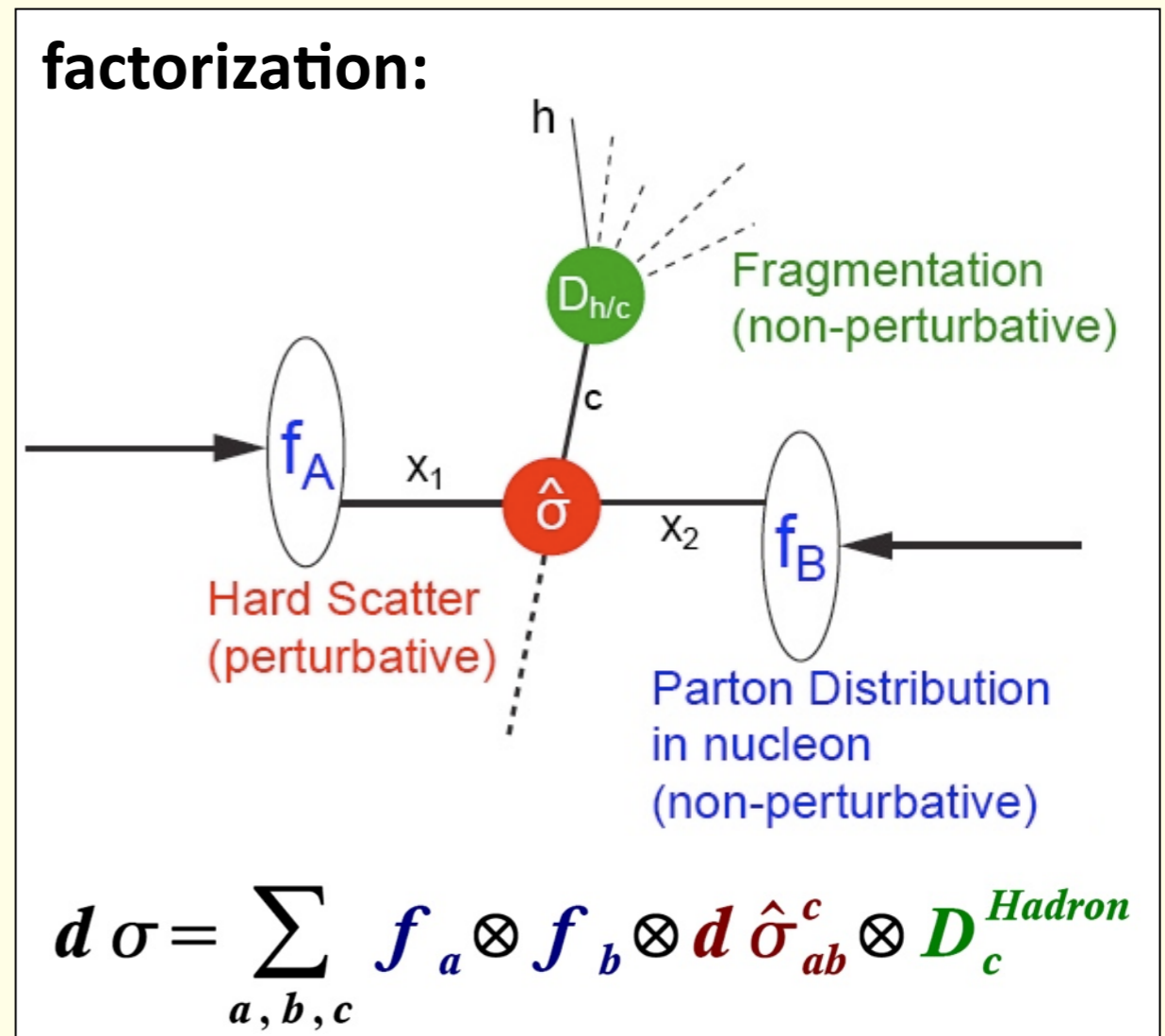
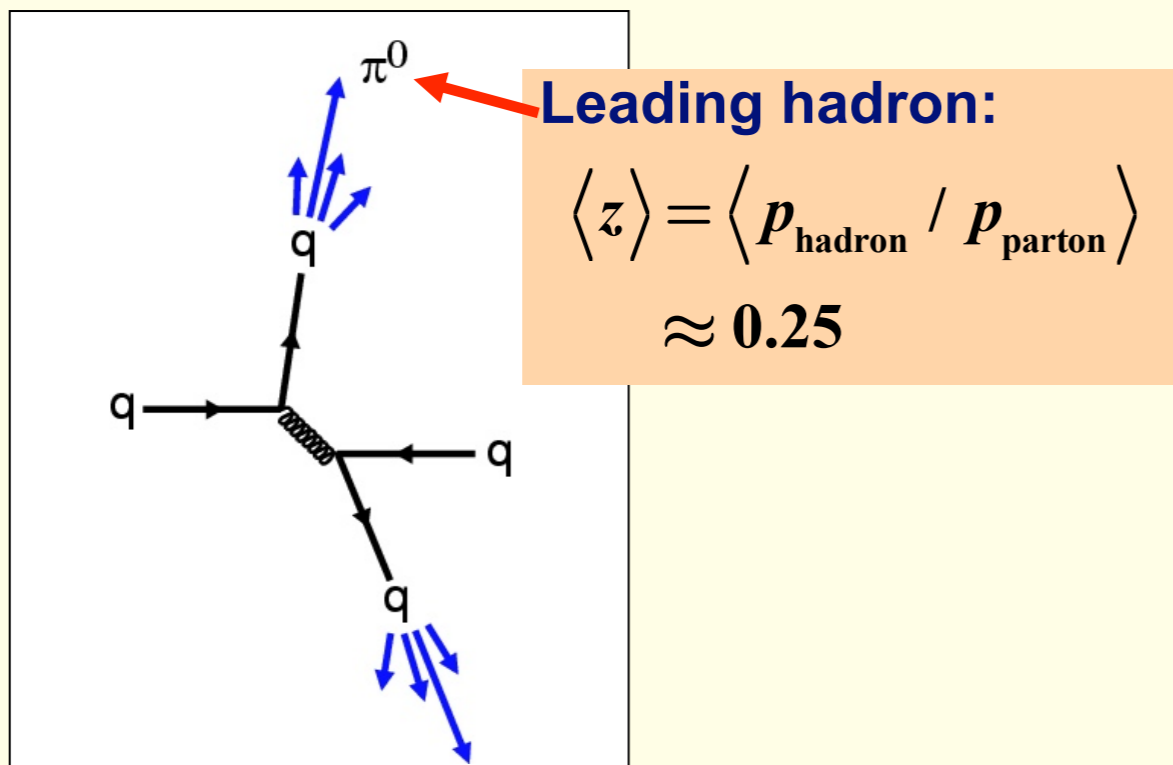
Fragmentation functions:

Number density for the production of a hadron h with fractional energy z in the fragmentation of a parton (e.g. determined from $e^+e^- \rightarrow Z^0 \rightarrow q\bar{q}$)

3.2 Hard Scattering and Particle Yields at High p_T in $p+p(\bar{p}p)$ Collisions

Theoretical Description of High- p_T Particle Production

- Scattering of pointlike partons described by QCD perturbation theory (pQCD)
- Soft processes described by **universal**, phenomenological functions
 - ▶ Parton distribution function from deep inelastic scattering
 - ▶ Fragmentation functions from e^+e^- collisions



Hadron Production in Leading Order QCD

Inv. Cross section

Parton distributions
(functions of x_{Bjorken}
and momentum transfer Q^2)

Fragmentation function

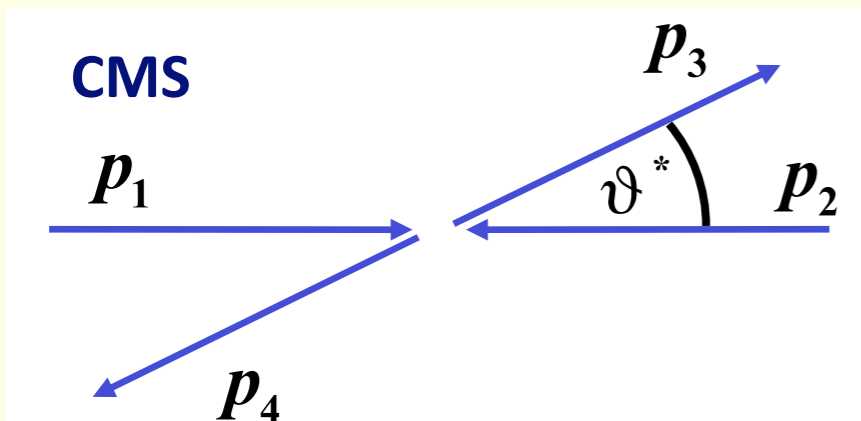
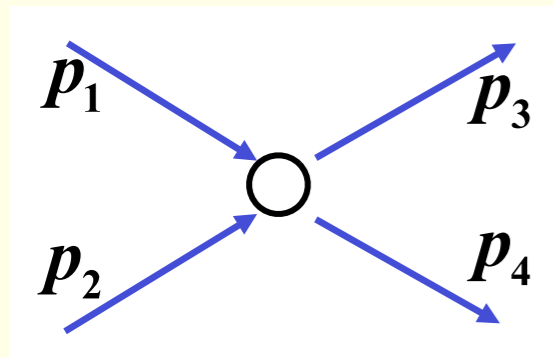
$$E \frac{d^3\sigma}{dp^3} = K \sum_{a,b,c,d=q,\bar{q},g} \int_{x_{a,\min}}^1 dx_a \int_{x_{b,\min}}^1 dx_b f_{a/A}(x_a, Q^2) f_{b/B}(x_b, Q^2) \frac{d\sigma^{ab \rightarrow cd}}{d\hat{t}} \frac{1}{\pi z_c} D_{h/c}(z_c, Q^2)$$

Phenomenological factor
which takes higher order
contributions into account

Elementary QCD
parton-parton
cross section

$$z_c = p_{T,\text{Hadron}} / p_{T,c}$$

Mandelstam Variables



Massless partons:

$$\hat{s} = (p_1 + p_2)^2$$

$$\hat{t} = (p_1 - p_3)^2 = -2p_1 p_3 = -\hat{s} \frac{1 - \cos \vartheta^*}{2}$$

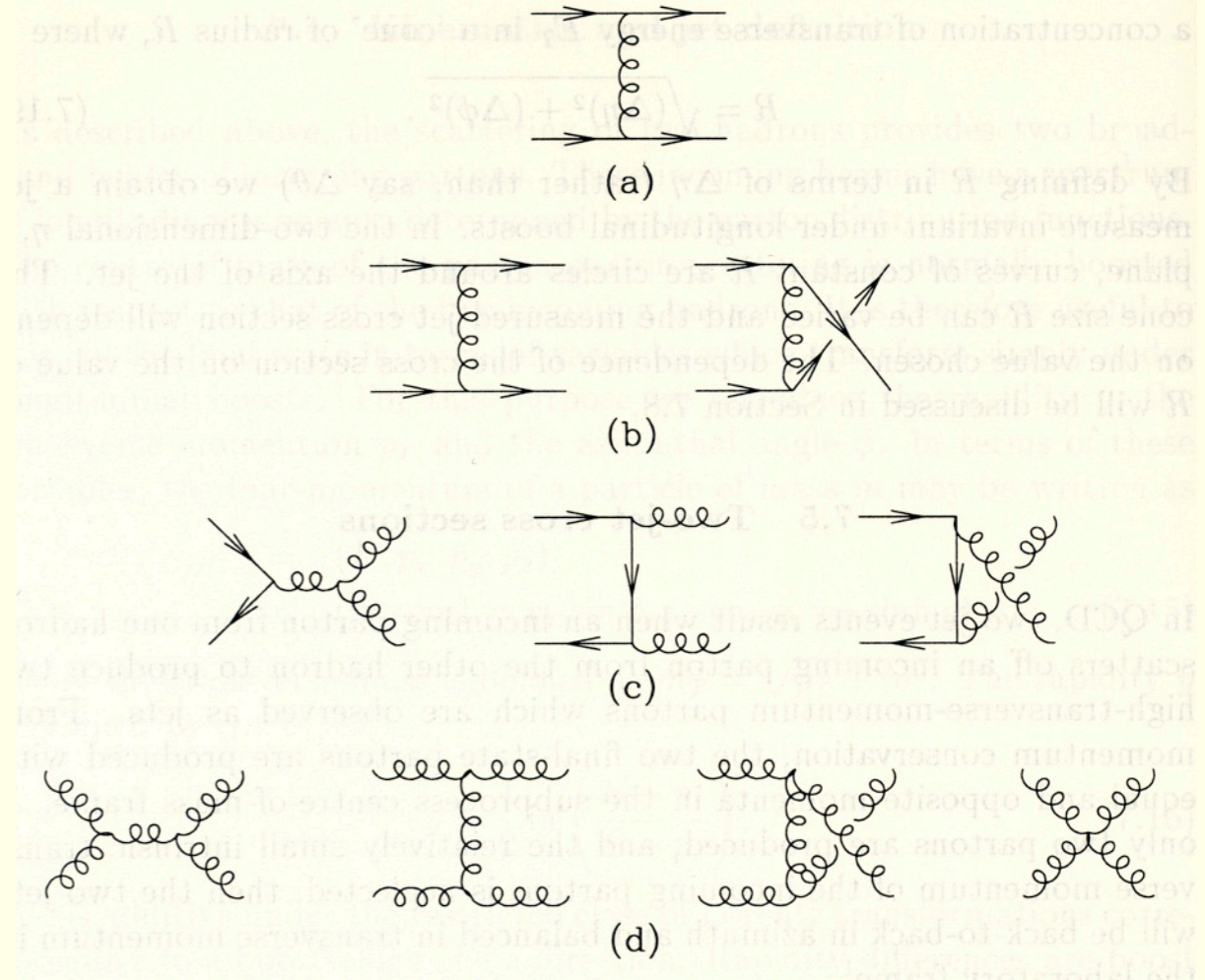
$$\hat{u} = (p_2 - p_3)^2 = -2p_2 p_3 = -\hat{s} \frac{1 + \cos \vartheta^*}{2}$$

Example: Jet cross section (i.e., no fragmentation function):

$$E_{\text{jet}} \frac{d^3\sigma}{d^3p_{\text{jet}}} = \frac{1}{16\pi s} \sum_{i,j,k,l=q,\bar{q},g} \int_0^1 \frac{dx_1}{x_1} \frac{dx_2}{x_2} f_i(x_1, \mu^2) f_j(x_2, \mu^2) \\ \times \sum |M(ij \rightarrow kl)|^2 \frac{1}{1 + \delta_{kl}} \delta(\hat{s} + \hat{t} + \hat{u})$$

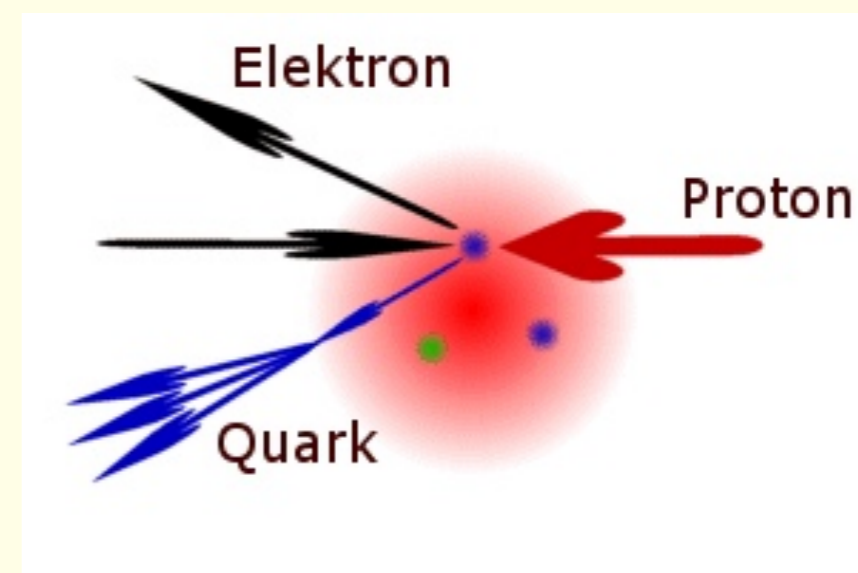
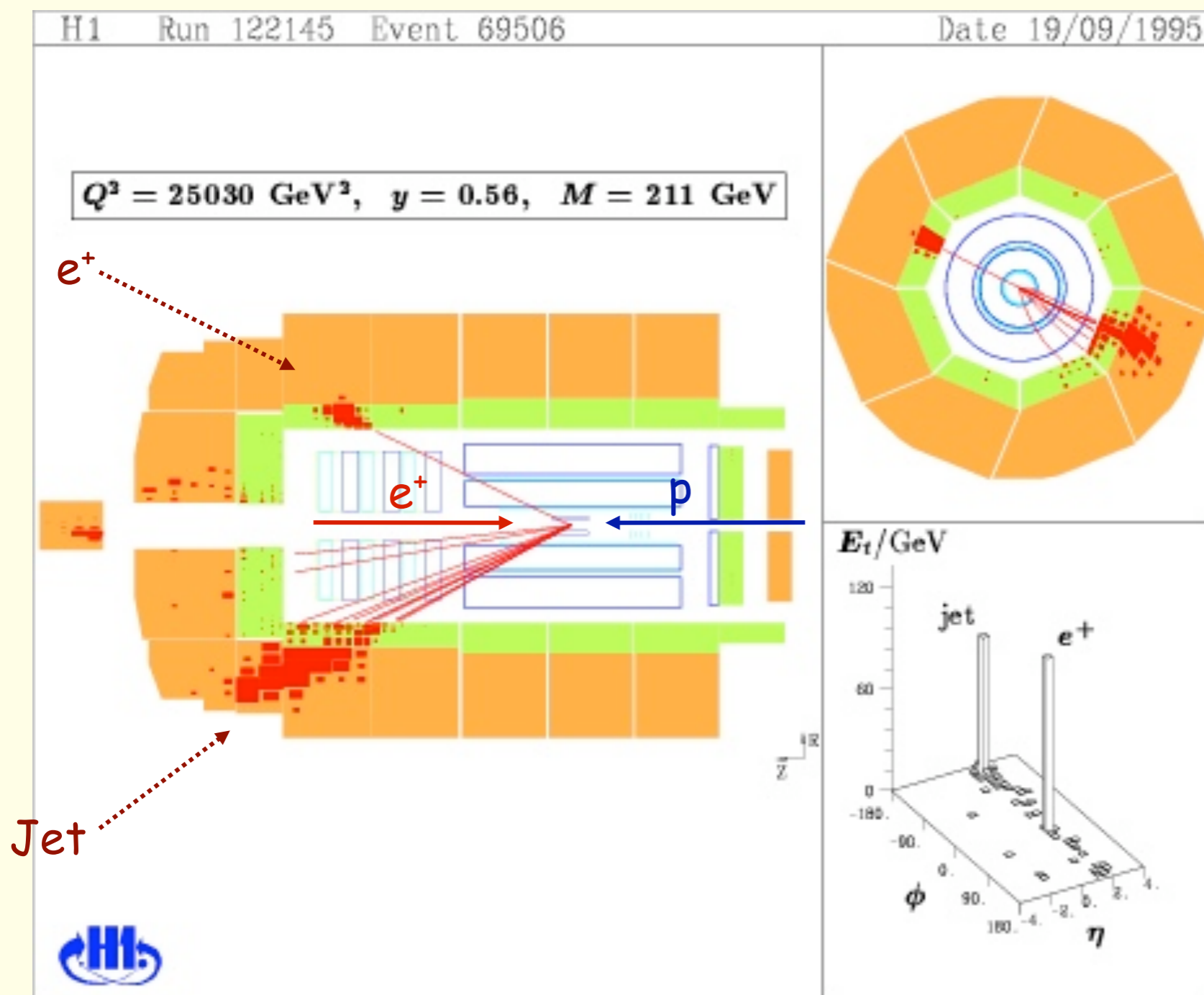
Point Cross Sections at Leading Order

Process	$\overline{\sum} \mathcal{M} ^2 / g^4$	$\theta^* = \pi/2$
$q q' \rightarrow q q'$	$\frac{4}{9} \frac{\hat{s}^2 + \hat{u}^2}{\hat{t}^2}$	2.22
$q \bar{q}' \rightarrow q \bar{q}'$	$\frac{4}{9} \frac{\hat{s}^2 + \hat{u}^2}{\hat{t}^2}$	2.22
$q q \rightarrow q q$	$\frac{4}{9} \left(\frac{\hat{s}^2 + \hat{u}^2}{\hat{t}^2} + \frac{\hat{s}^2 + \hat{t}^2}{\hat{u}^2} \right) - \frac{8}{27} \frac{\hat{s}^2}{\hat{u}\hat{t}}$	3.26
$q \bar{q} \rightarrow q' \bar{q}'$	$\frac{4}{9} \frac{\hat{t}^2 + \hat{u}^2}{\hat{s}^2}$	0.22
$q \bar{q} \rightarrow q \bar{q}$	$\frac{4}{9} \left(\frac{\hat{s}^2 + \hat{u}^2}{\hat{t}^2} + \frac{\hat{t}^2 + \hat{u}^2}{\hat{s}^2} \right) - \frac{8}{27} \frac{\hat{u}^2}{\hat{s}\hat{t}}$	2.59
$q \bar{q} \rightarrow g g$	$\frac{32}{27} \frac{\hat{t}^2 + \hat{u}^2}{\hat{t}\hat{u}} - \frac{8}{3} \frac{\hat{t}^2 + \hat{u}^2}{\hat{s}^2}$	1.04
$g g \rightarrow q \bar{q}$	$\frac{1}{6} \frac{\hat{t}^2 + \hat{u}^2}{\hat{t}\hat{u}} - \frac{3}{8} \frac{\hat{t}^2 + \hat{u}^2}{\hat{s}^2}$	0.15
$g q \rightarrow g q$	$-\frac{4}{9} \frac{\hat{s}^2 + \hat{u}^2}{\hat{s}\hat{u}} + \frac{\hat{u}^2 + \hat{s}^2}{\hat{t}^2}$	6.11
$g g \rightarrow g g$	$\frac{9}{2} \left(3 - \frac{\hat{t}\hat{u}}{\hat{s}^2} - \frac{\hat{s}\hat{u}}{\hat{t}^2} - \frac{\hat{s}\hat{t}}{\hat{u}^2} \right)$	30.4

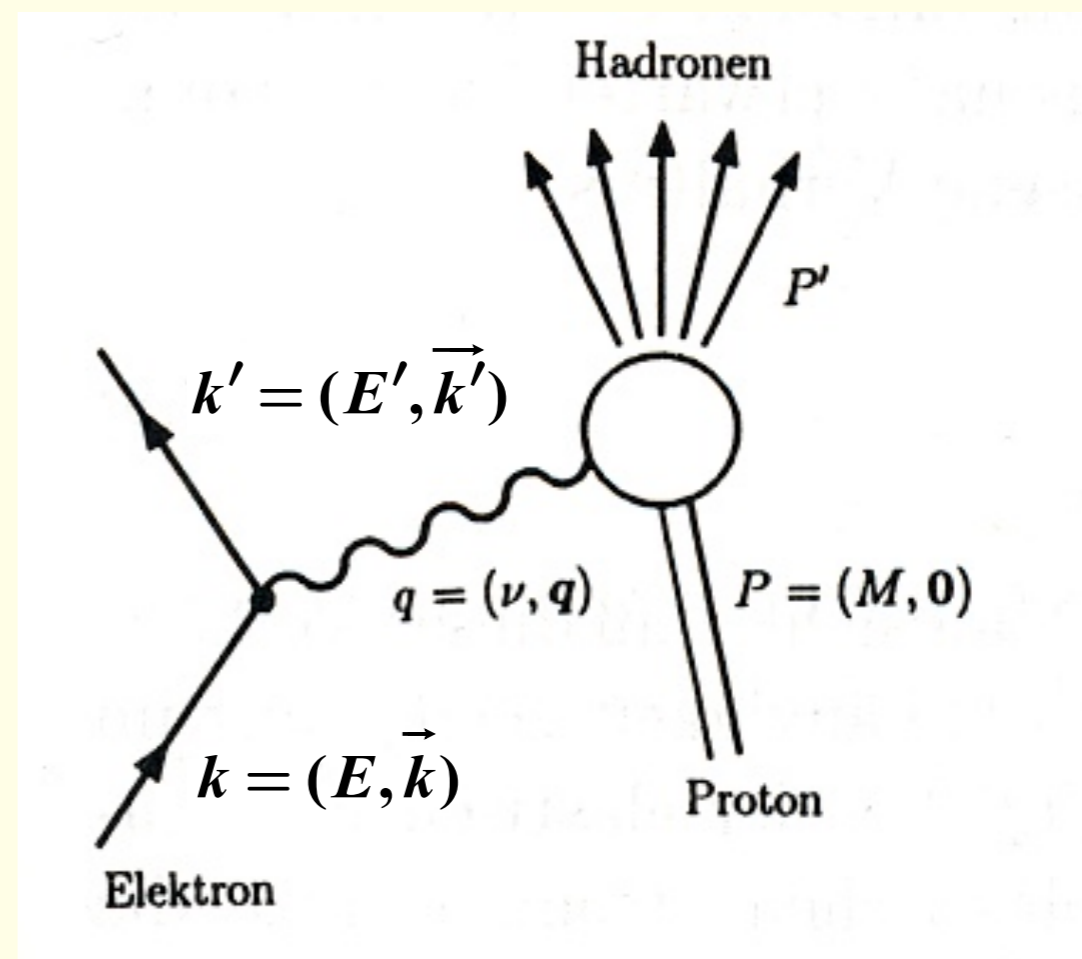
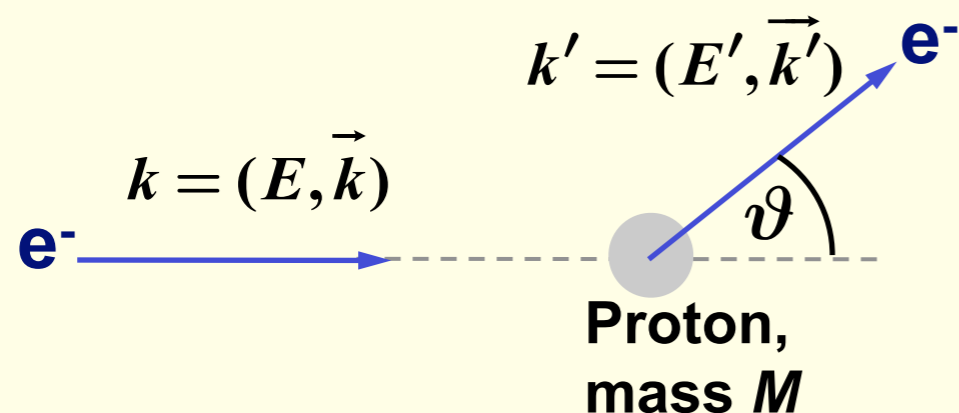


Determination of Parton Distribution Functions: Deep-Inelastic Lepton-Nucleon Scattering

e^+p Scattering: H1 event display



Determination of Parton Distribution Functions: Deep-Inelastic Lepton-Nucleon Scattering: Kinematic Variables



$$\nu = E - E' \quad (\text{in lab. frame})$$

$$Q^2 = -q^2 :$$

Structure functions to be determined in the experiment

$$\frac{d^2\sigma}{dQ^2 d\nu} = \frac{4\pi\alpha^2}{(Q^2)^2} \cdot \frac{E}{E'} \left(W_2(Q^2, \nu) \cos^2 \frac{\vartheta}{2} + 2W_1(Q^2, \nu) \sin^2 \frac{\vartheta}{2} \right)$$

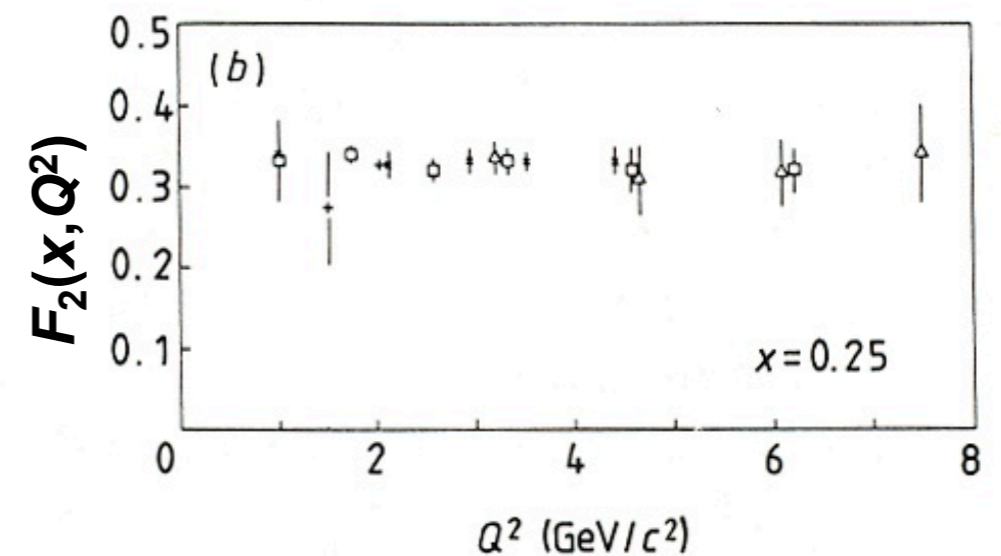
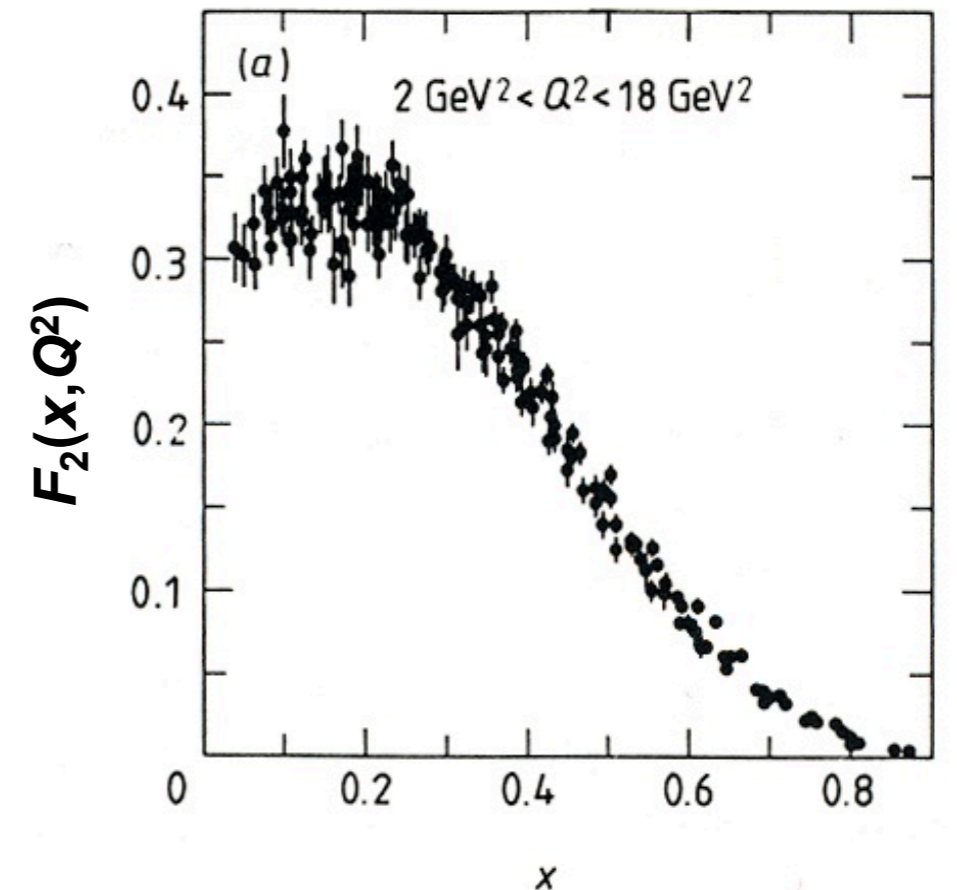
Discovery of Scaling at SLAC

Bjorken-x: $x := \frac{Q^2}{2M\nu}$

In the limit $Q^2, \nu \rightarrow \infty$
the structure functions only depend
on x . This is called *scaling*:

$$W_1(Q^2, \nu) \rightarrow F_1(x),$$
$$\frac{\nu}{M} \cdot W_2(Q^2, \nu) \rightarrow F_2(x)$$

Interpretation:
Inelastic lepton-nucleon scattering
can be regarded as incoherent
elastic scattering of the lepton off
pointlike constituents of the nucleon,
called **partons**.



Quark-Parton Model

Quark-Parton Model:

- View nucleon in infinite momentum frame so that transverse momenta of the partons can be neglected
- The Bjorken- x can be interpreted as the momentum fraction x ($0 \leq x \leq 1$) of the nucleon that is carried by the parton that participated in the scattering
- Identify partons with quarks and gluons

The structure function $F_2(x)$ is then given by

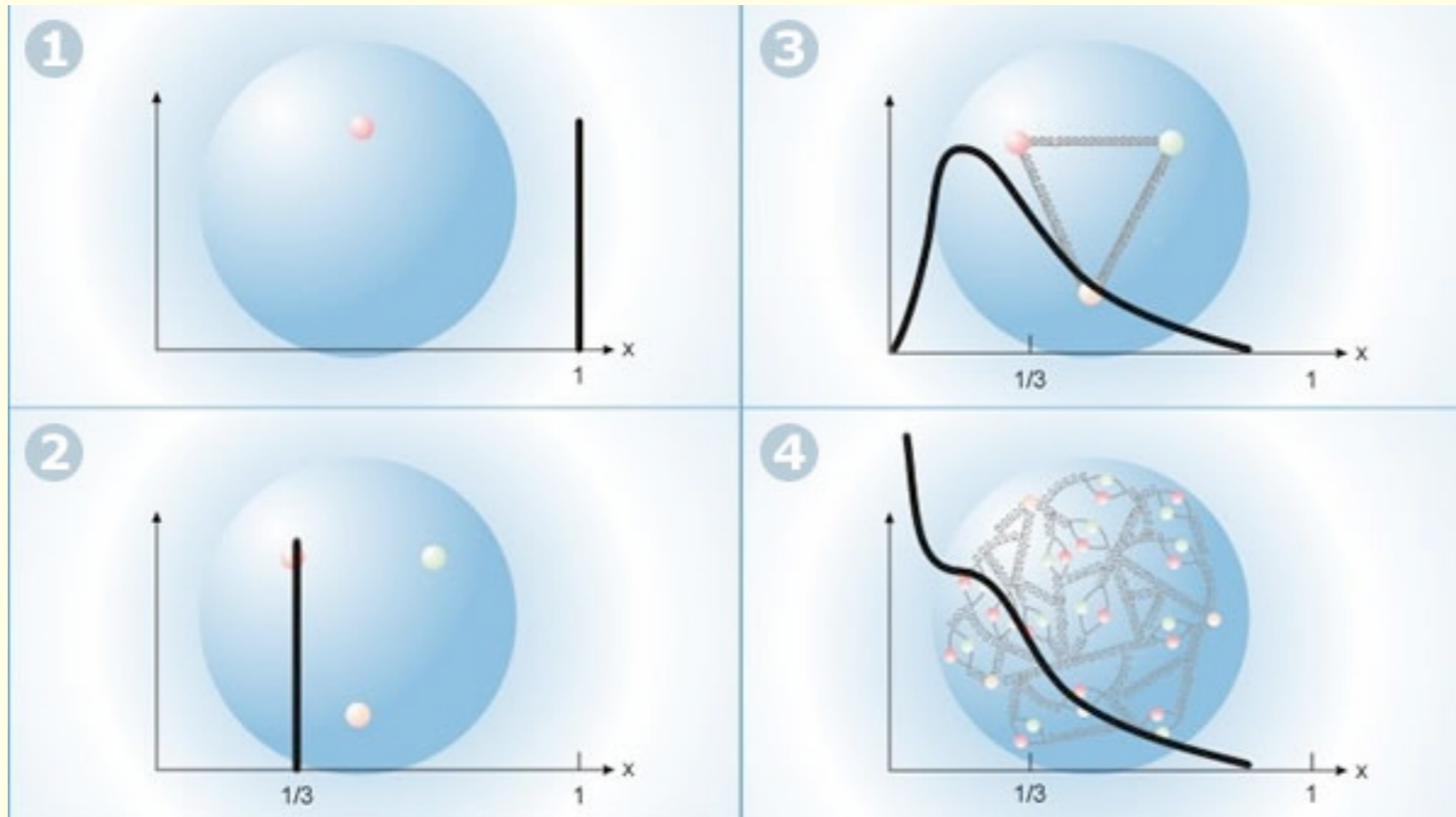
$$F_2(x) = x \sum_f z_f^2 (q_f(x) + \bar{q}_f(x))$$

where

$q_f(x) dx$ [$\bar{q}_f(x) dx$]: number of quarks [antiquarks] of flavor f with fractional momenta between $x \dots x+dx$

z_f : quark charge (e.g. 2/3 for u-quark)

Parton Distributions (I)



Proton =

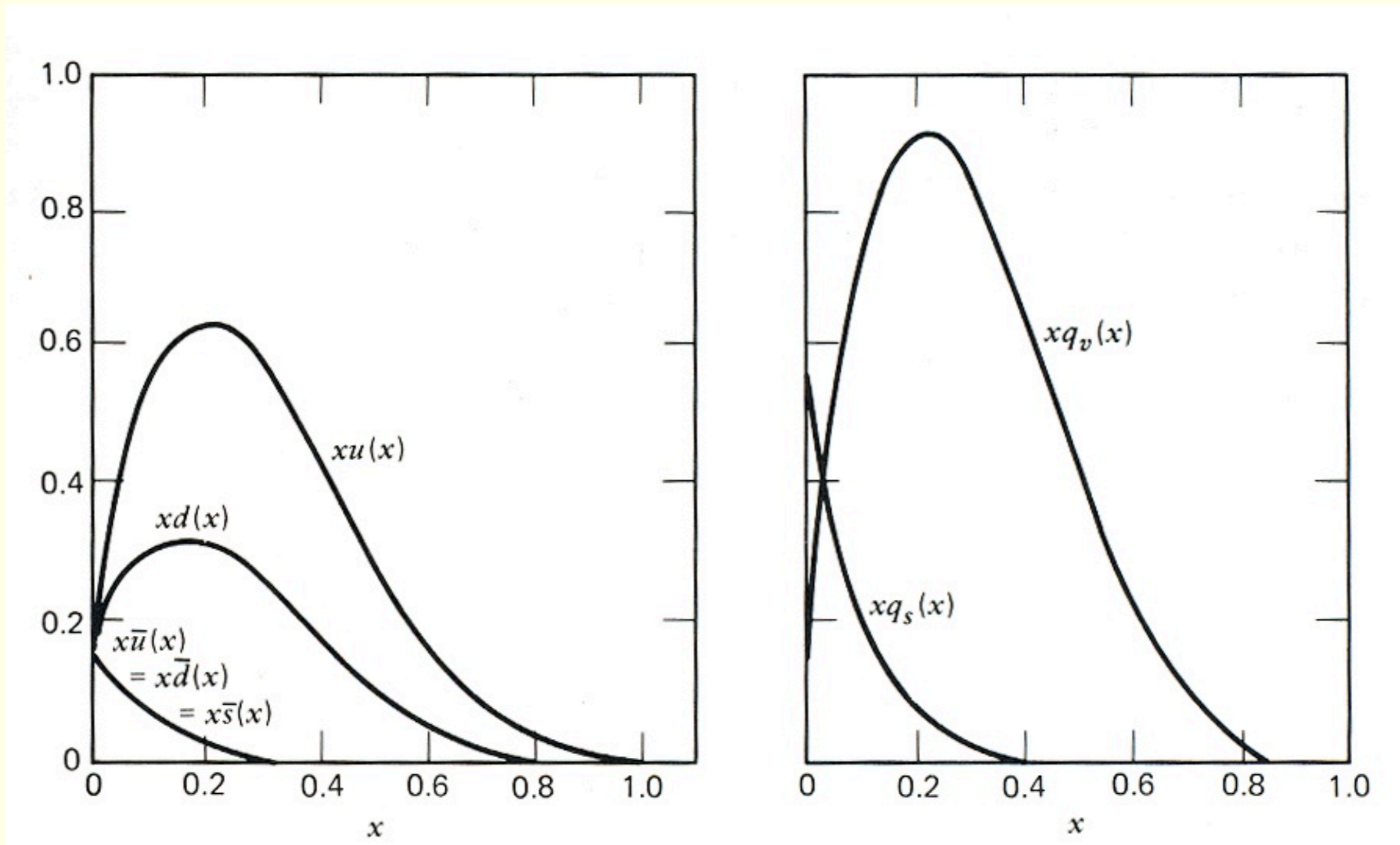
1. 1 valence quark
2. 3 valence quarks
3. 3 valence quarks + gluons
4. 3 valence quarks + gluons + sea quarks

Interpretation of x_{Bjorken} in the parton model:

In a reference frame in which the parton transverse momentum can be neglected (infinite momentum frame) x_{Bjorken} represents the fraction of the 4-momentum of the nucleon carried by the parton

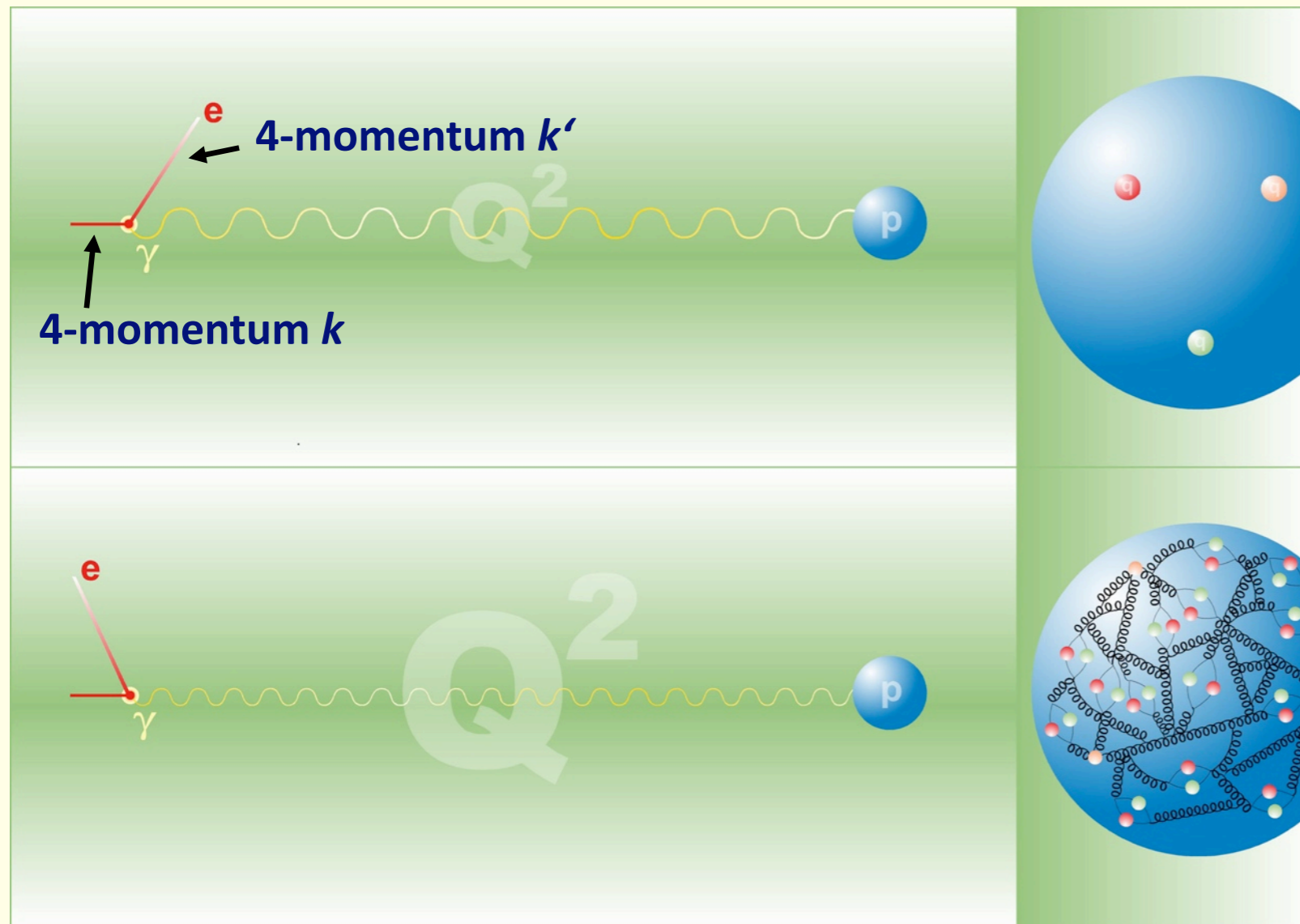
Parton Distributions (II)

parton distributions in the proton:



$q(x) dx$: parton distribution = number of partons in $[x, x+dx]$

Resolution of the Virtual Photon



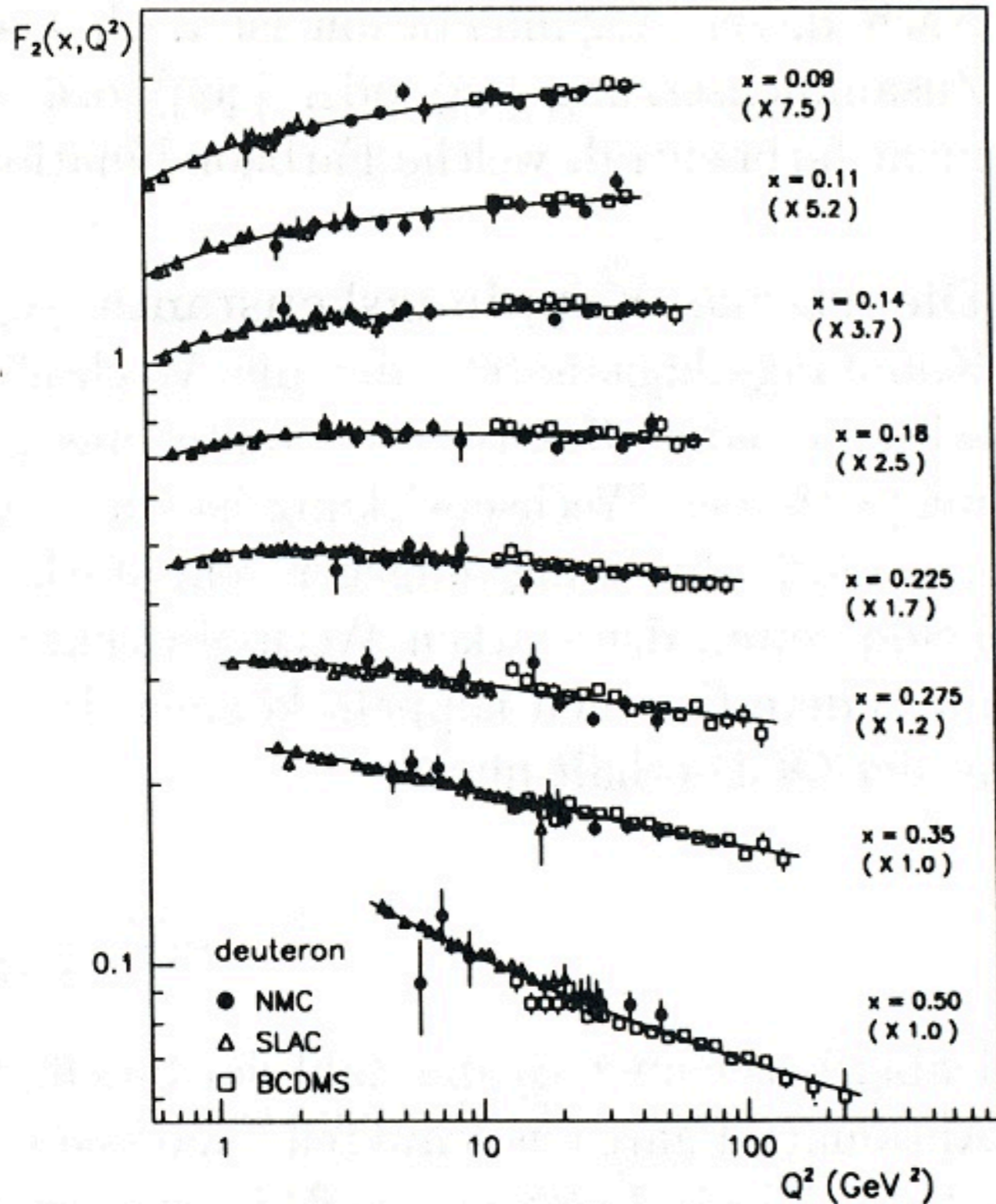
Valence quarks

Valence quarks +
sea quarks

4-momentum transfer: $q = (k - k')$, $Q^2 := -q^2$

wave length of the virtual photon: $\lambda = \frac{\hbar}{\sqrt{Q^2}}$

Scaling Violations



- **Scaling violation**

- ▶ **Small x (< 0.1):**

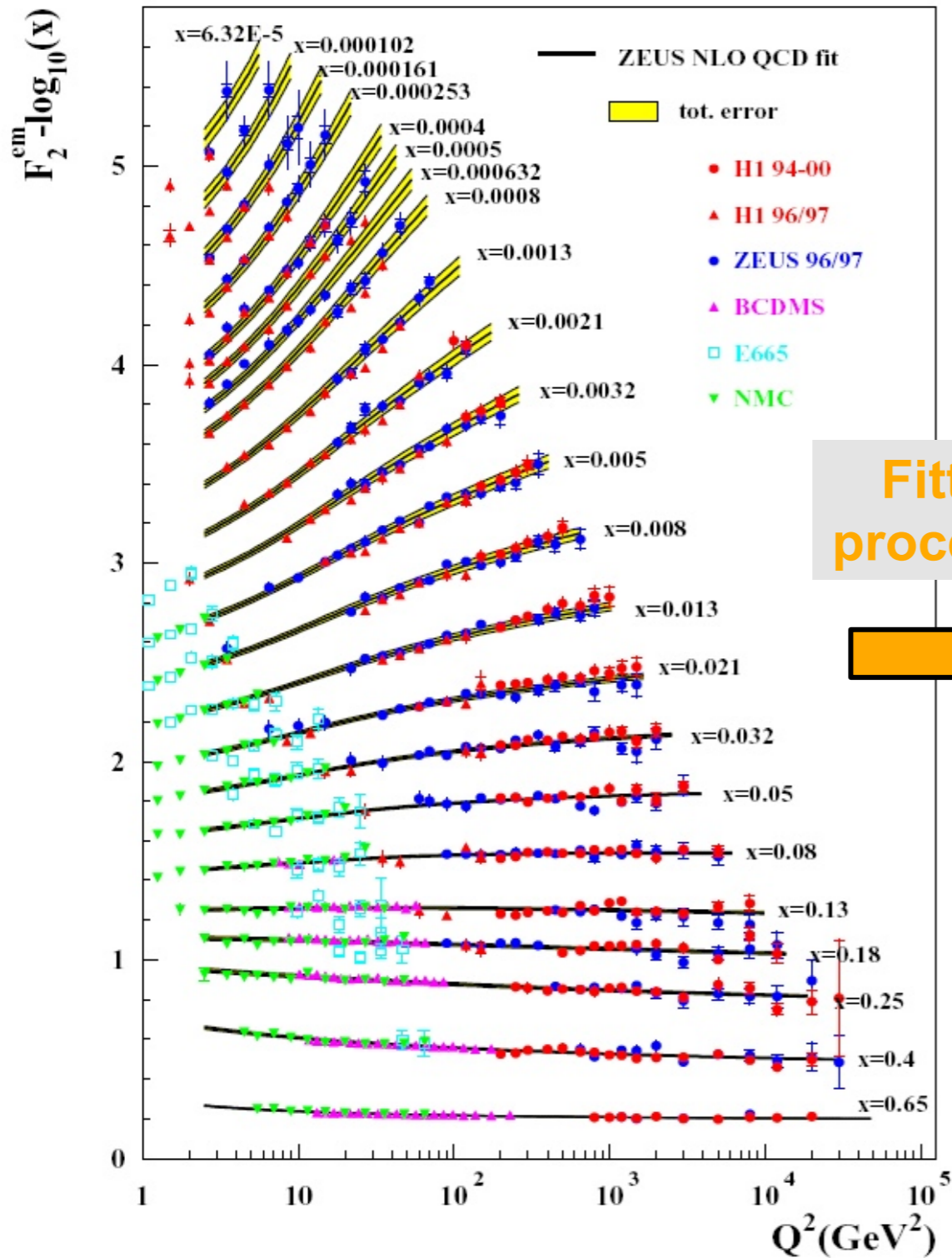
- $F_2(x, Q^2)$ increases with Q^2

- ▶ **Large x (> 0.3):**

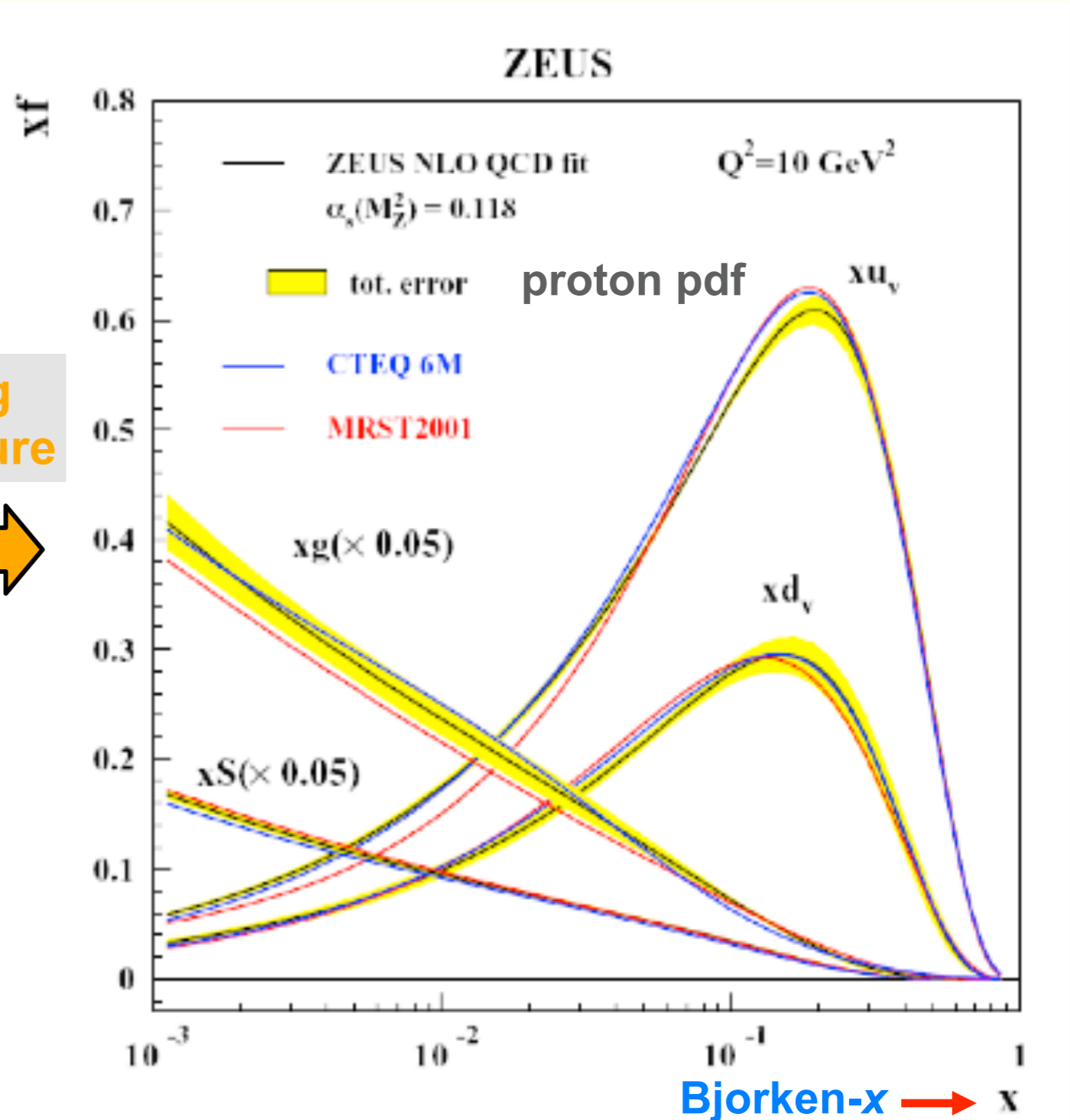
- $F_2(x, Q^2)$ decreases with Q^2

Parton Distributions: High Precision Data from HERA

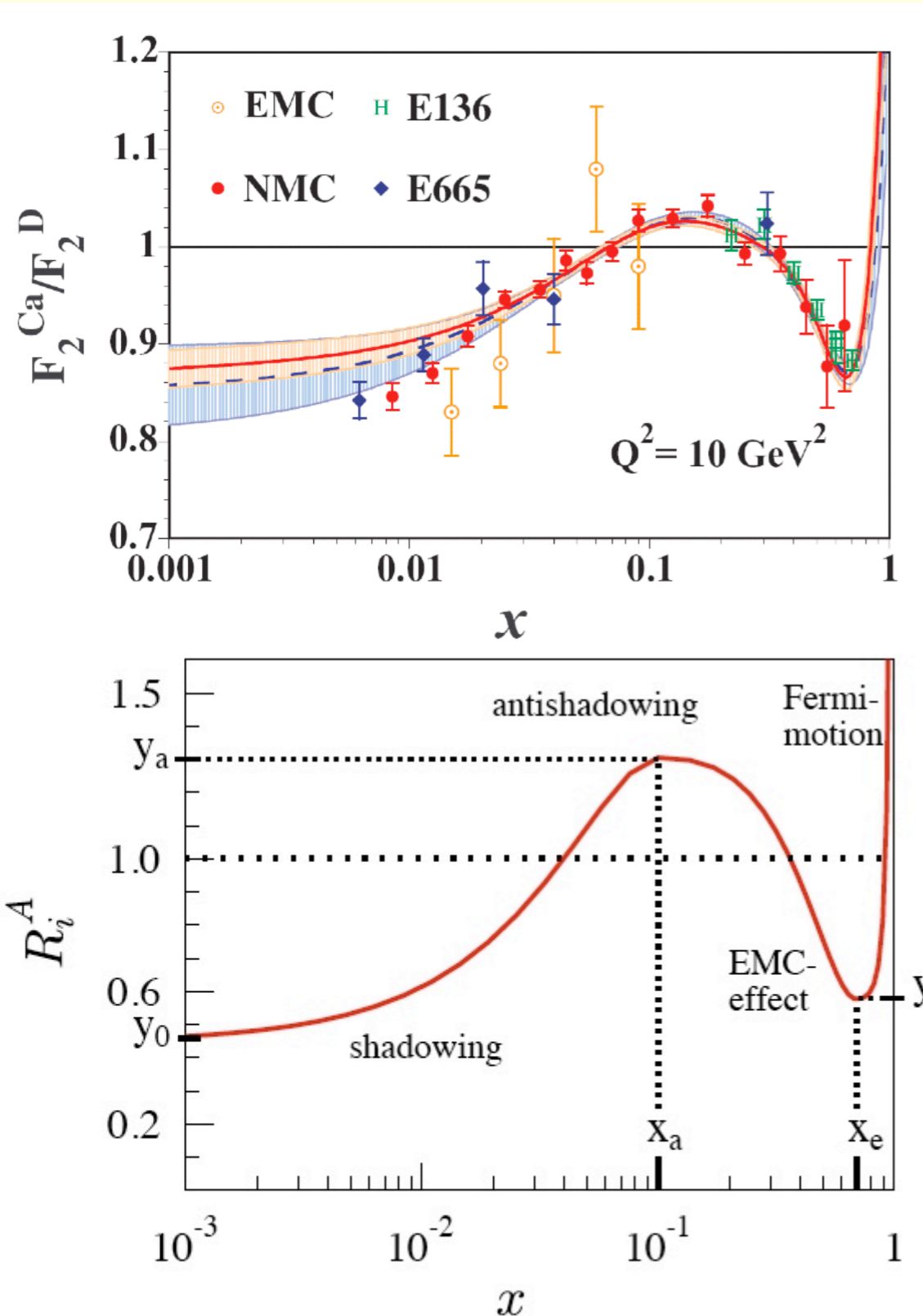
$$d\sigma = \sum_{a,b,c} f_a \otimes f_b \otimes d\hat{\sigma}_{ab}^c \otimes D_c^{Hadron}$$



Fitting procedure

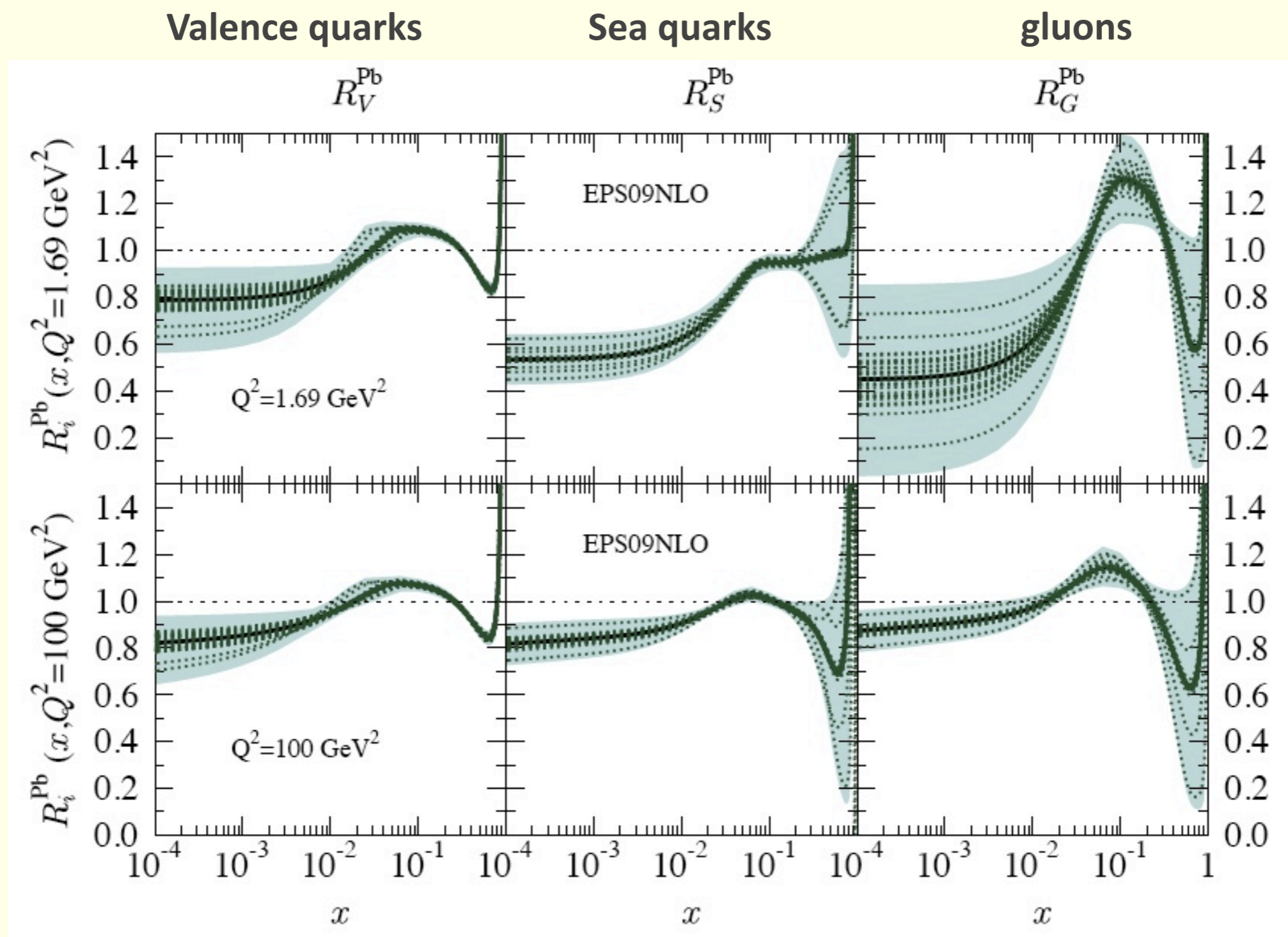


Modification of the Structure Functions in Nuclei



- $x < 0.1$: “shadowing region”
- $0.1 < x < 0.3$: “anti-shadowing”
- $0.3 < x < 0.7$: “EMC effect”
- $0.7 < x < 1.0$: Fermi-motion of nucleons in nuclei

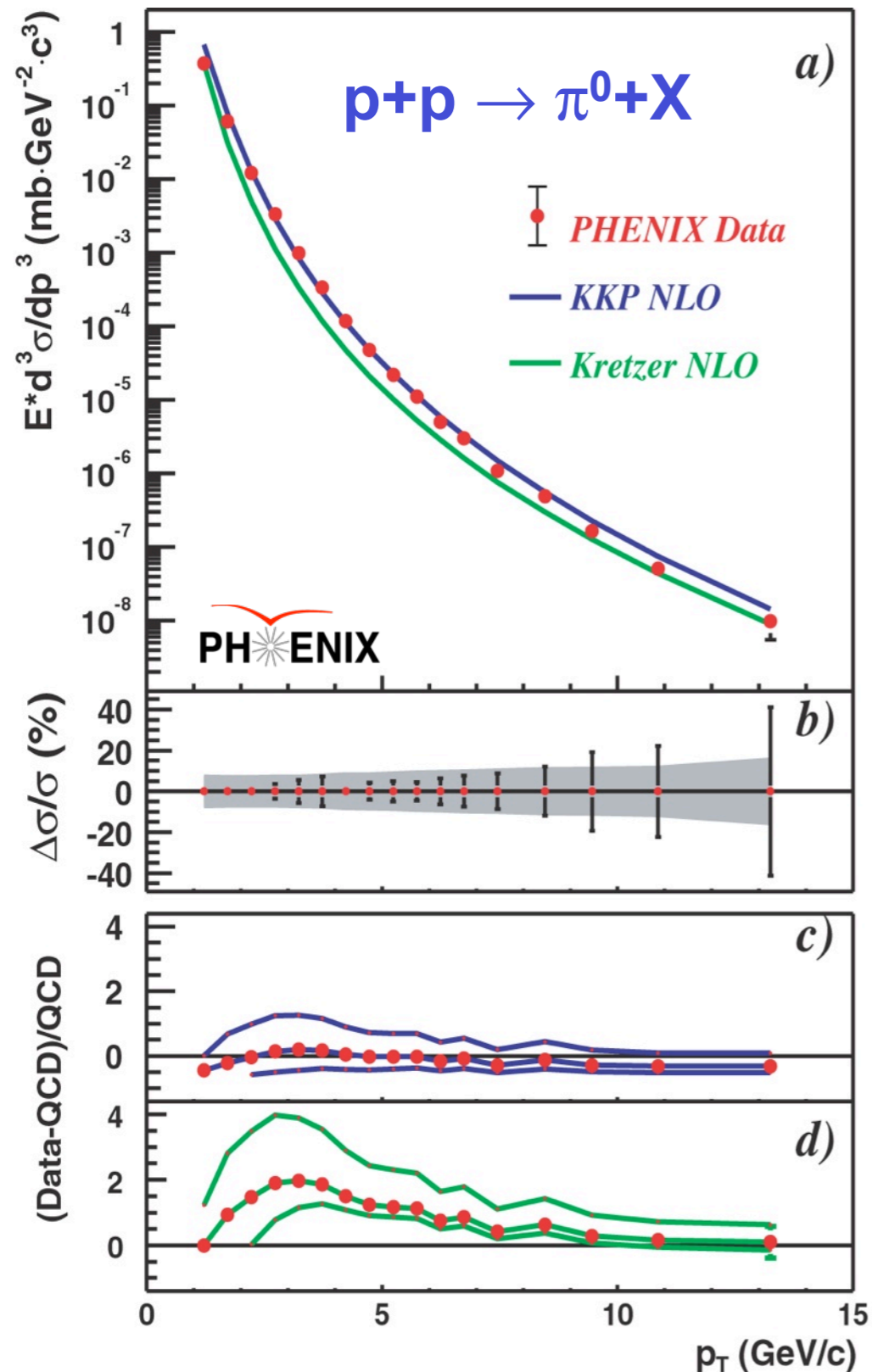
An Example: Nuclear PDF's in Pb (EPS09NLO)



Large uncertainties for gluon PDF's at small x

Eskola et al.,
arXiv:0902.4154v2 [hep-ph]

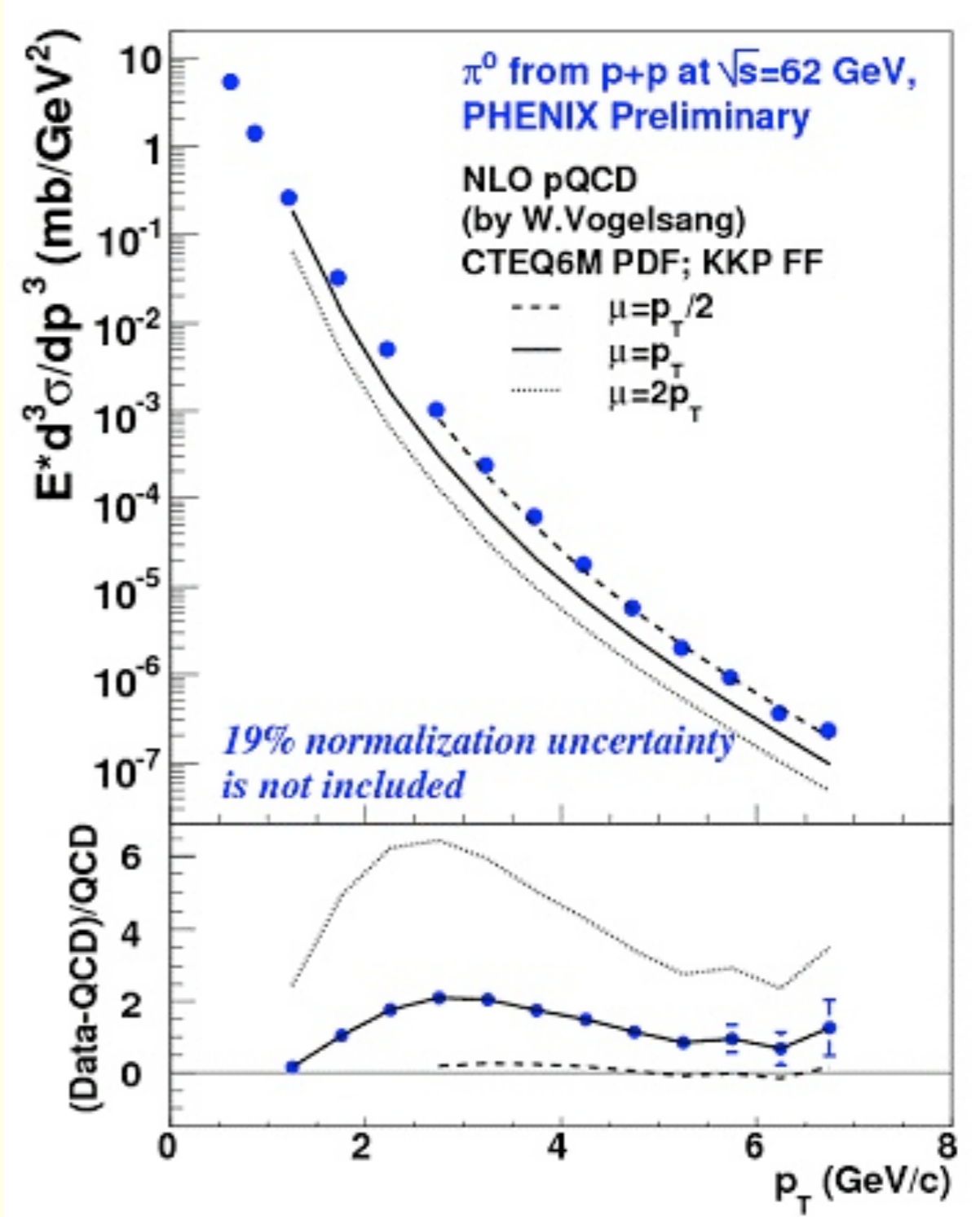
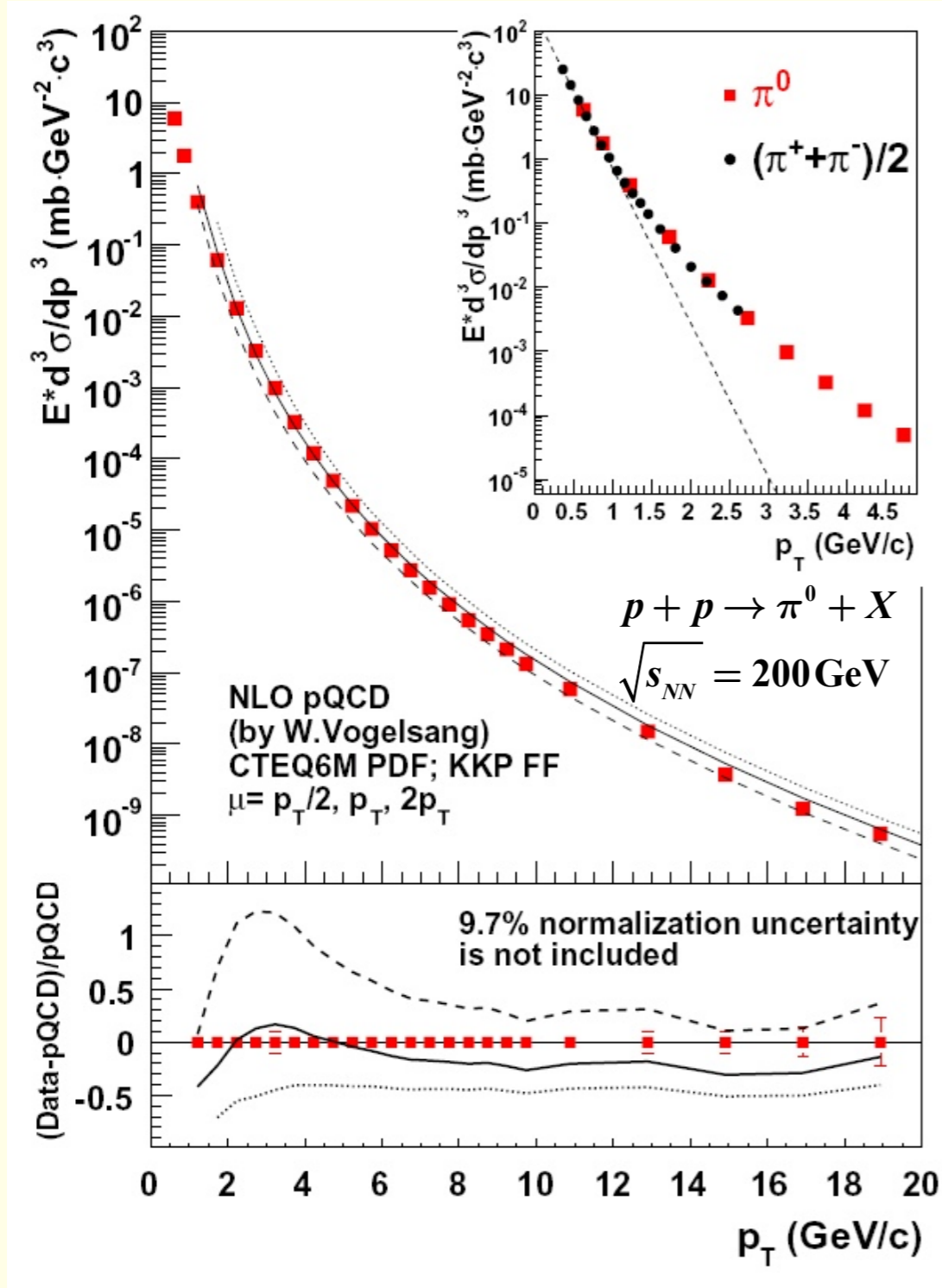
pQCD works in p+p at $\sqrt{s} = 200$ GeV



- π^0 production in p+p well described by perturbative QCD
- Data sensitive to differences in gluon fragmentation function (KKP vs. Kretzer)
- Reference for Au+Au
- Description of hard processes under control at RHIC energy

PRL 91, 241802 (2003)

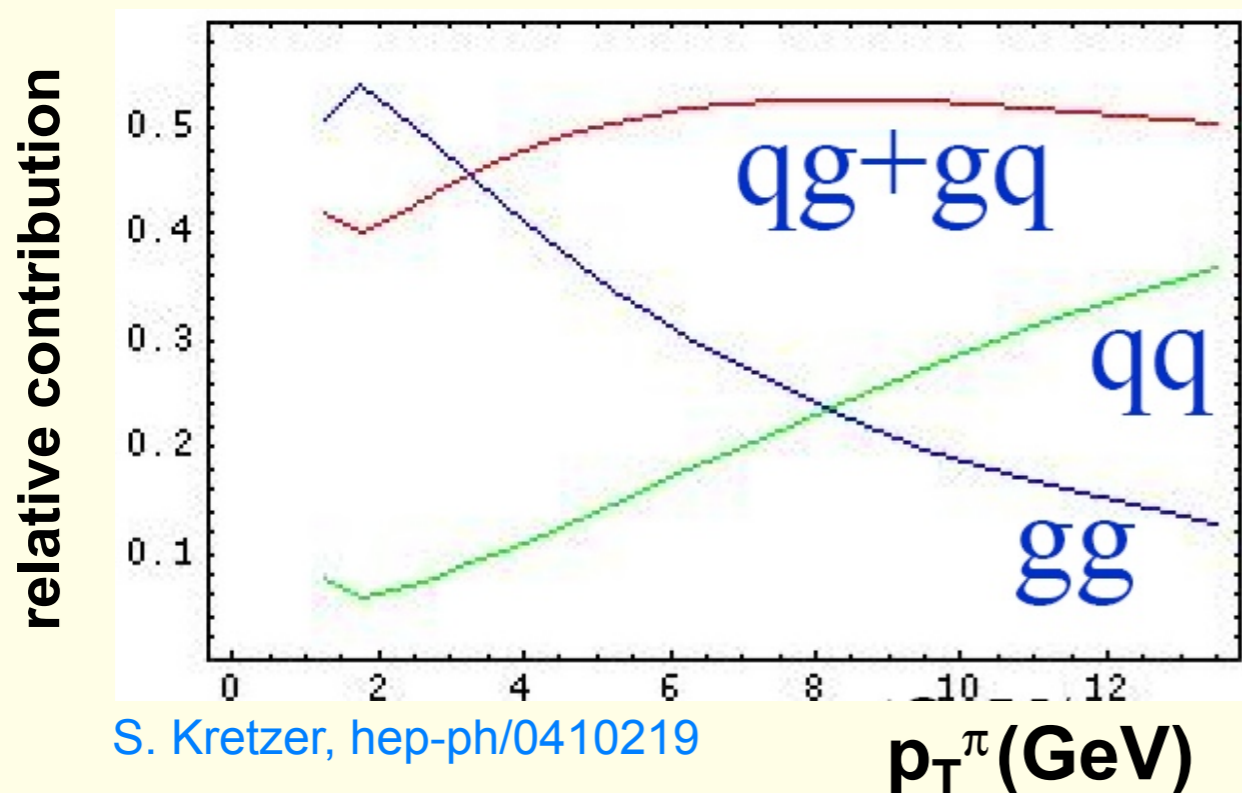
More Recent Data with Higher Statistics: Same Conclusion: pQCD Works at RHIC Energies



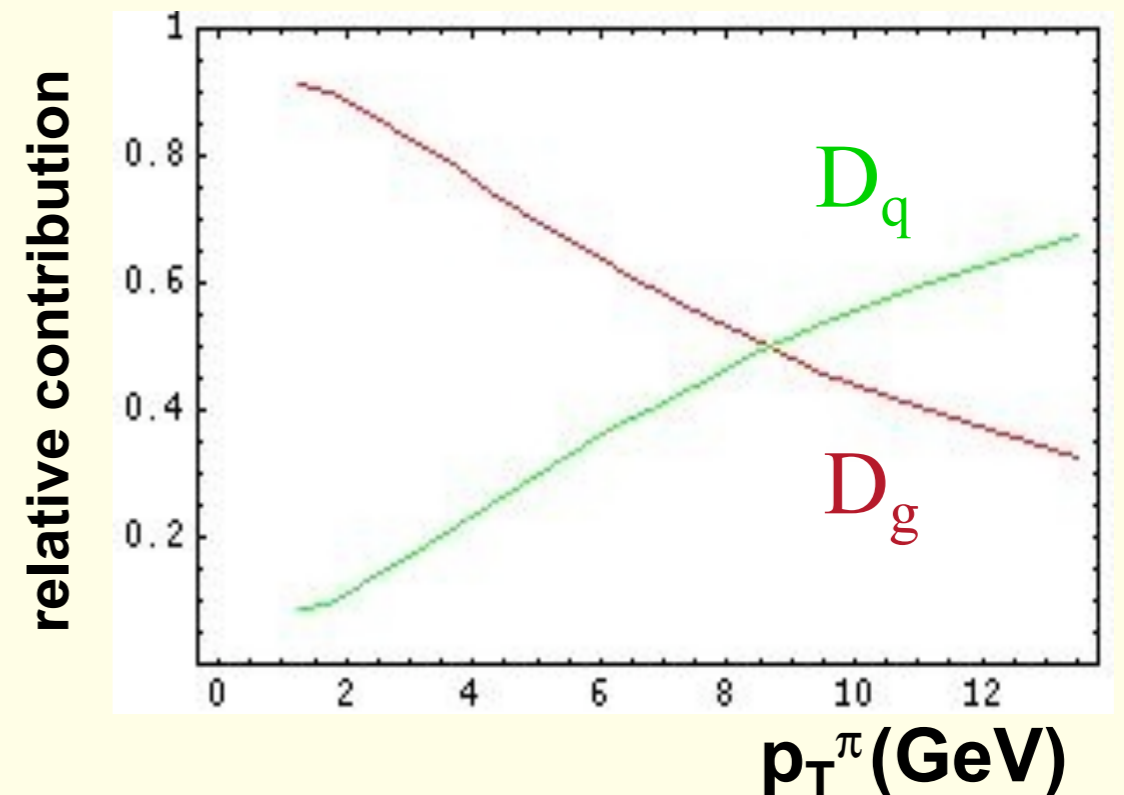
Agreement with pQCD in p+p is a prerequisite for parton energy loss calculations

Different Contributions to the Pion Spectrum in p+p at $\sqrt{s} = 200$ GeV

parton parton scattering



fragmentation

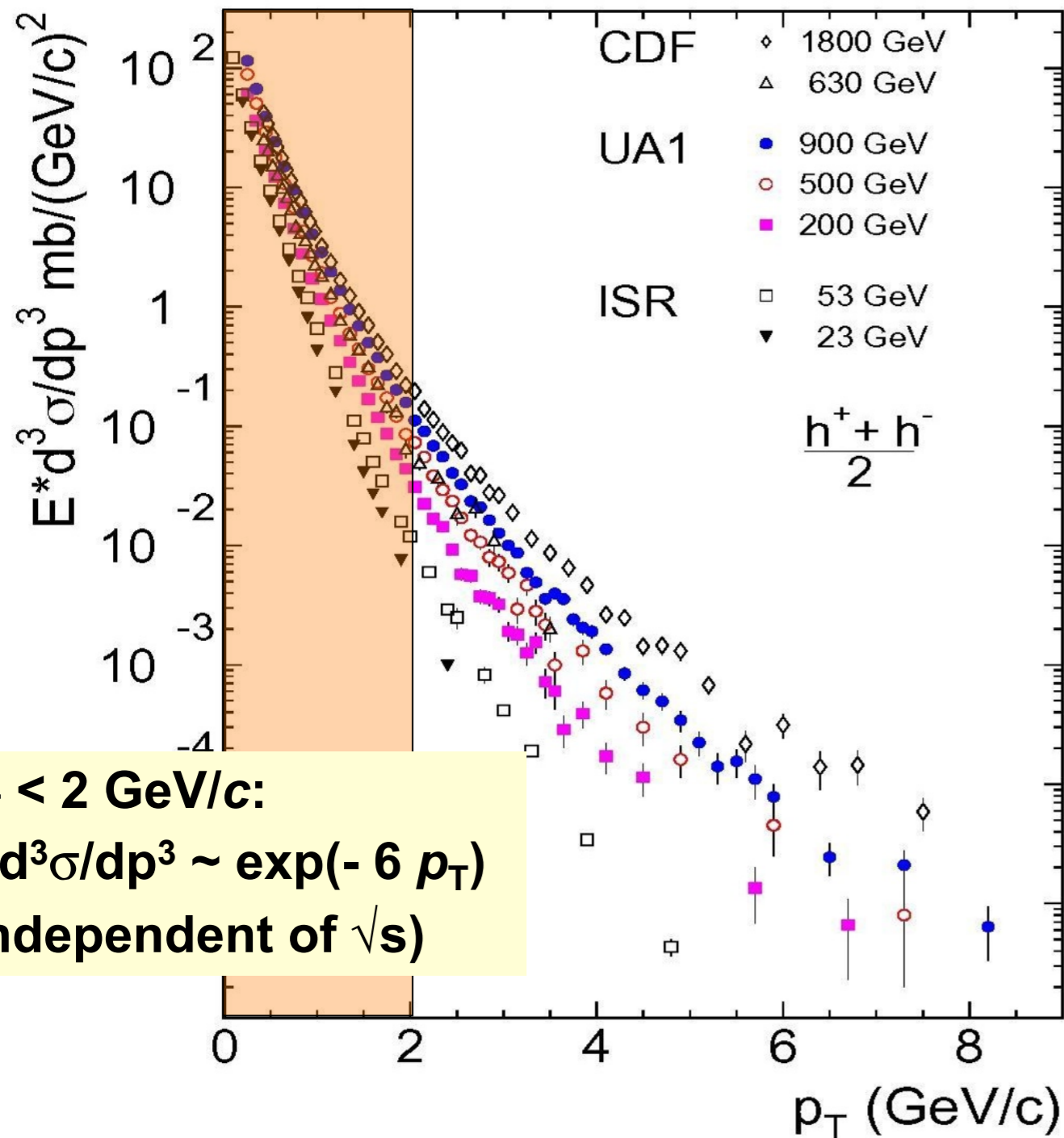


$p_T < 9$ GeV/c: gluon fragmentation dominates

$p_T > 9$ GeV/c: quark fragmentation dominates

Particle Production at High p_T (I)

p_T spectra of charged particles for various \sqrt{s}



$p_T < 2$ GeV/c:
 $E \cdot d^3\sigma/dp^3 \sim \exp(-6 p_T)$
 (independent of \sqrt{s})

High p_T part of the spectrum flattens with increasing \sqrt{s}

Low $p_T (< 2$ GeV/c):

$$\frac{1}{p_T} \frac{dN_x}{dp_T} = A(\sqrt{s}) \cdot e^{-6 p_T}$$

High p_T :

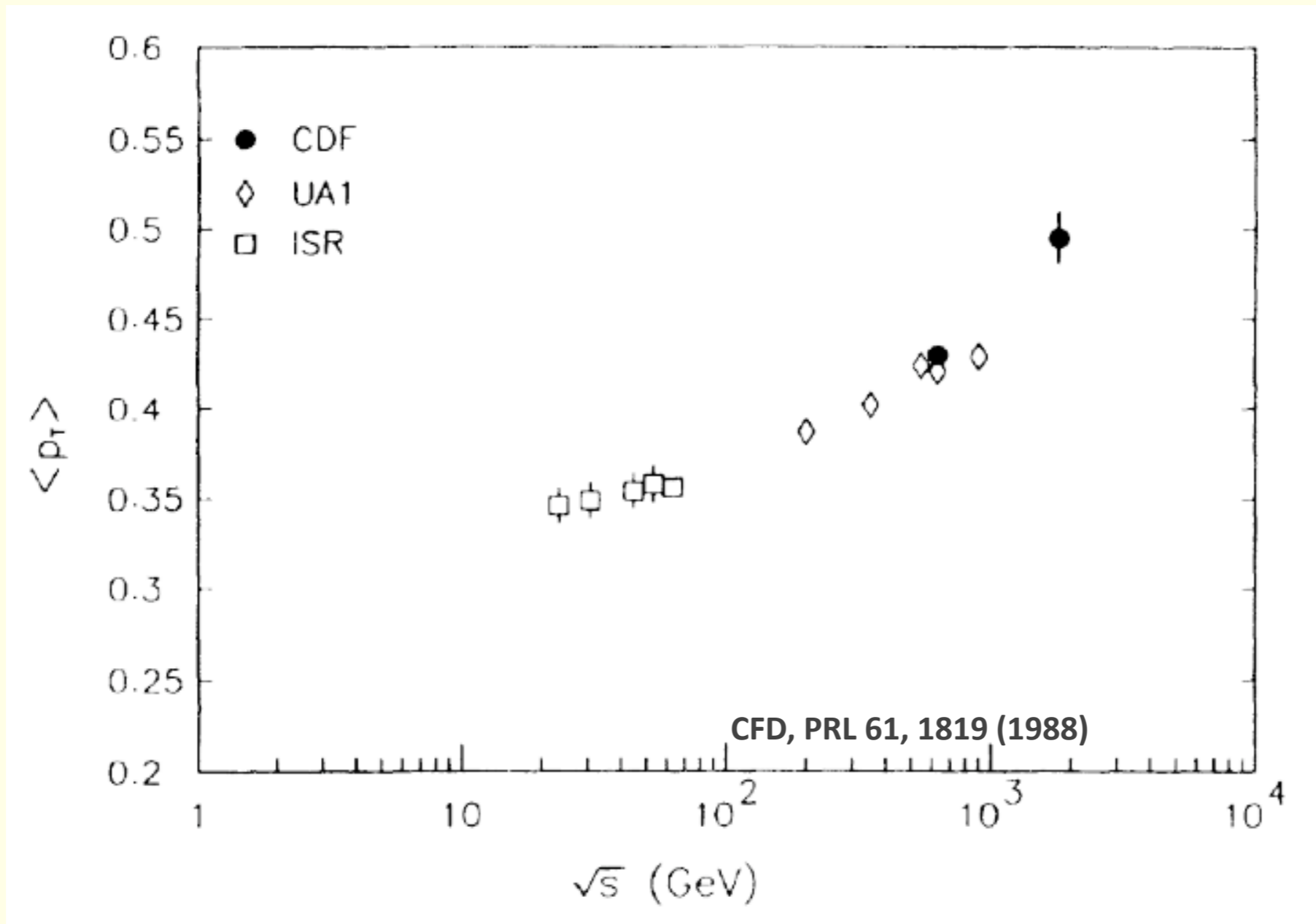
$$\frac{1}{p_T} \frac{dN_x}{dp_T} = A(\sqrt{s}) \cdot \frac{1}{p_T^n}$$

Average transverse momentum:

$$\langle p_T \rangle = \frac{\int_0^\infty p_T \frac{dN_x}{dp_T} dp_T}{\int_0^\infty \frac{dN_x}{dp_T} dp_T} \approx 300 - 400 \text{ MeV}/c$$

Largely independent of \sqrt{s} (for $\sqrt{s} < 200$ GeV)

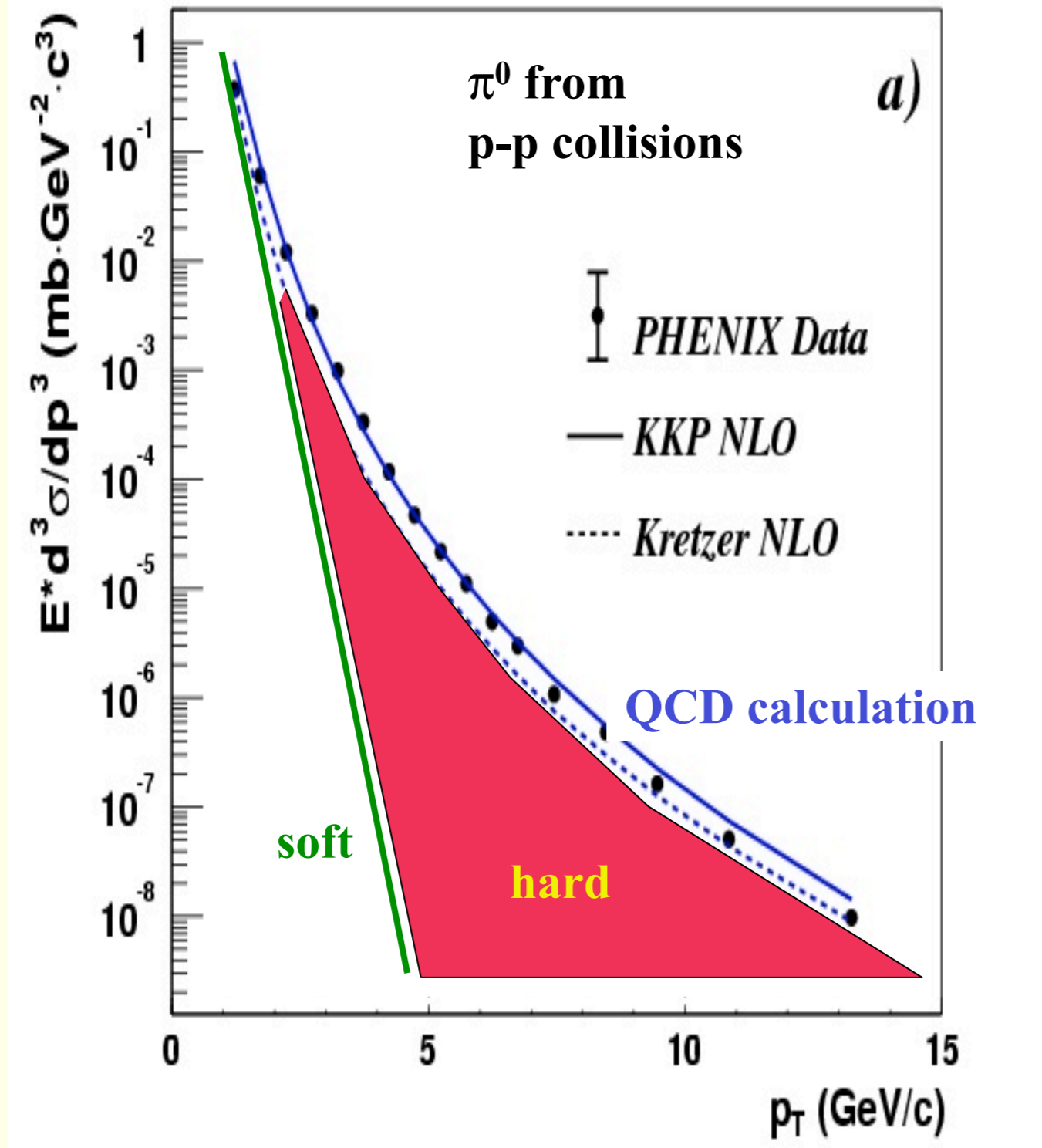
$\langle p_T \rangle$ vs. \sqrt{s} in p+p(bar p)



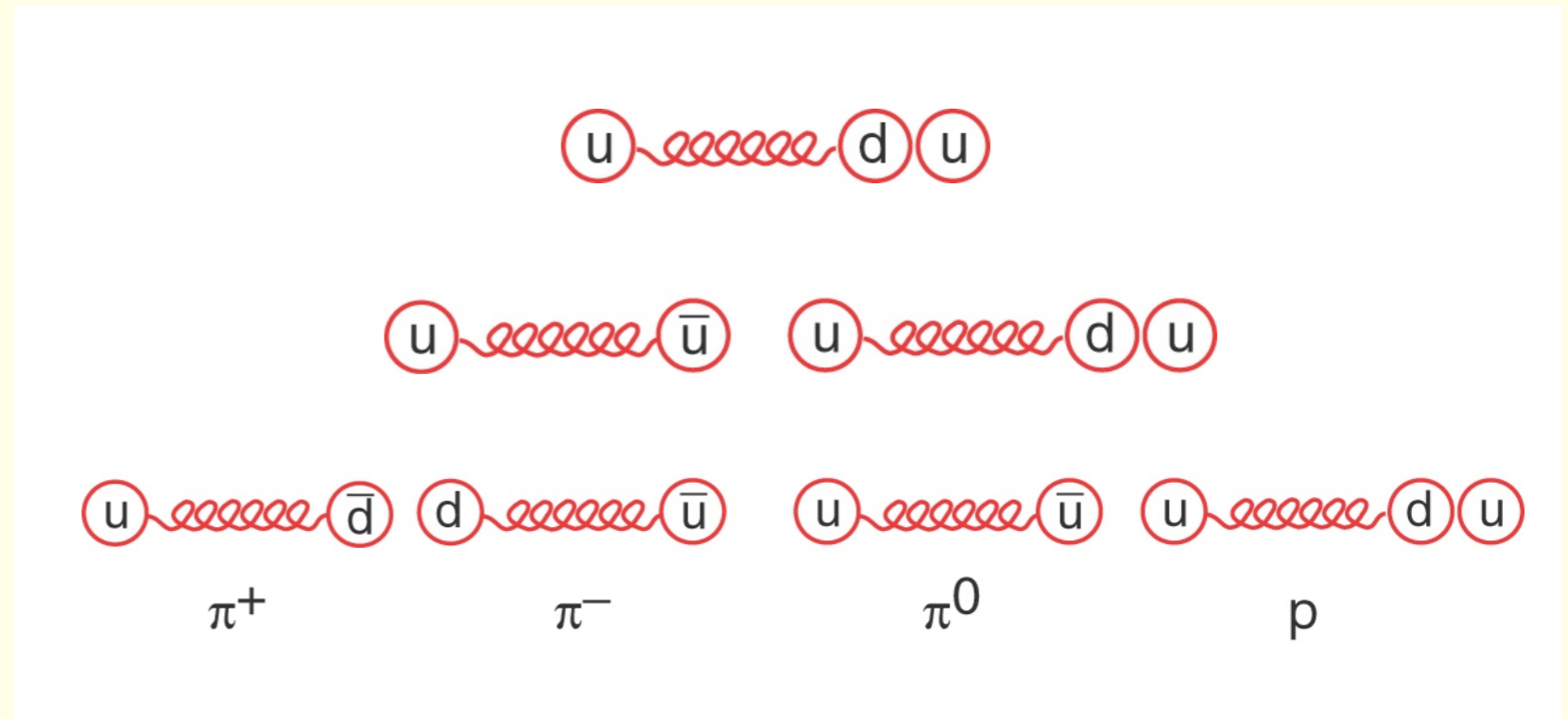
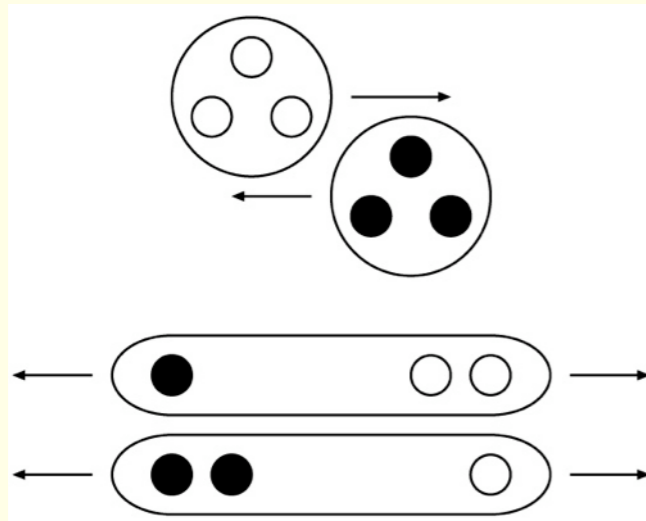
Increase of $\langle p_T \rangle$ reflects increase in hard scattering

Particle Production at High p_T (II)

Hard vs. soft particle production



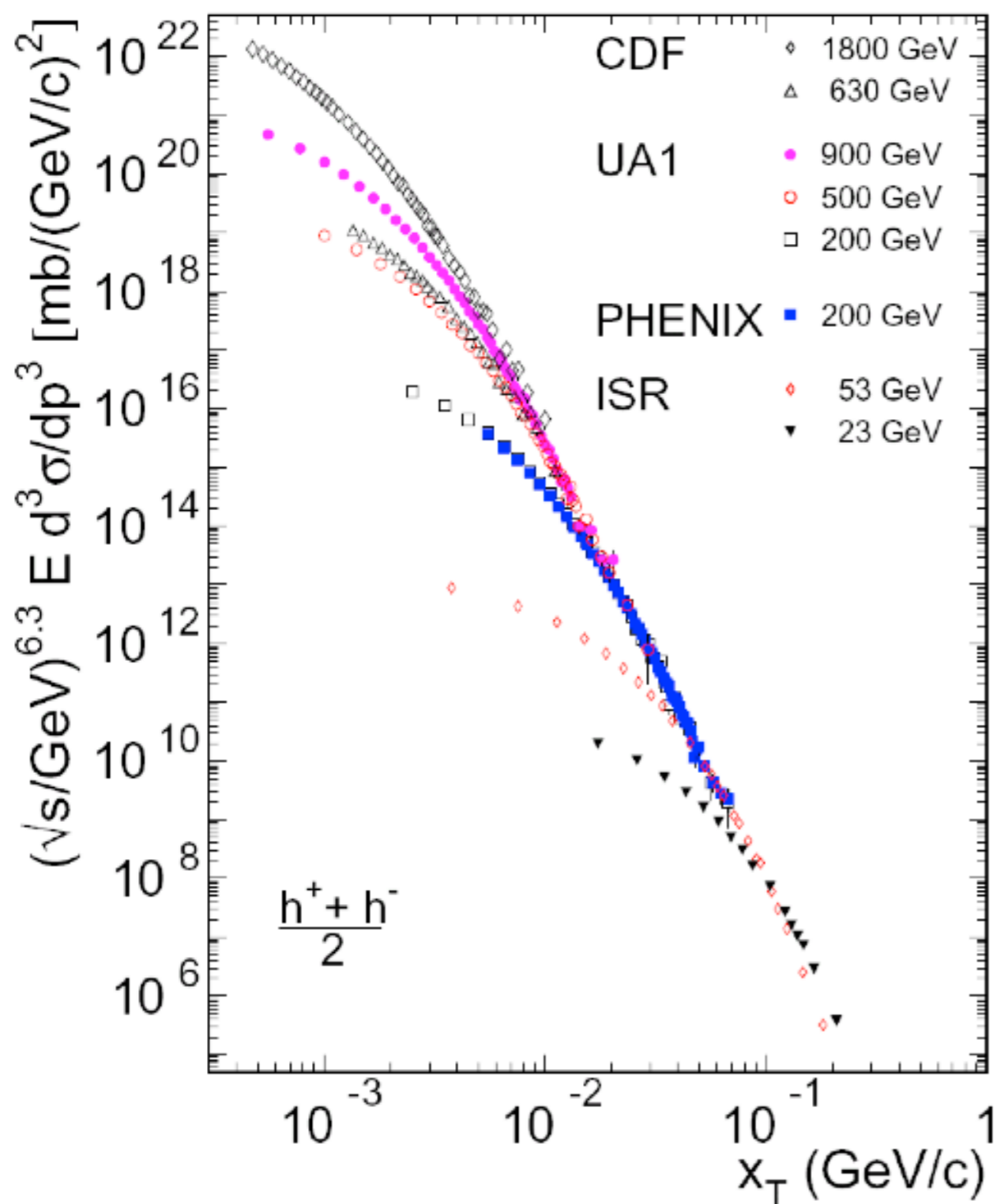
A Model for Particle Production at Low p_T in Nucleon-Nucleon Collisions: String Fragmentation



String fragmentation models explains:

- \sqrt{s} independence of the p_T of produced particles ($p_T \sim 350 \text{ MeV}/c$) („string breaking is a local process“)
- Shape of the rapidity distribution of produced particles, in particular the plateau at mid-rapidity

Where is the Transition from Soft to Hard Particle Production?



Scaling expected for parton-parton scattering with high momentum transfer (hard scattering):

$$E \frac{d^3 \sigma}{dp^3} = \frac{1}{\sqrt{s}^{n(x_T, \sqrt{s})}} G(x_T)$$

$$x_T = \frac{2p_T}{\sqrt{s}}$$

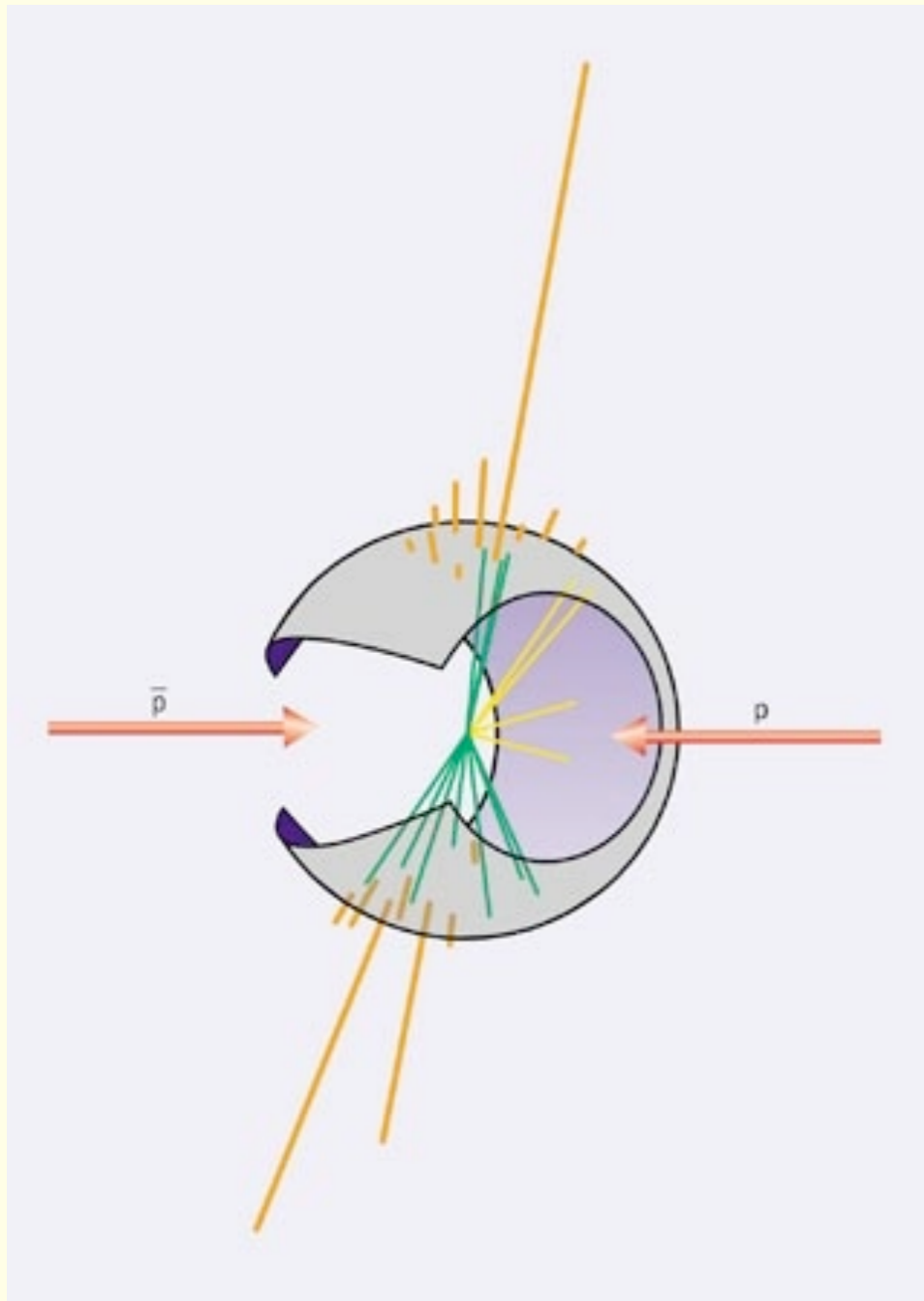
x_T at which scaling behavior is observed decreases with increasing \sqrt{s} .

Upshot: Particle production dominated by hard processes for

$$p_T > \sim 2 \text{ GeV}/c$$

3.3 Jets in Nucleon-Nucleon Collisions

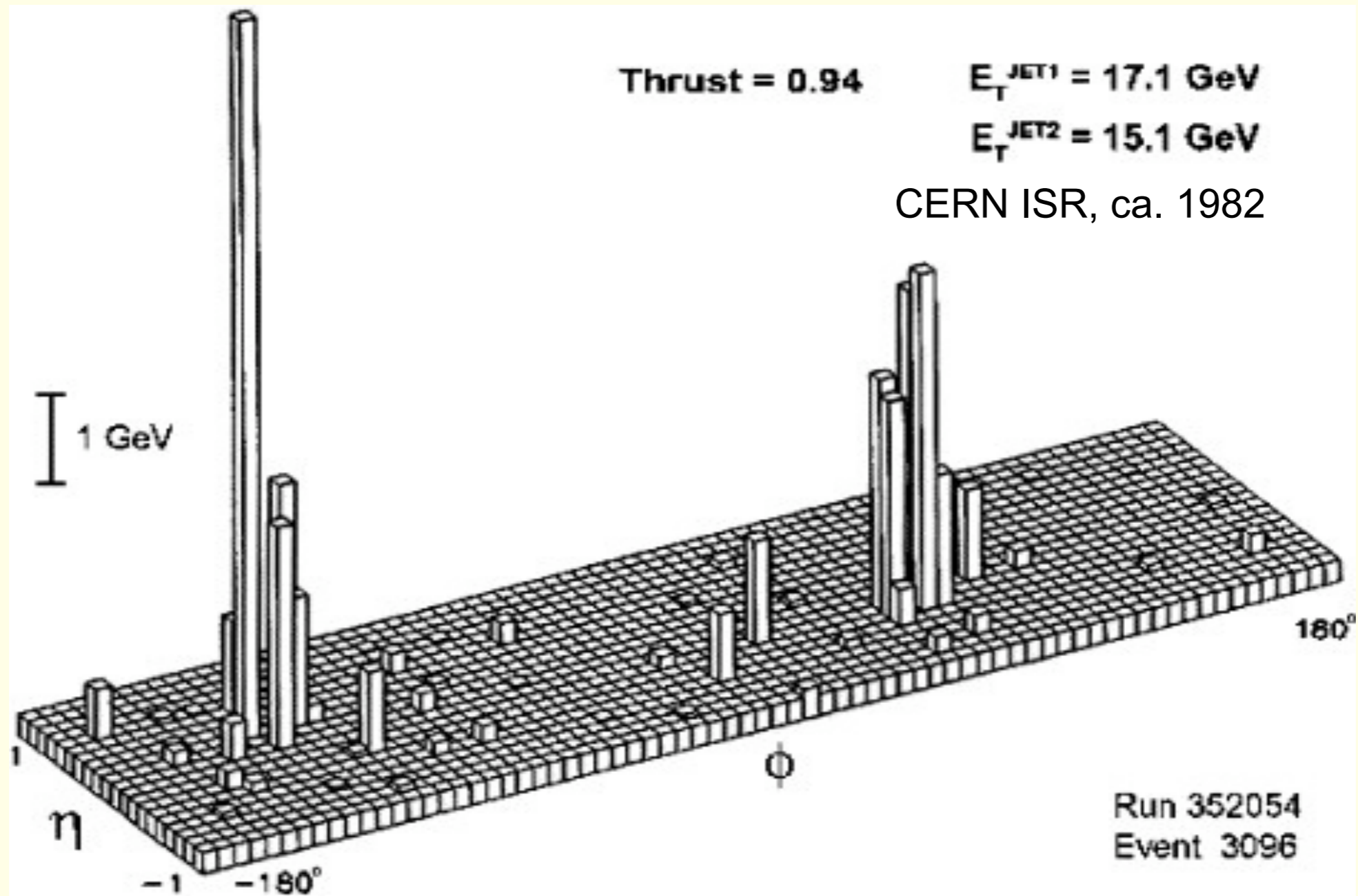
Jets and Hard Scattering in p+p



UA2 two-jet event, ca 1982

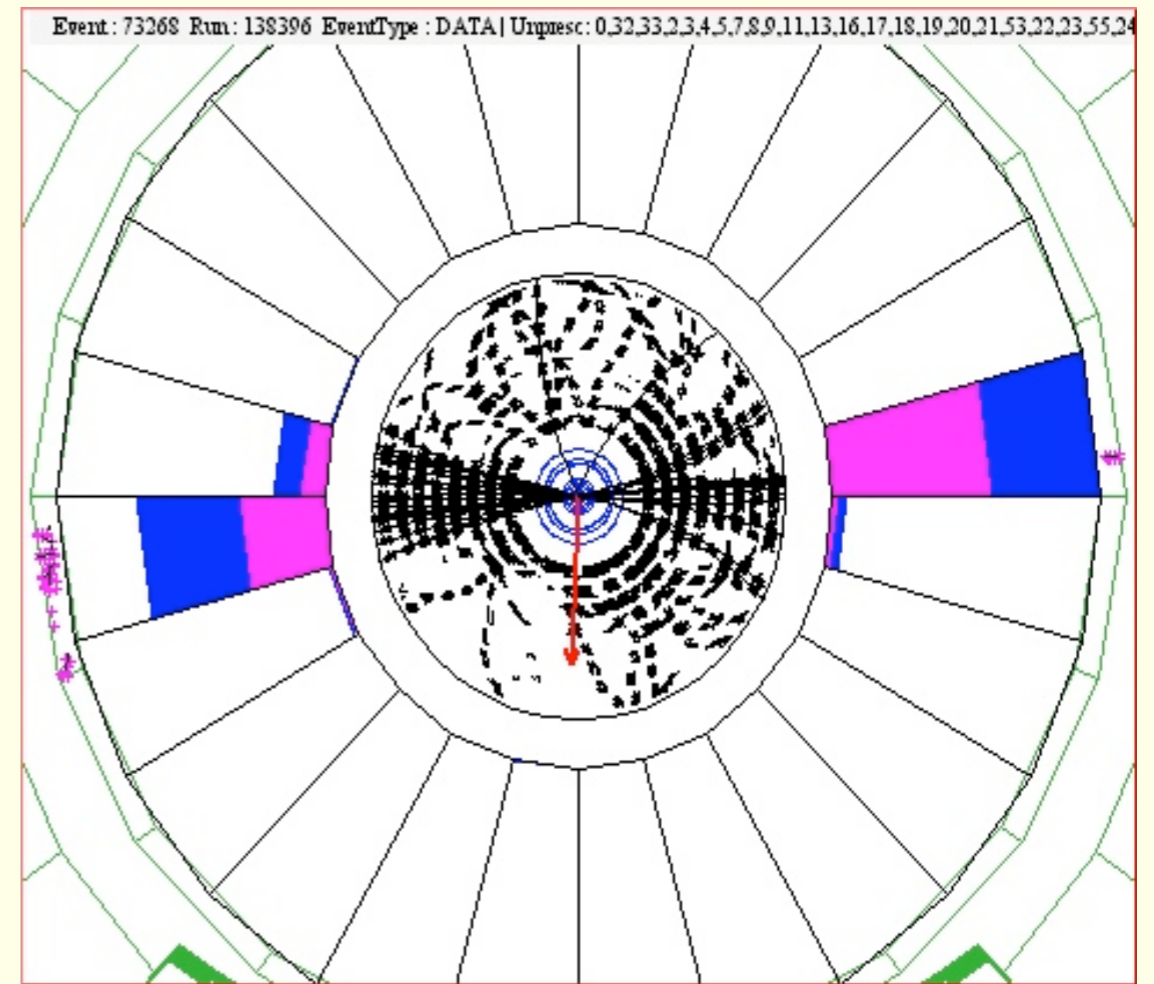
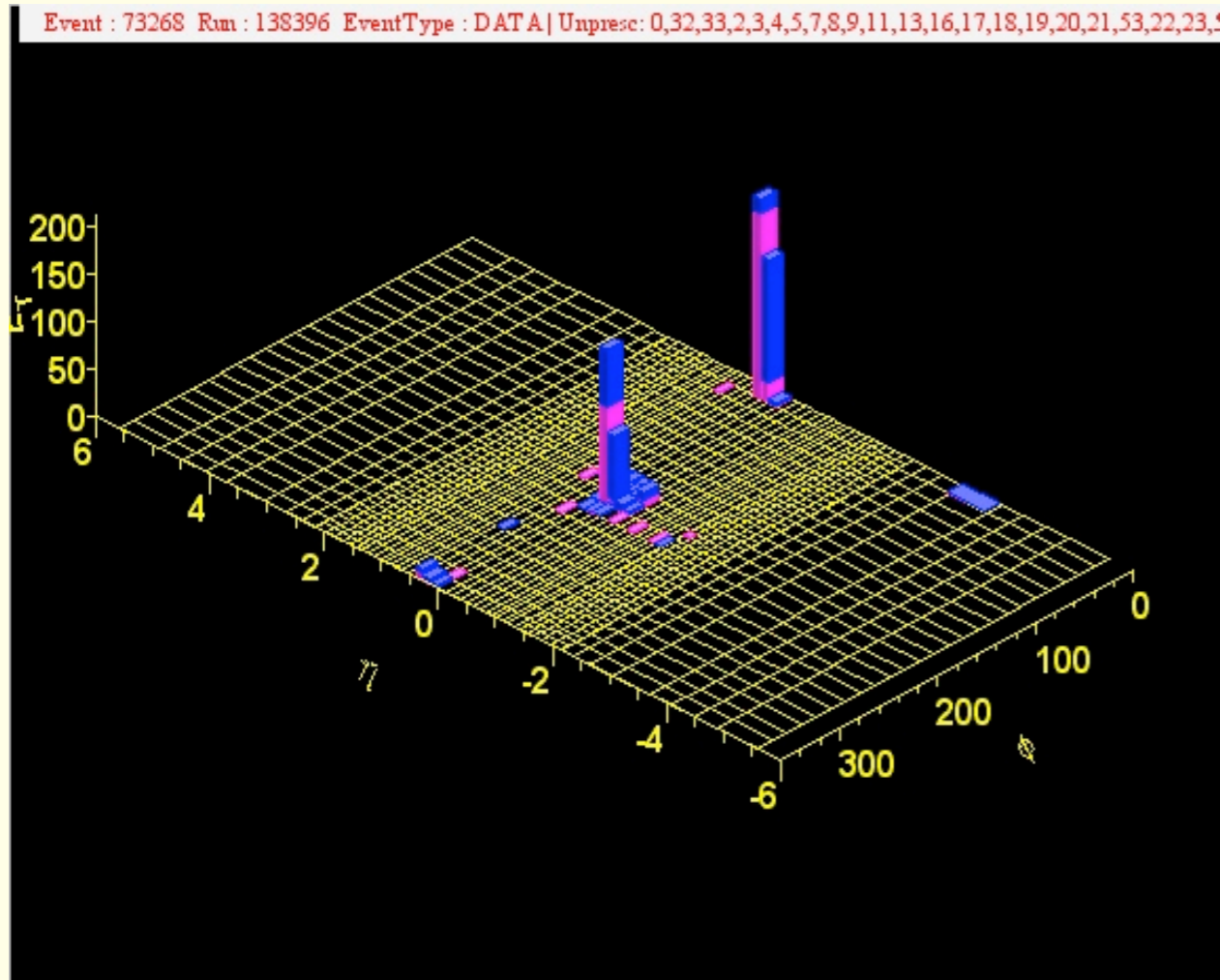
- Jets in p+p were discovered in the late seventies, early eighties
- Confirmation of QCD
- Note: jet cross section small (a typical „minimum bias“ event looks different)

Jet Event in a p+p Collision at $\sqrt{s} = 63$ GeV

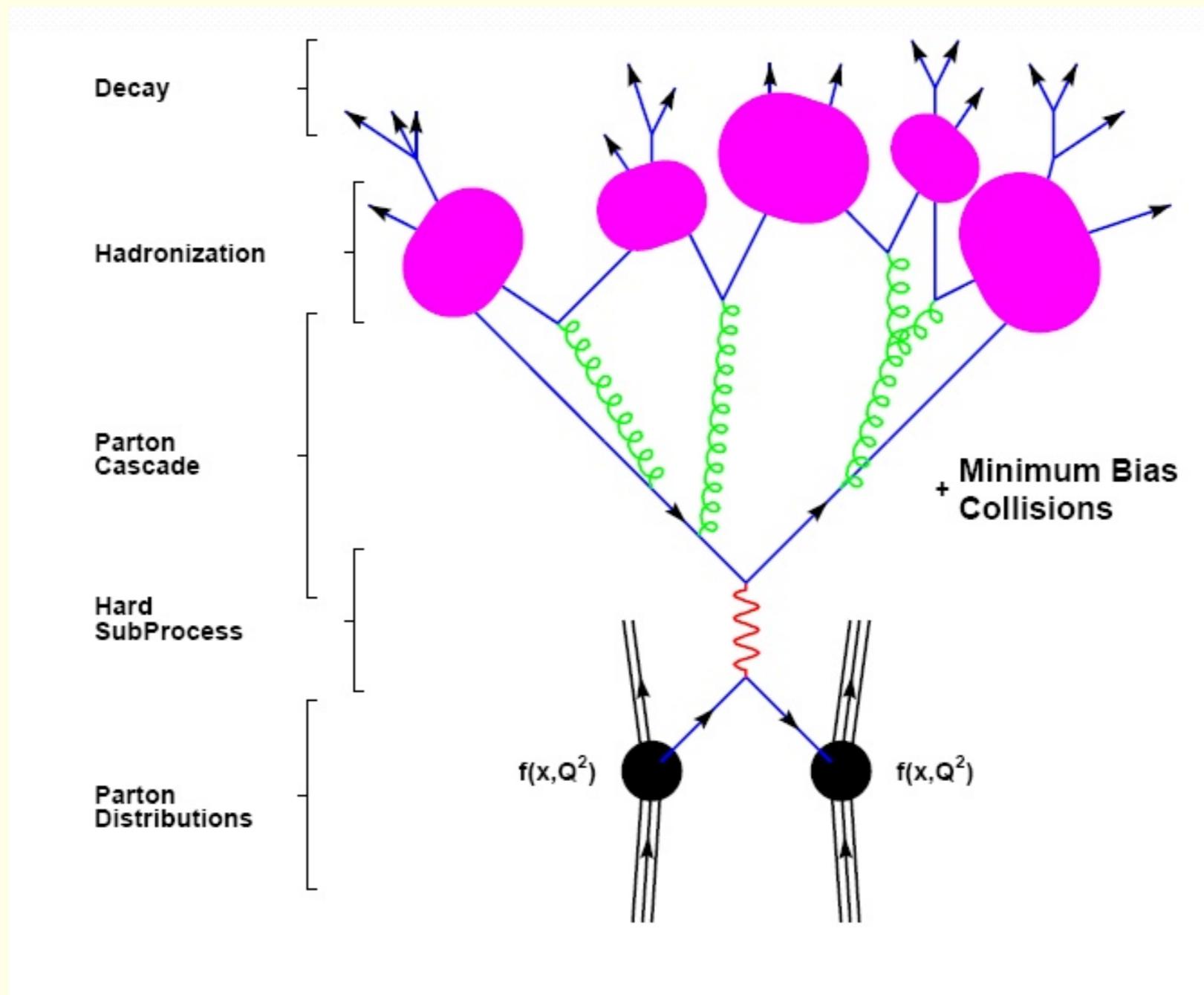


Lego plot shows energy vs. pseudorapidity η and azimuthal angle ϕ

Jet Event at the Tevatron



Evolution of a Jet Event



Hard Process → Parton Cascade → Hadronization

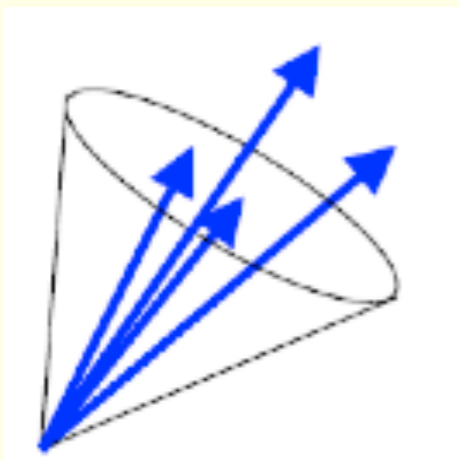
describable with pQCD

not describable with pQCD
(only phenomenological models)

Jet-Finding Algorithms

- **Objective:** reconstruct energy and direction of initial parton
- **Must be unambiguously applicable** at level of experimental data (tracks/towers) and in perturbative QCD calculation (parton level)
- **Starting point:** list of calorimeter towers and/or charged hadron tracks
- **Two classes of algorithms:**
 - ▶ **Cone algorithm:** traditional choice in hadron-hadron collisions
 - ▶ k_T algorithm: traditional choice in e^+e^- collisions

Cone algorithm:

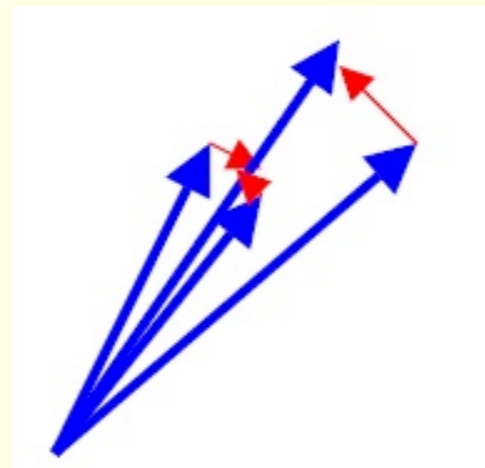


Sum content in
cone with radius

$$R = \sqrt{(\Delta\eta)^2 + (\Delta\phi)^2}$$

Typical choice:
 $R = 0.7$

k_T algorithm:



Successively merge
“particles” in order of
relative transverse
momentum.

Termination of merging
controlled by a
parameter D

- (Normally) start with seed (e.g. calorimeter module with high energy)
- Consider all particles in cone around seed and calculate

$$\eta^C = \frac{\sum_{i \in C} E_T^i \eta^i}{E_T^C}, \quad \phi^C = \frac{\sum_{i \in C} E_T^i \phi^i}{E_T^C} \quad (E_T = E \sin \vartheta)$$

- Repeat this procedure with new cone center (η^C, ϕ^C)
- Terminate when “flow” of cone center stops
- Calculate jet energy as

$$E_T^C = \sum_{i \in C} E_T^i$$

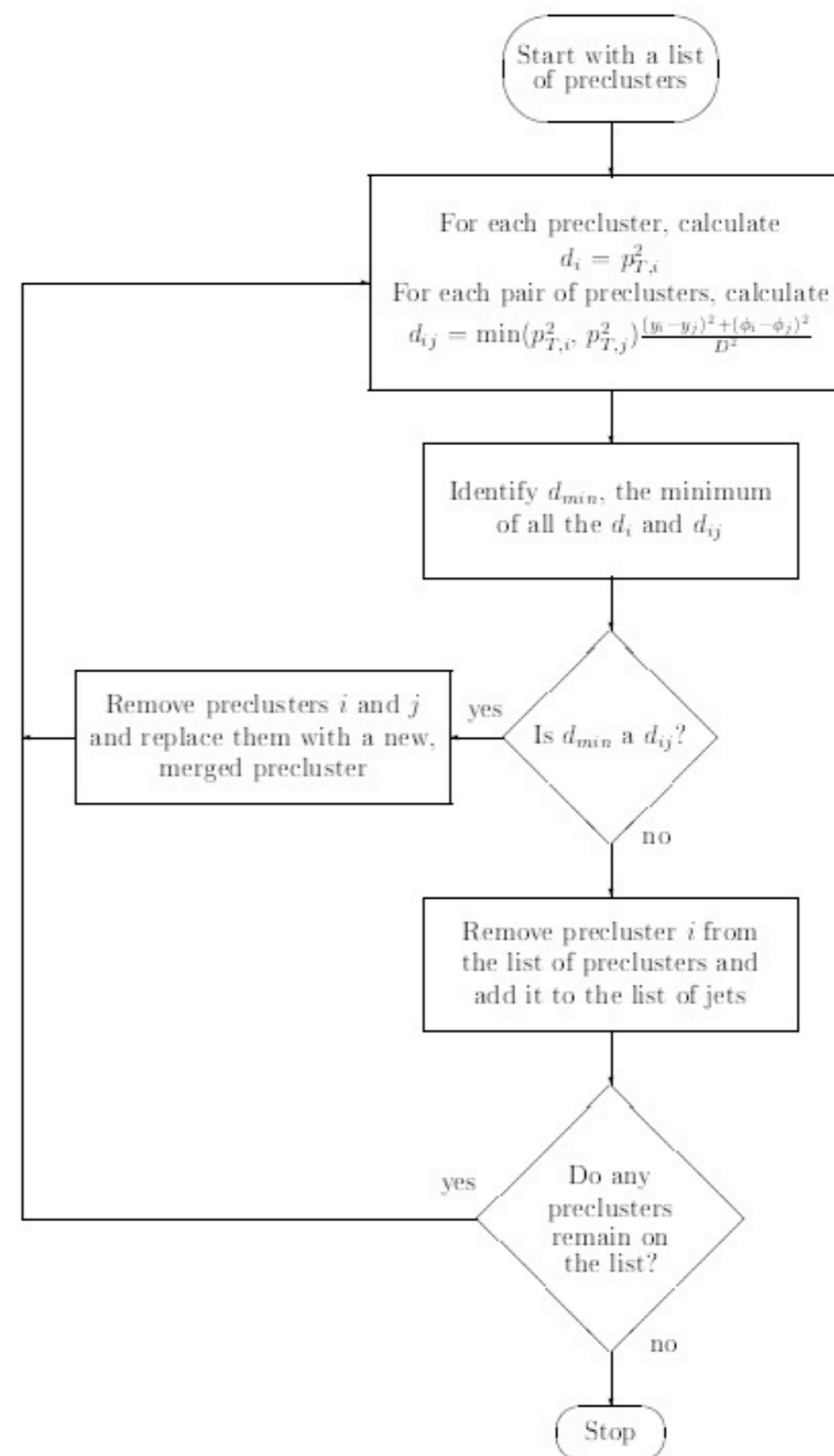
- A particle may belong to two cones:
split energy among jets
- Subtract background energy from underlying event

k_T Algorithm (I)

- Algorithm starts with a list of preclusters (calorimeter cells, particles, or partons)
- Calculate p_T and rapidity y for each precluster
- For each precluster define $d_i = p_{T,i}^2$
- For each pair (i,j) of preclusters define

$$d_{ij} = \min(p_{T,i}^2, p_{T,j}^2) \frac{\Delta\mathcal{R}_{ij}^2}{D^2}$$
$$= \min(p_{T,i}^2, p_{T,j}^2) \frac{(y_i - y_j)^2 + (\phi_i - \phi_j)^2}{D^2}$$

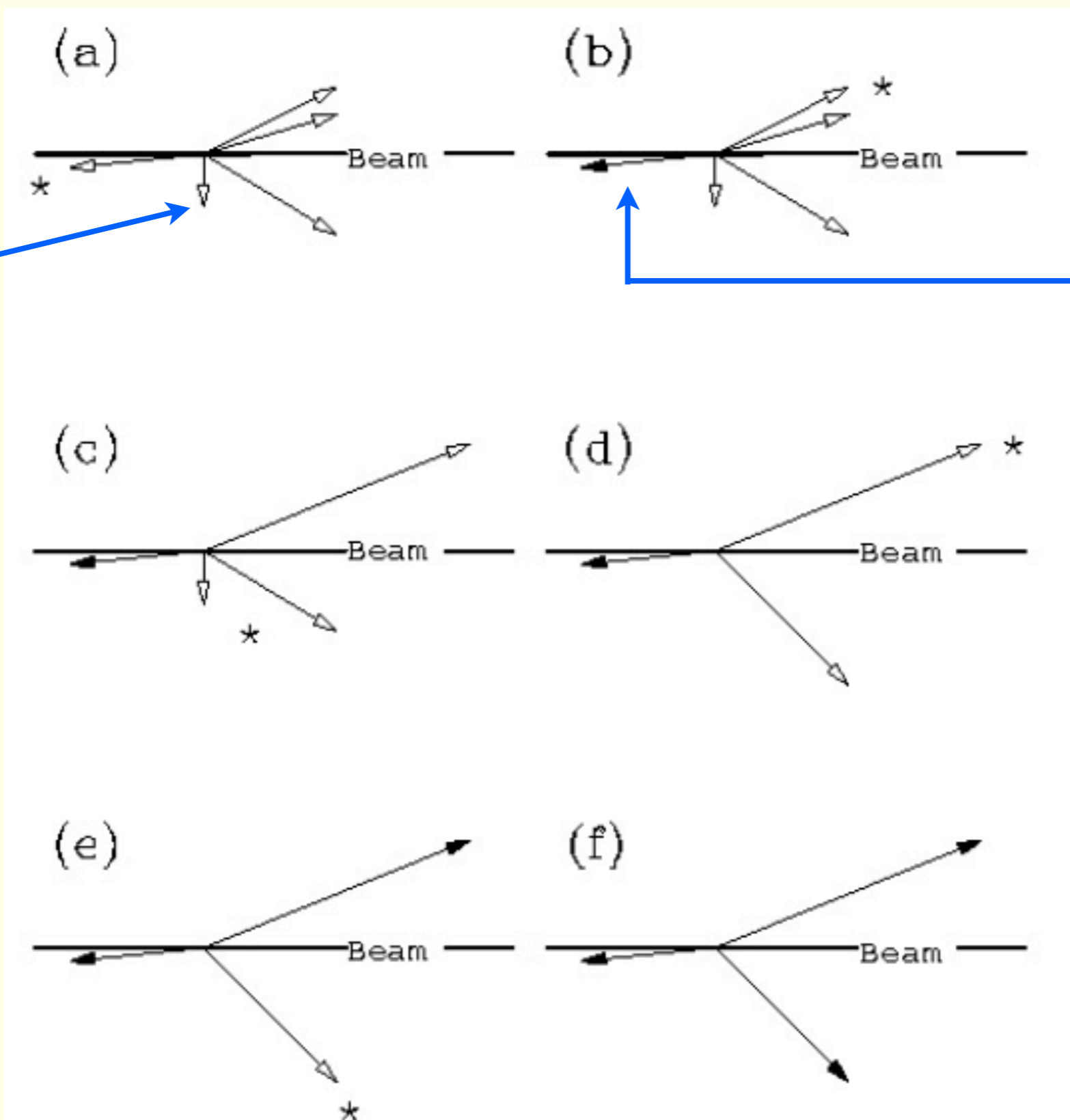
- For $D = 1$ and $\Delta R_{ij}^2 \ll 1$, d_{ij} is the minimal transverse momentum k_T (squared) of one vector with respect to the other
- Find minimum d_{\min} of all d_i and d_{ij}
- Merge preclusters i and j if d_{\min} is a d_{ij}
- Else: Remove precluster i with $d_{\min} = d_i$ from list of preclusters and add it to the list of jets
- Repeat until list of preclusters is empty



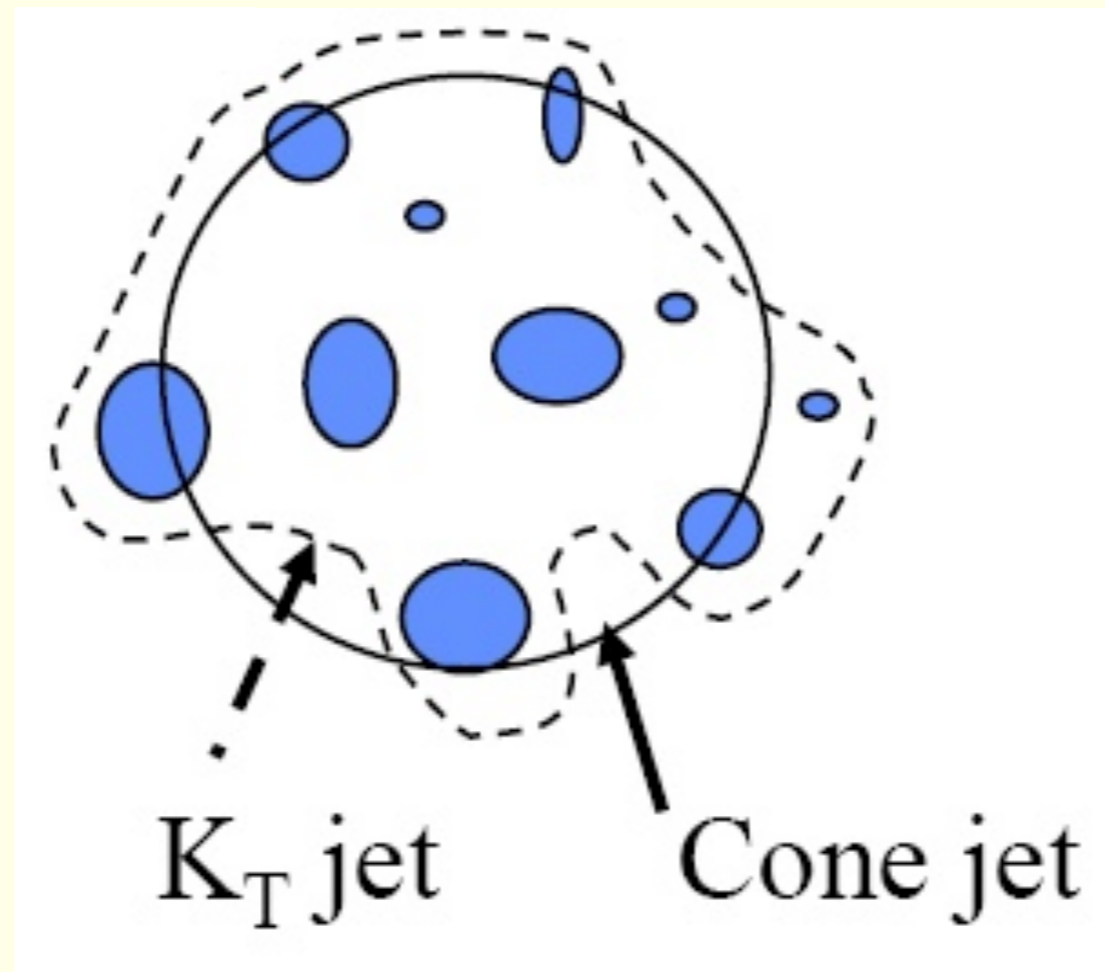
k_T Algorithm (II): A Simple Example

open arrows:
preclusters

closed arrows:
jets



Why the k_T Algorithm is Typically only used in e^+e^- Collisions?

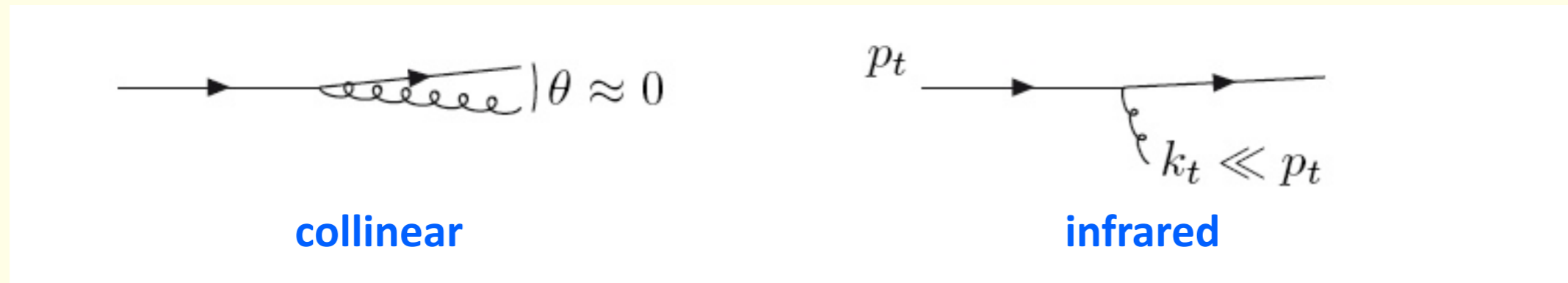


k_T jet has no fixed shape/area

→ Difficult to subtract background from underlying event

Jet Finding Algorithms: Typical Requirements (I)

Two types of divergences:

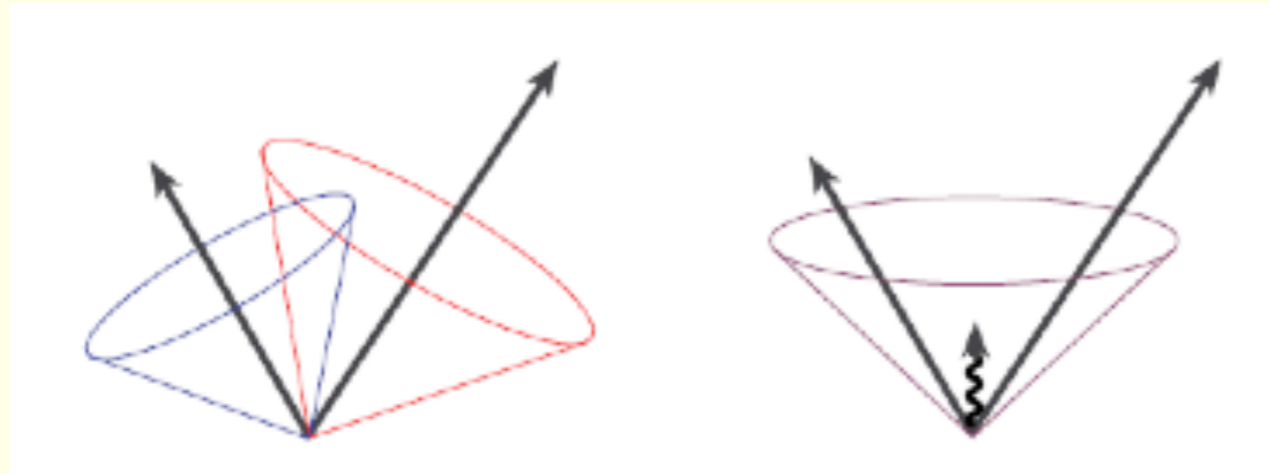


The reconstructed jets should not change in case of

- collinear splitting, i.e., if one parton is replaced by two partons at the same place
- soft emission, i.e., if a low energy parton is added

Jet Finding Algorithms: Typical Requirements (II)

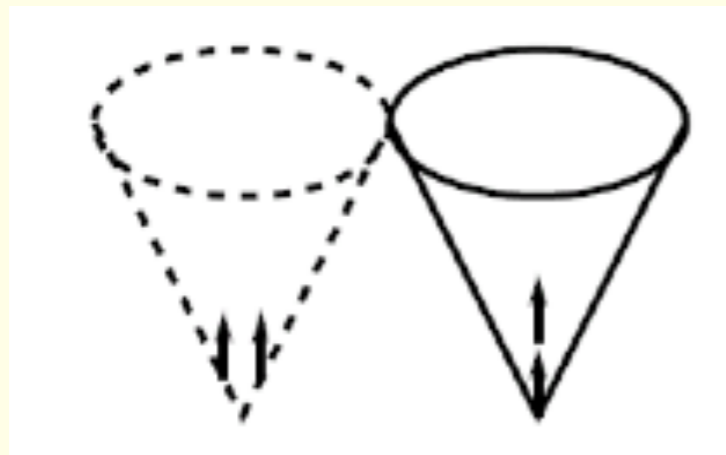
- **Infrared safety**



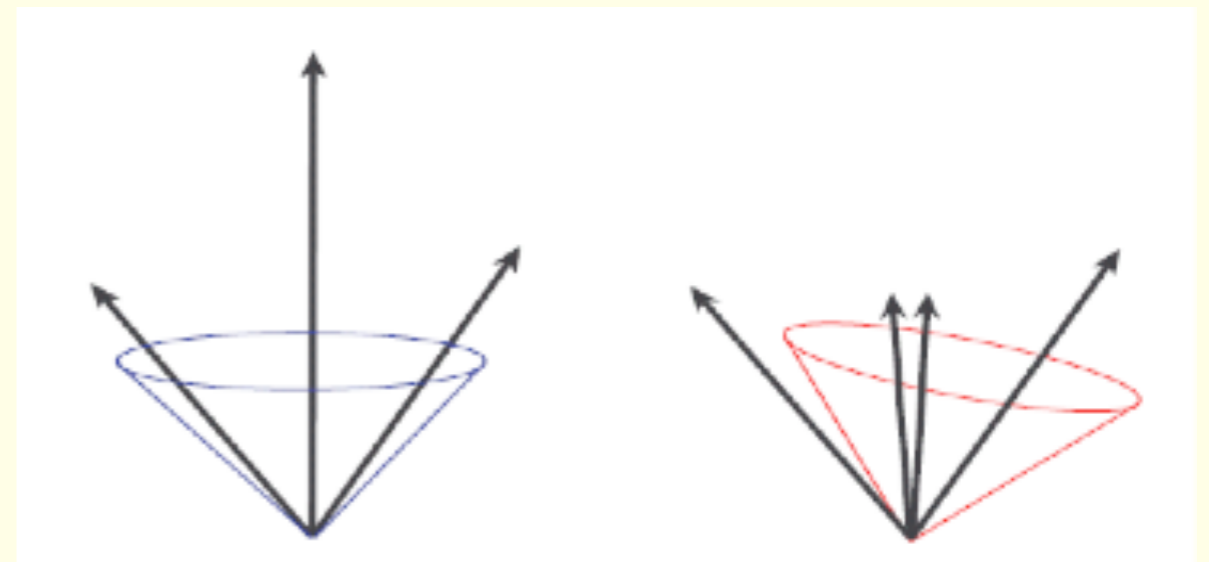
Fermilab Run II jet physics: hep-ex/0005012

Example of infrared sensitivity:
Soft radiation (right plot) causes
merging of jets which would
have been separated otherwise

- **Collinear safety**

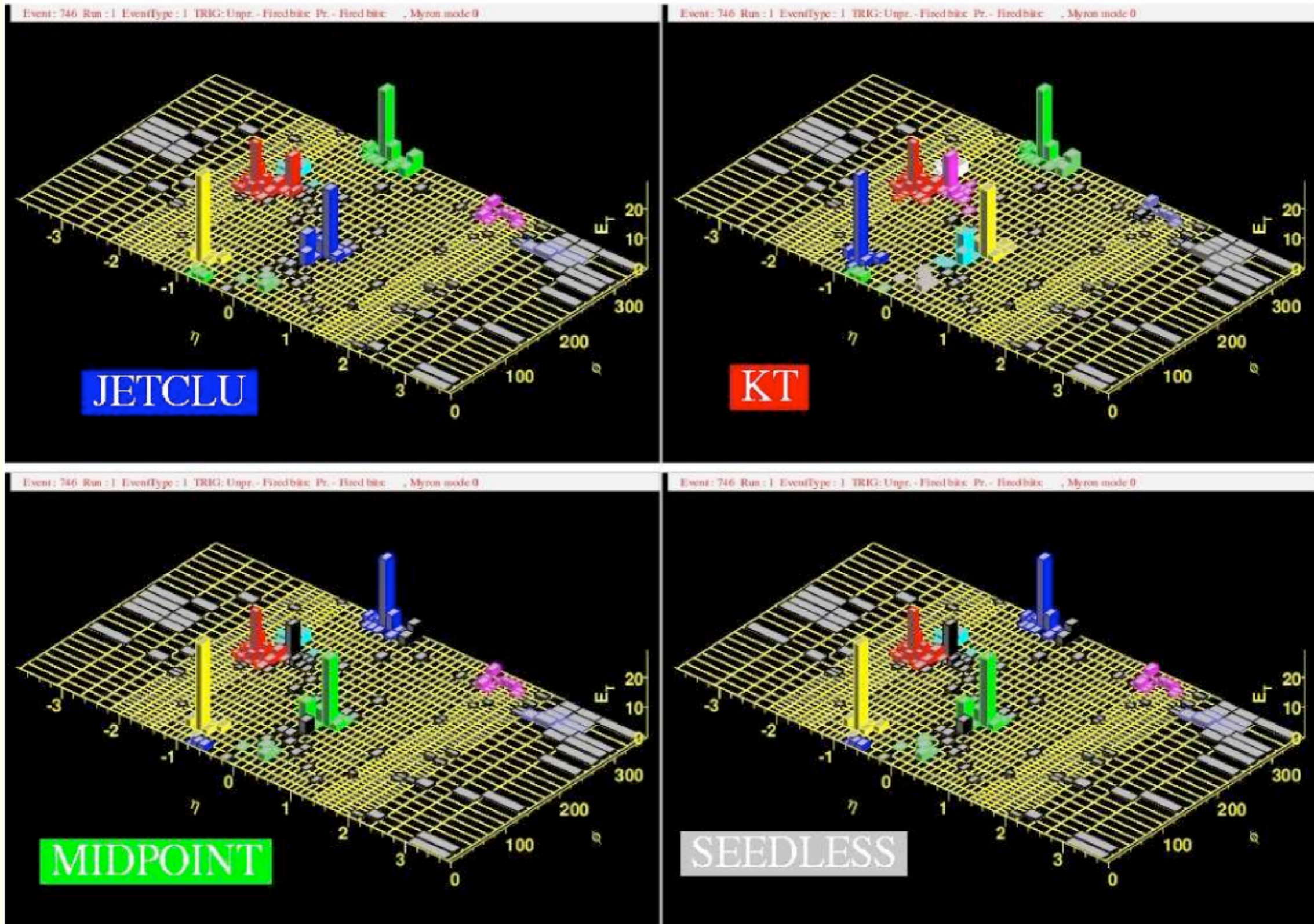


Example of collinear sensitivity:
Seed and therefore jet not found
in left picture



Example of collinear sensitivity:
Reconstructed jet depends on seed

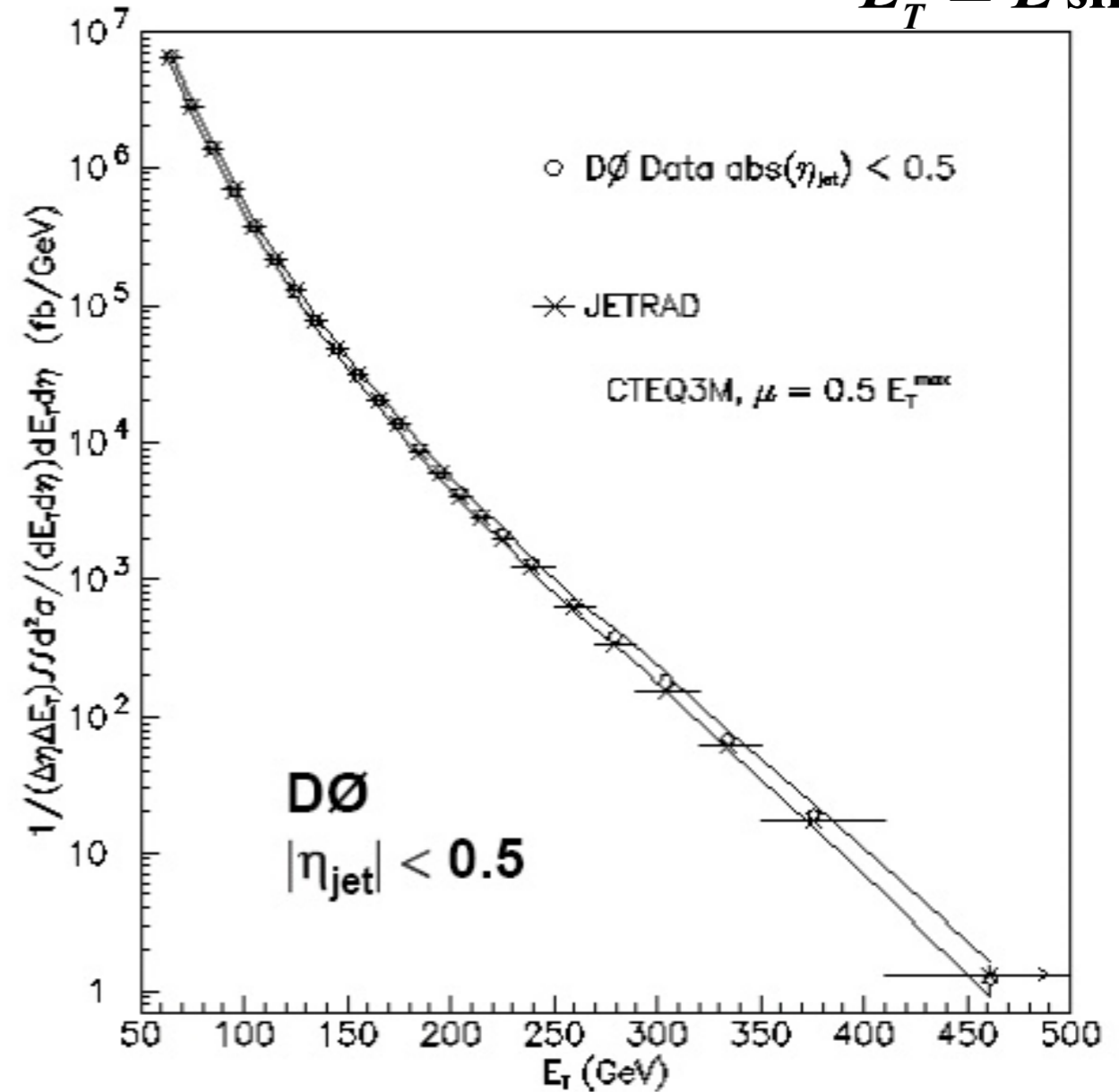
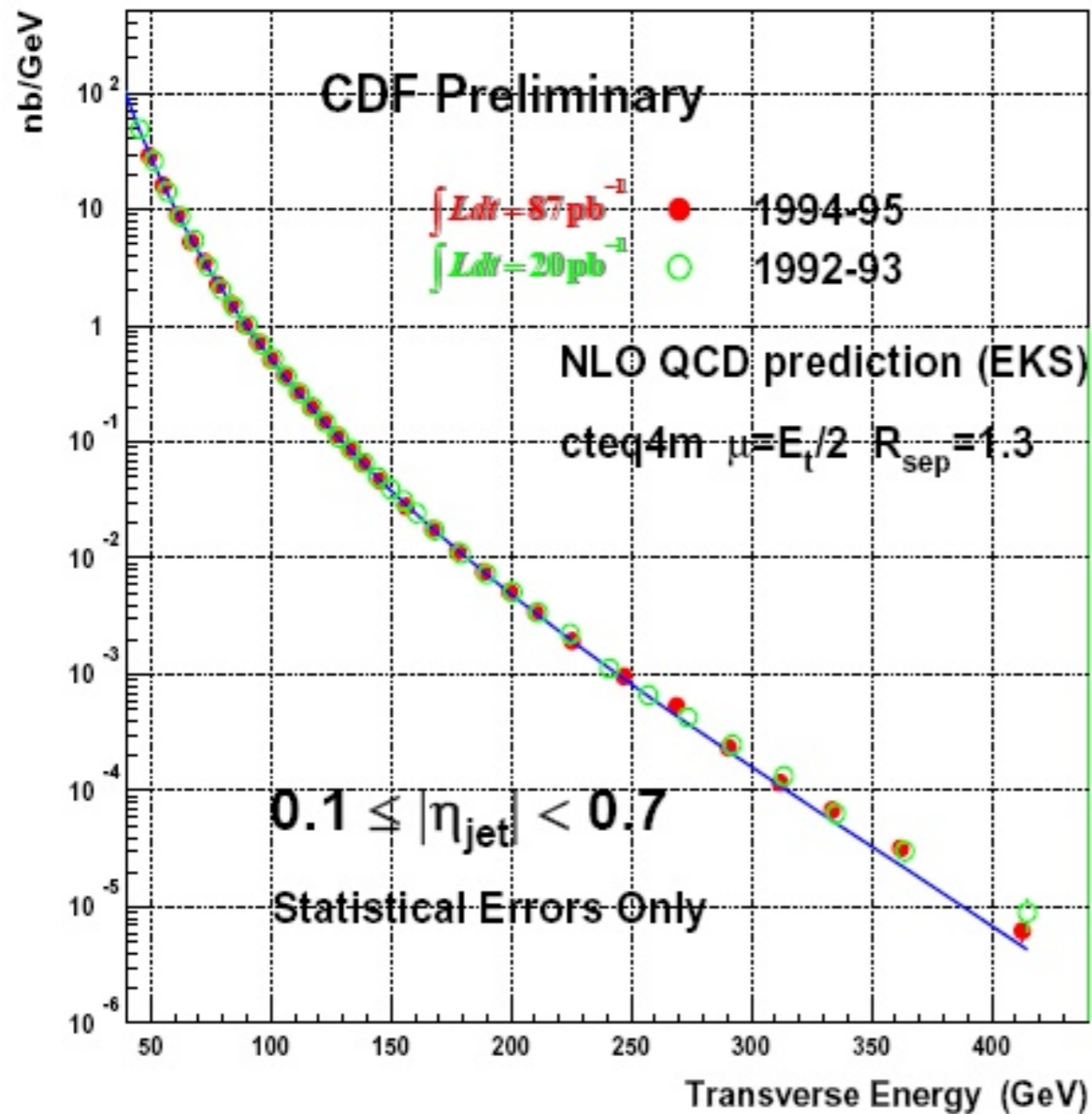
Jet Ambiguities: Different Algorithms Find Different Jets



Jet Cross Sections at the Tevatron

http://www-d0.fnal.gov/Run2Physics/displays/presentations/klima_lecture_jan2003/Lecture_1.pdf

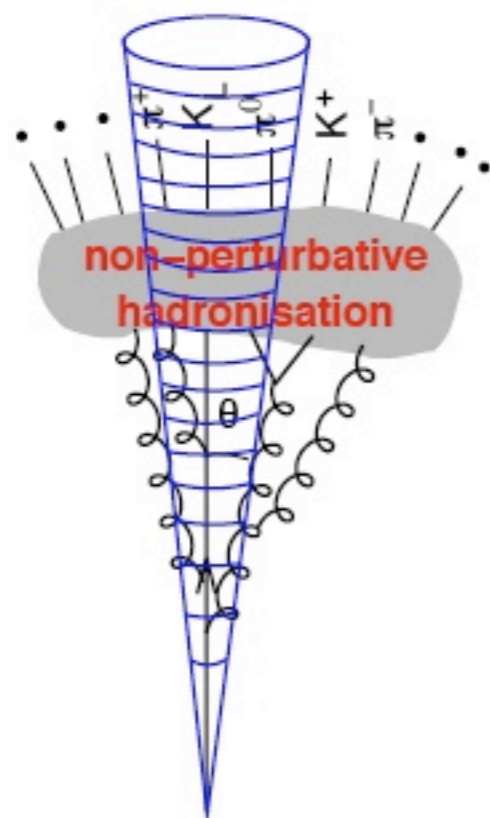
$$E_T = E \sin \vartheta$$



Pretty good agreement between data and NLO pQCD predictions

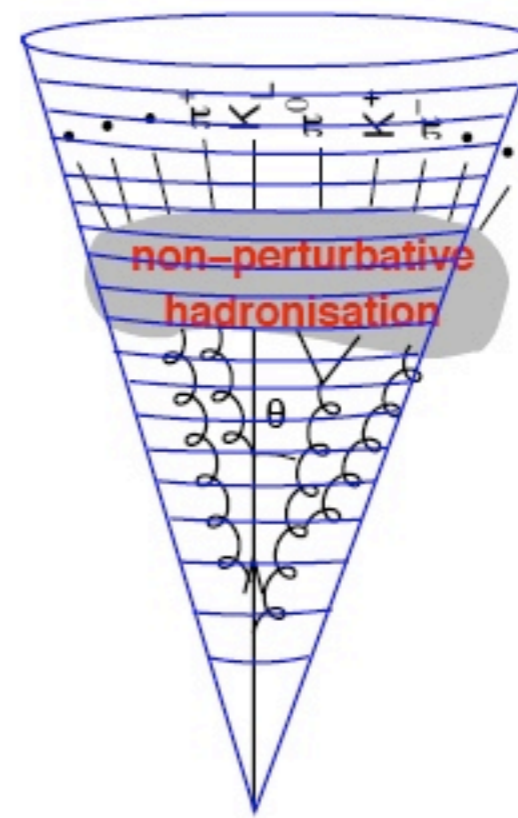
Choice of the Optimal Cone Radius

Small jet radius



Small cone radius:
Small background from the underlying event at the expense of some loss of jet particles

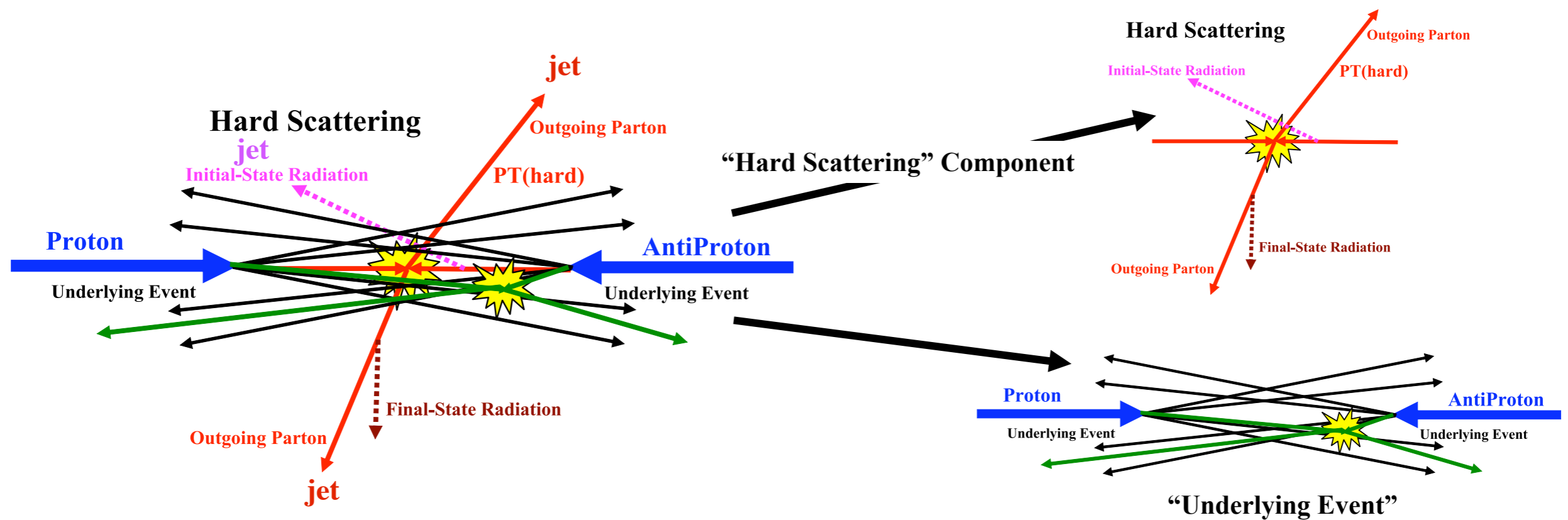
Large jet radius



Large cone radius:
Large background from the underlying event but nearly all jet particles included

Due to higher backgrounds the cone radius in heavy-ion collisions typically smaller than in p+p

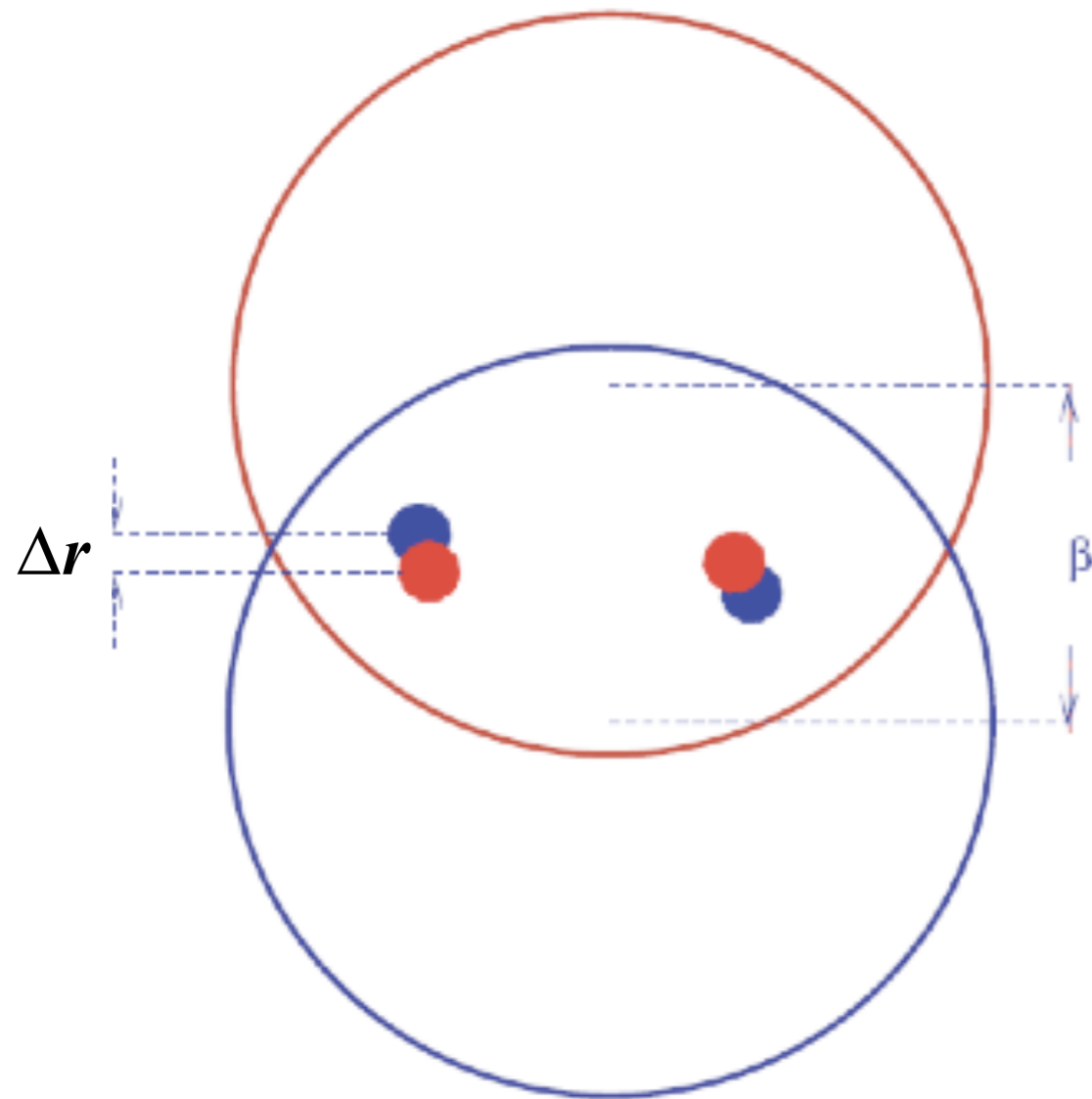
Underlying Event (UE)



Rick Field: <https://agenda.infn.it/conferenceDisplay.py?confId=599>

- The hard scattering component (the „signal“):
 - ▶ $2 \rightarrow 2$ (sometimes $2 \rightarrow 3$) parton-parton scattering
 - ▶ plus initial and final state radiation (however, sometimes also attributed to the UE)
- The “underlying event” consists of the “beam-beam remnants” and from particles arising from soft or semi-soft multiple parton interactions (MPI).

What are Multiple Partonic Interactions?



$$\Delta p_T^{\min} \cdot \Delta r \approx \hbar$$

$$\Delta r \approx \frac{\hbar c}{\Delta p_T^{\min} \cdot c} = \frac{0,2 \text{ GeV fm}}{\Delta p_T^{\min} \text{ (GeV)}}$$

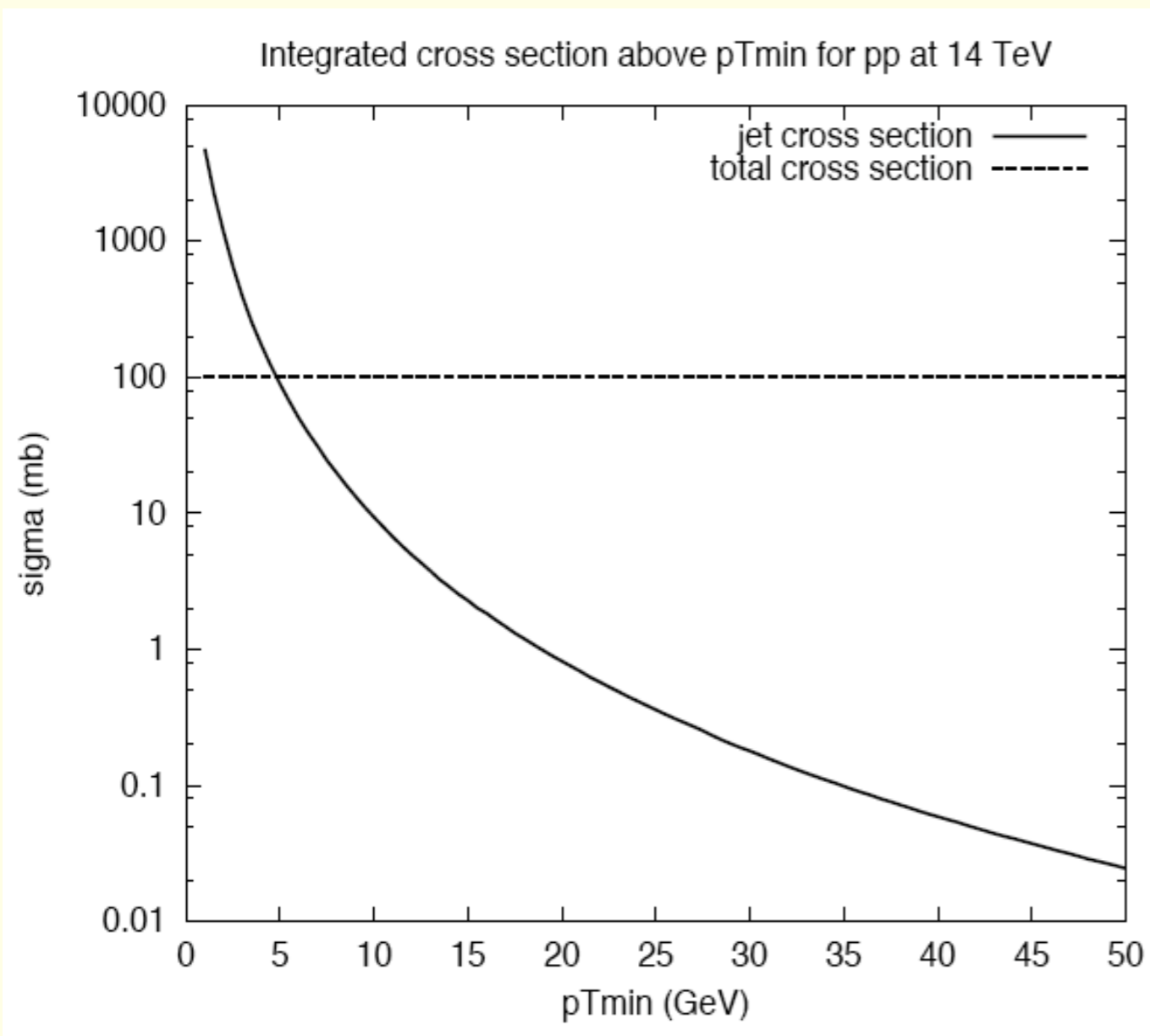
Multiple parton interaction:

- Two or more pairs of partons interacting in the same inelastic p+p collision
- Momentum transfer larger than some lower cut-off p_T^{\min} which establishes the hard scale
- p_T^{\min} should correspond to a transverse size much smaller than the overlap area
- Thus, the two interaction region are well separated in space and should contribute incoherently to the cross section

Multiple Partonic Interactions are Inevitable

Mini-jet cross section
diverges for $p_{\perp\min} \rightarrow 0$:

$$\sigma_{\text{int}}(p_{\perp\min}) = \int_{p_{\perp\min}}^{\sqrt{s}/2} \frac{d\sigma}{dp_{\perp}} dp_{\perp} \propto \frac{1}{p_{\perp\min}^2}$$



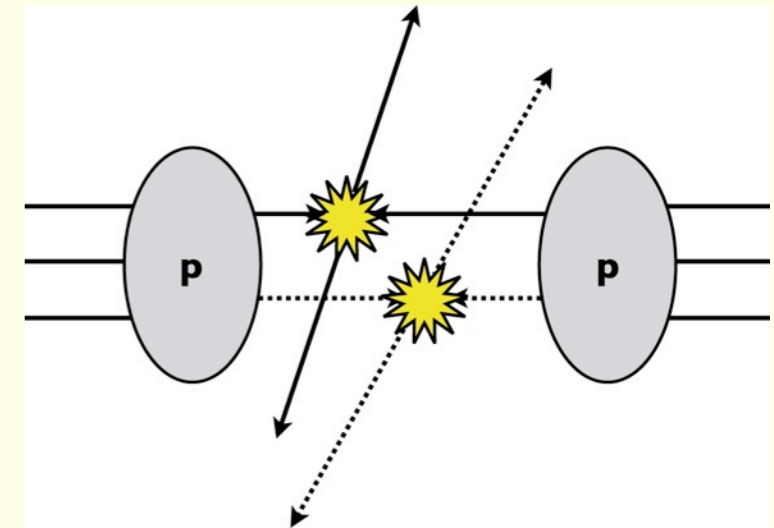
Even for scales $p_{\perp\min} \gg \Lambda_{QCD}$
one has $\sigma_{\text{int}}(p_{\perp\min}) > \sigma_{\text{tot}}$

The number of hard interactions
per p+p collisions is thus given by

$$\langle n_{\text{hard}} \rangle(p_{\perp\min}) = \frac{\sigma_{\text{int}}(p_{\perp\min})}{\sigma_{\text{tot}}}$$

Motivation for Studying Multiple Parton Interactions (I)

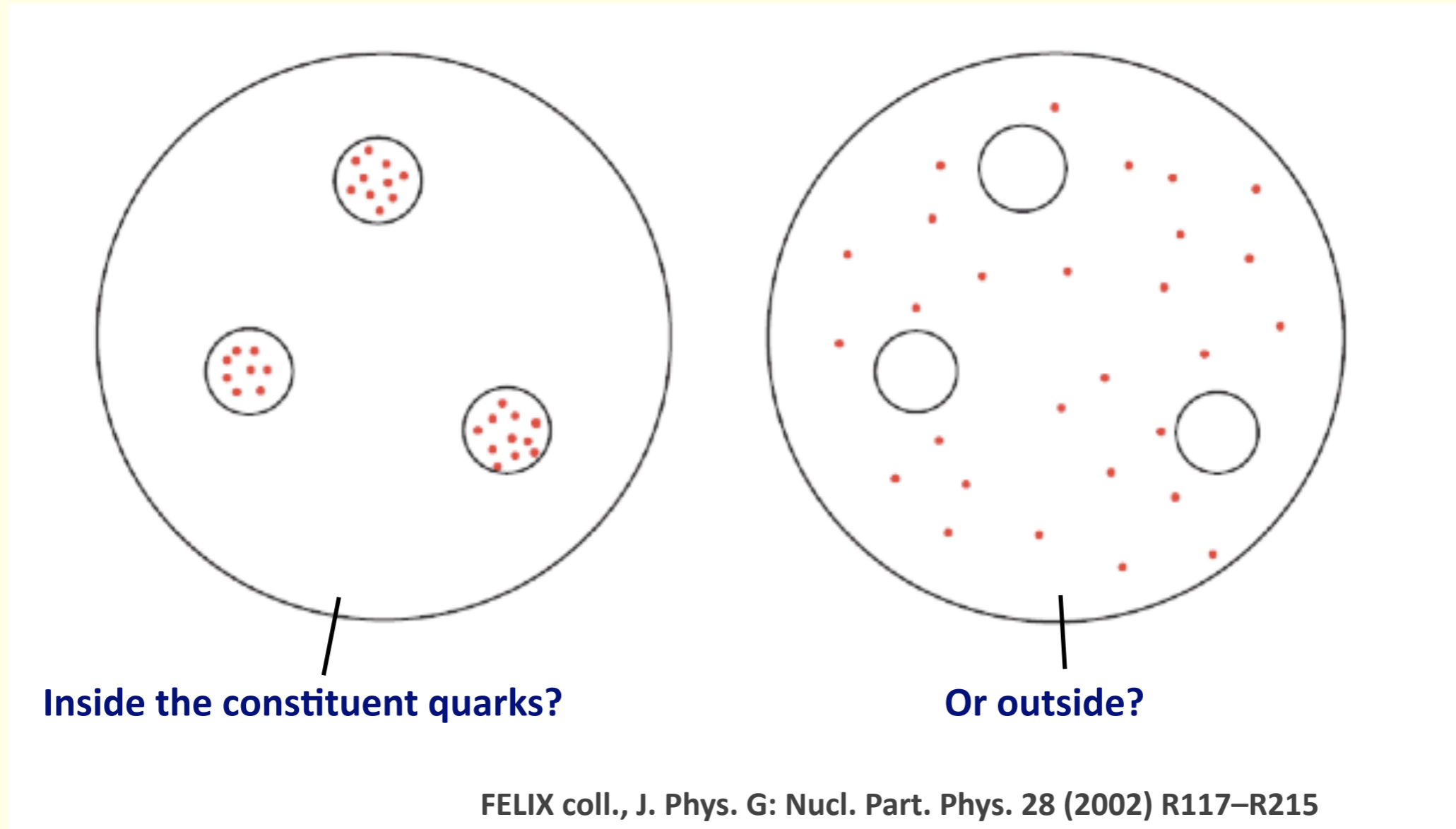
- Important for understanding of minimum bias p+p collisions at the Tevatron and the LHC
 - ▶ Tevatron: $\sim 2 - 6$ hard interactions per collision
 - ▶ LHC: $\sim 4 - 10$ hard interactions per collision
- Understanding of the “underlying event” important in specialized analyses, e.g., Higgs searches, jet production
 - ▶ Pedestal effect:
Events with high- p_T jets have more underlying activity than minimum-bias events
- Study distribution of the partons and parton correlations in the plane transverse to the beam axis



Motivation for Studying Multiple Parton Interactions (II)

Transverse Profile of the Proton:

Where are the sea quarks and gluons inside the proton in the plane transverse to the beam axis?

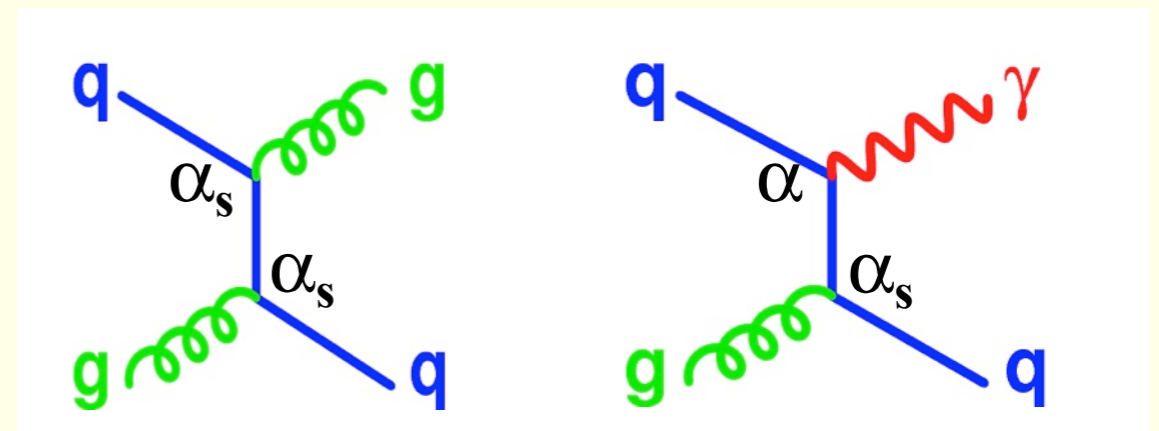


→ Study multiple parton interactions

3.4 Direct Photons

Direct Photons

- **Direct photons:**
Photons emerging from parton-parton scattering
(as opposed to hadron decay photons)
- No complication due to parton-to-hadron fragmentation at the expense of smaller cross section
- Direct Photons allow to test QCD
- Sensitive to gluon distribution in the proton at leading order
(though this turns out to be difficult largely due to theoretical uncertainties and some possible inconsistencies in the data)

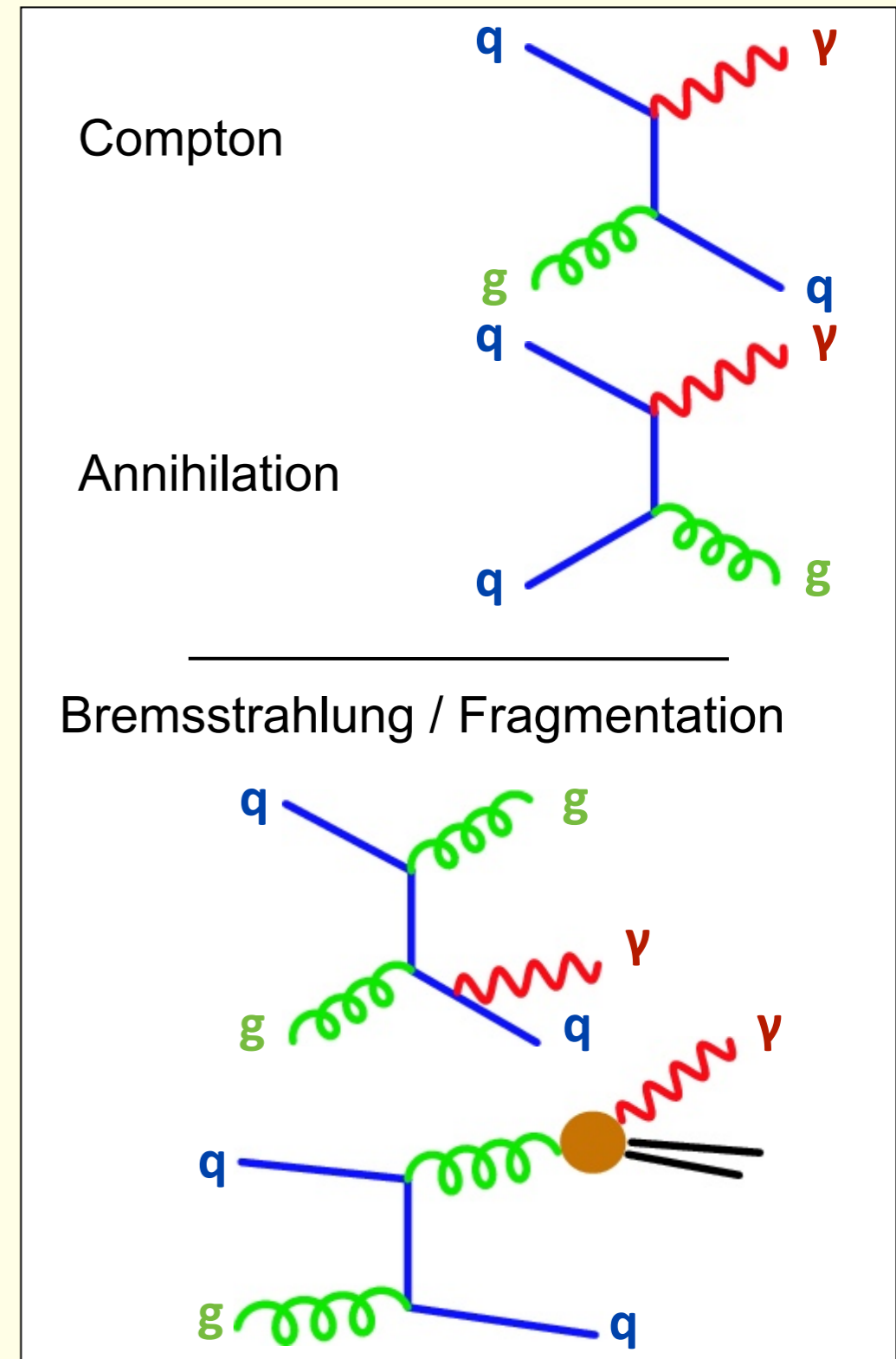


Direct Photon Production in p+p: Hard Scattering

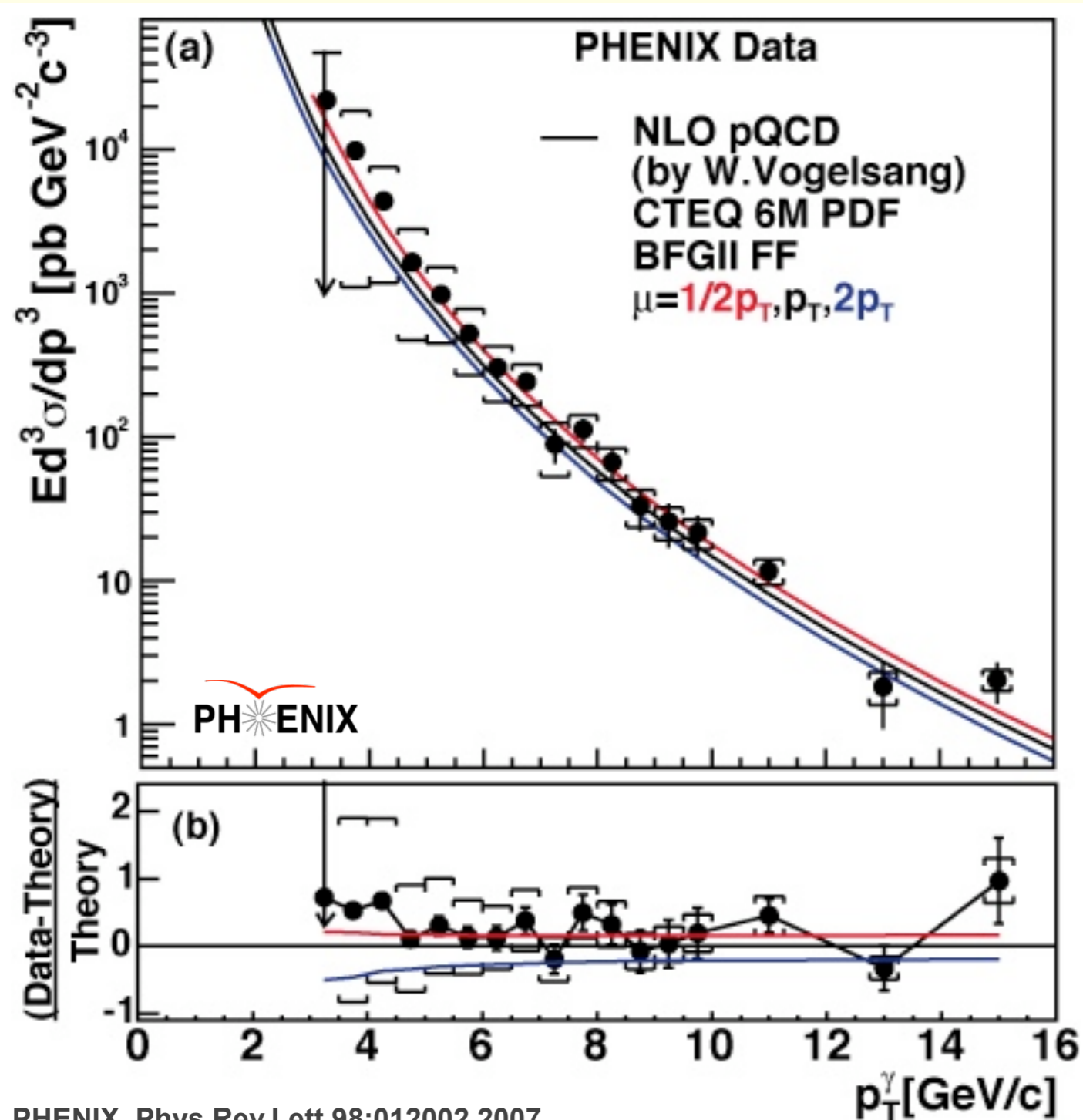
- Processes in perturbative QCD

- ▶ Compton: $q + g \rightarrow \gamma + q$
 - ▶ Annihilation: $q + \bar{q} \rightarrow \gamma + g$
 - ▶ Bremsstrahlung
- } LO } NLO

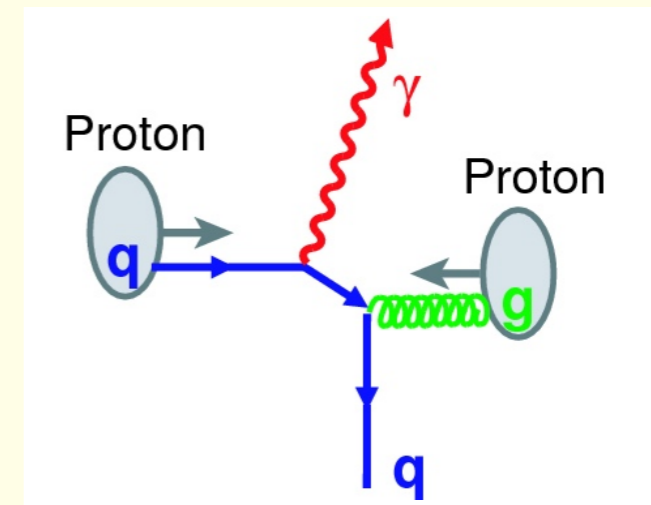
- Typically 20-30% uncertainty in pQCD calculations related to choice of unphysical scales



Direct Photons at RHIC: p+p at $\sqrt{s} = 200$ GeV



PHENIX, Phys.Rev.Lett.98:012002,2007



- Direct photons measured on statistical basis

$$\gamma_{\text{direct}} = \gamma_{\text{total}} - \gamma_{\text{decay}}$$

Calculated based on measured π^0, η spectra

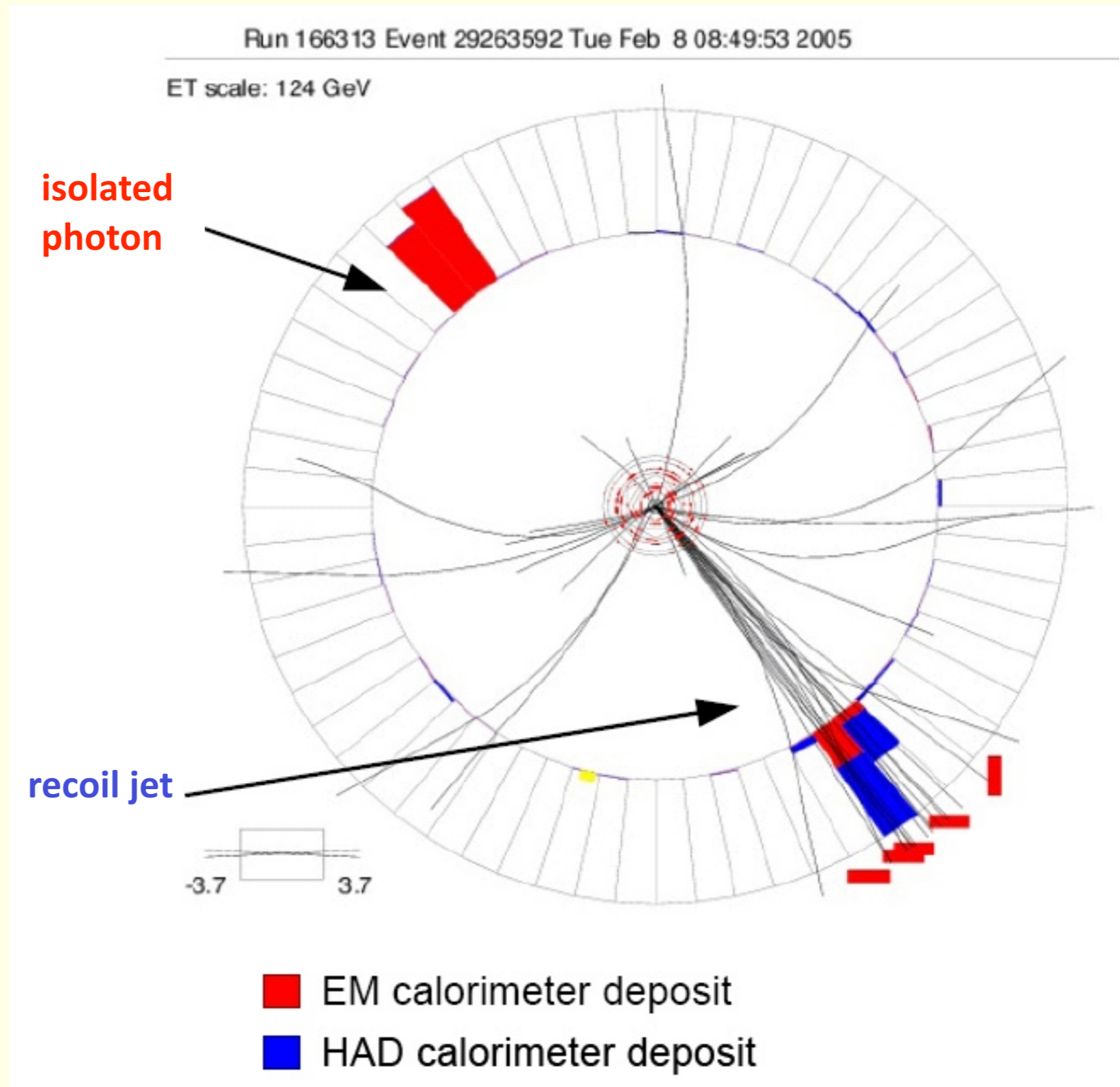
- Good agreement with NLO pQCD prediction
- Reference for Au+Au

Direct Photons at the Tevatron (I): Isolated Photons

Tevatron experiments measure **isolated direct photons** (photons without associated charged track and small associated hadronic energy)

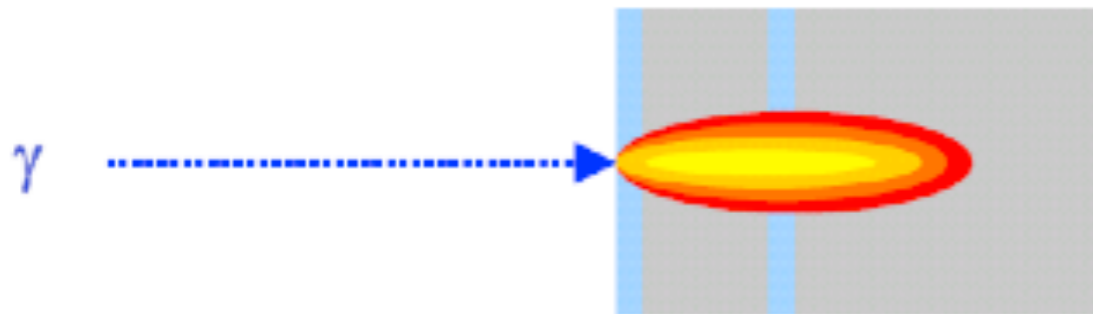
This rejects direct photons from fragmentation and bremsstrahlung

Rejection of background from $\pi^0 \rightarrow \gamma\gamma$ with measurement of shower profile

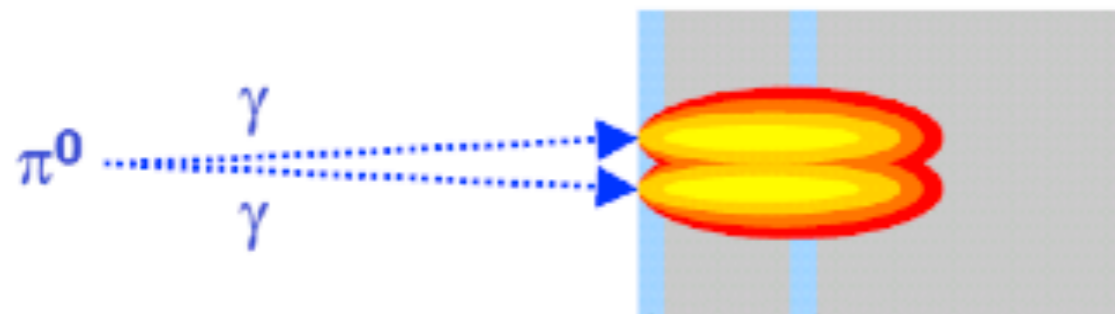


Direct Photons at the Tevatron (II): Rejection of $\pi^0 \rightarrow \gamma\gamma$ background

Signal



Background



Preshower
detector

Shower maximum
detector

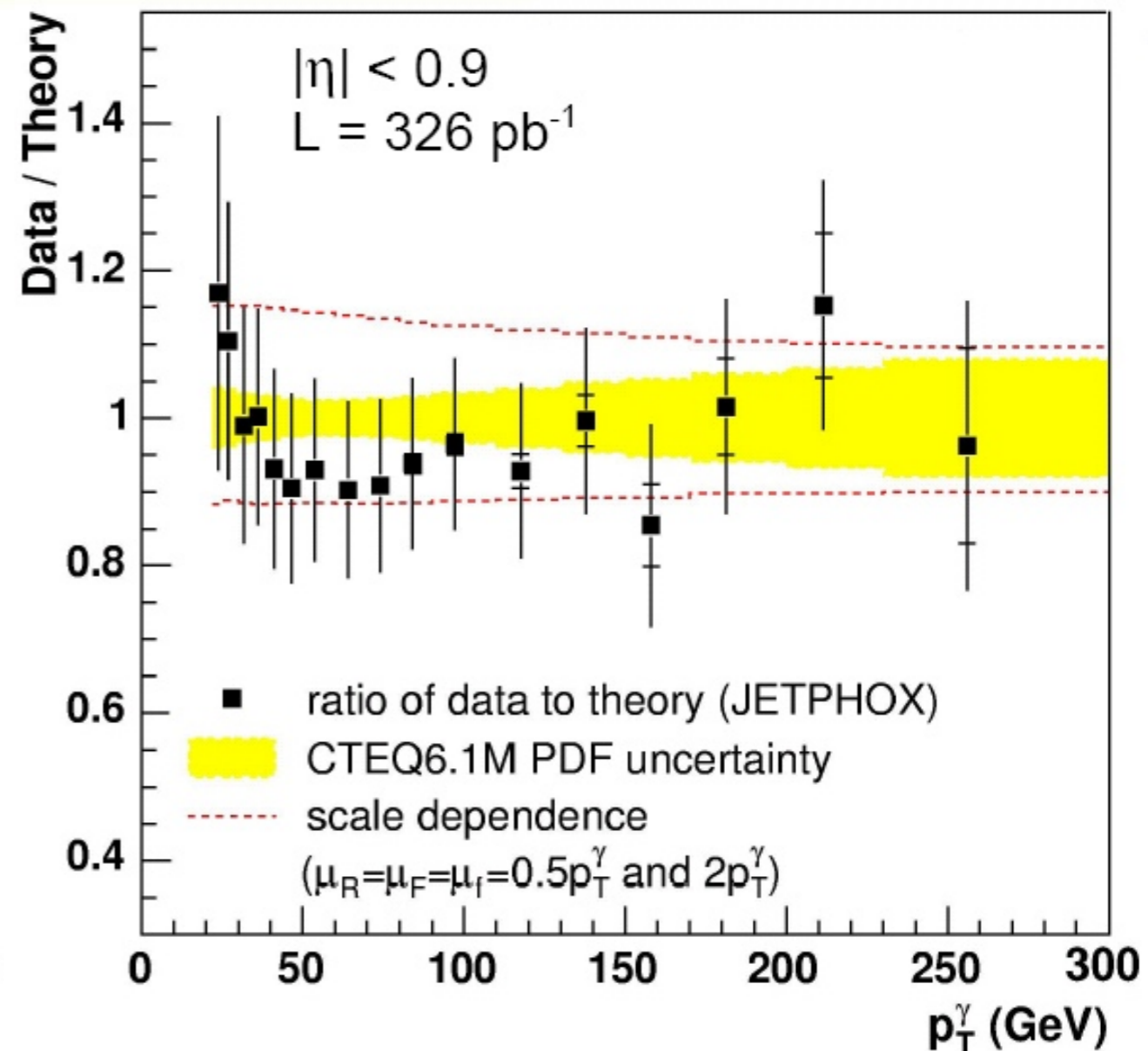
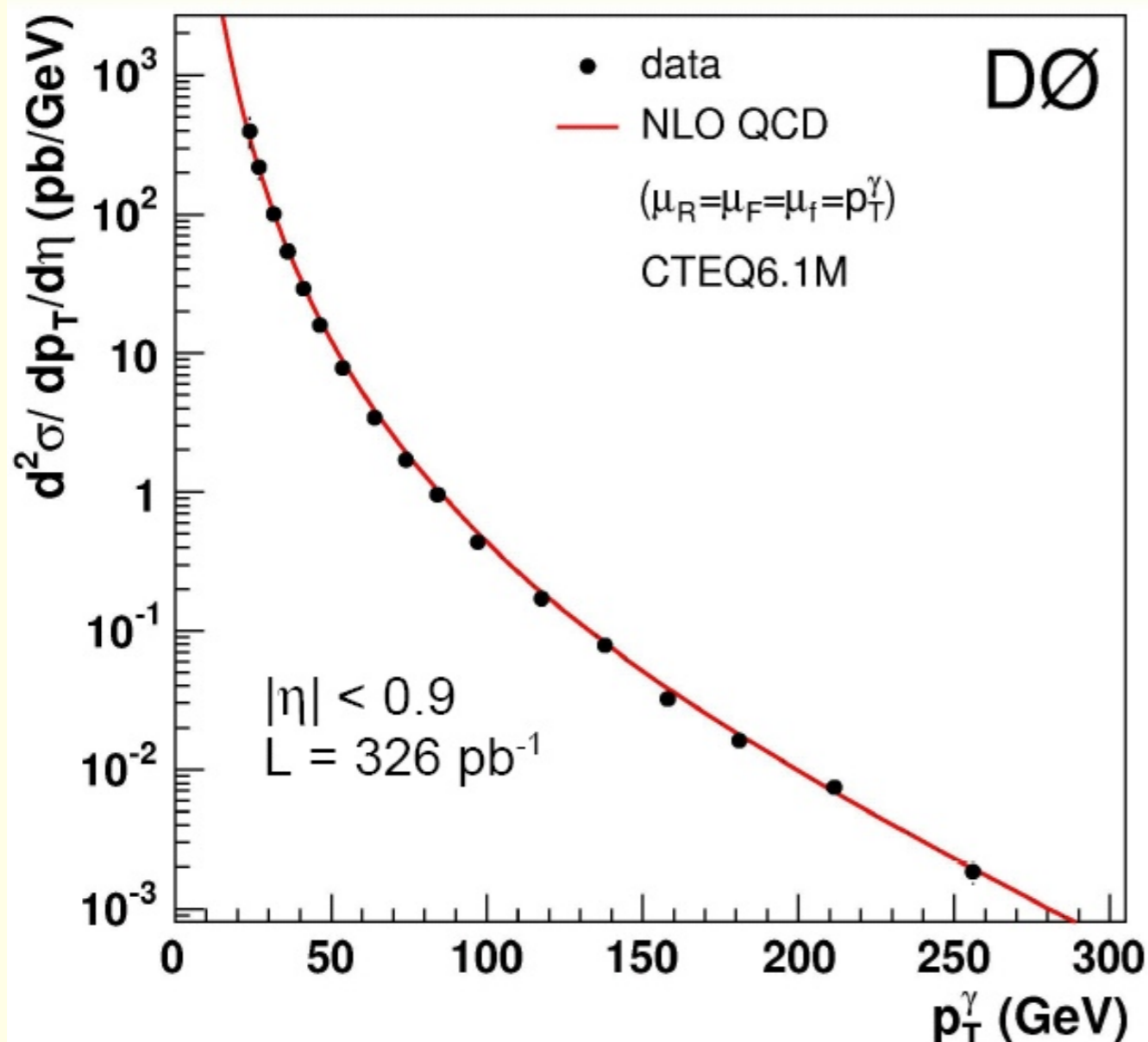
Experimental techniques

- DØ measures longitudinal shower development at start of shower
- CDF measures transverse profile at start of shower (preshower detector) and at shower maximum

Direct Photons at the Tevatron (III)

Isolated Photons (γ + jet):

PLB 639 (2006) 151



Good agreement with NLO QCD

Extra Slides

Mean z of the Fragmentation Products and the “Leading-Particle Effect” (I)

Consider exponential fragmentation function: $D(z) = B e^{-bz}$

Mean multiplicity of the fragments: $\langle m \rangle = \int_0^1 D(z) dz = B \int_0^1 e^{-bz} dz = \frac{B}{b} (1 - e^{-b})$

B and b are not independent since FF must satisfy:

$$1 \equiv \int_0^1 z D(z) dz = \frac{B}{b^2} (1 - e^{-b} (1 + b))$$

In particular:

$$B \approx b^2 \Rightarrow \langle m \rangle \approx b$$

Mean z of the fragments:

$$\langle z \rangle = \frac{\int_0^1 z D(z) dz}{\int_0^1 D(z) dz} = \frac{1}{\langle m \rangle}$$

RHIC: mean number of charged particles in a jet

$$\langle m \rangle \approx b \approx 8 - 10 \Rightarrow \langle z \rangle \approx 0.1 - 0.125$$

Mean z of the Fragmentation Products and the “Leading-Particle Effect” (II)

Mean z for a fixed value of p_T :

$$\frac{1}{p_T} \frac{d^2 n_\pi}{dp_T dz} = f\left(\frac{p_T}{z}\right) \cdot D_{q/\pi}(z) \cdot z^{-2} \longrightarrow \langle z(p_T) \rangle = \frac{\int_0^1 dz z f\left(\frac{p_T}{z}\right) \cdot D_{q/\pi}(z) \cdot z^{-2}}{\int_{x_T}^1 dz f\left(\frac{p_T}{z}\right) \cdot D_{q/\pi}(z) \cdot z^{-2}}$$

$$= \dots \approx \frac{n-1}{b}$$

$\langle z(p_T) \rangle$ is $n - 1$ times larger than the unconditional $\langle z \rangle$

This is called the leading-particle or “trigger bias” effect.

RHIC: $\langle z \rangle \approx 0.1 - 0.125 \quad \Rightarrow \quad \langle z(p_T) \rangle = 0.7 - 0.8$

A Simplified Analytic Model for the Calculation of the Inclusive Hadron p_T Spectrum (I)

How can we calculate the inclusive pion p_T distribution given the parton p_T distribution and the parton-to-pion fragmentation function?

Parton p_T distribution: $\frac{1}{\hat{p}_T} \frac{dn}{d\hat{p}_T} = A \cdot \frac{1}{\hat{p}_T^n} =: f(\hat{p}_T)$ ($n \approx 8$ for p+p at $\sqrt{s_{NN}} = 200$ GeV)

Start with pion p_T spectrum as function of the parton \hat{p}_T and $z = p_T / \hat{p}_T$:

$$\frac{1}{\hat{p}_T} \frac{d^2 n_\pi}{d\hat{p}_T dz} = f(\hat{p}_T) \cdot D_{q/\pi}(z)$$

pion transverse momentum

Change of variables:

$$\hat{p}_T = \frac{p_T}{z}, \quad \left. \frac{d\hat{p}_T}{dp_T} \right|_z = \frac{1}{z} \quad \longrightarrow \quad \frac{1}{p_T} \frac{d^2 n_\pi}{dp_T dz} = f\left(\frac{p_T}{z}\right) \cdot D_{q/\pi}(z) \cdot z^{-2}$$

A Simplified Analytic Model for the Calculation of the Inclusive Hadron p_T Spectrum (II)

Pion yield dN/dp_T at fixed p_T : Integration over z

$$\frac{1}{p_T} \frac{dn_\pi}{dp_T} = \int_{x_T}^1 dz f\left(\frac{p_T}{z}\right) \cdot D_{q/\pi}(z) \cdot z^{-2}$$

Maximum parton energy: $\frac{\sqrt{s}}{2} \Rightarrow z_{\min} = \frac{p_T}{\sqrt{s}/2} \equiv x_T$

Using the power law form of the parton spectrum:

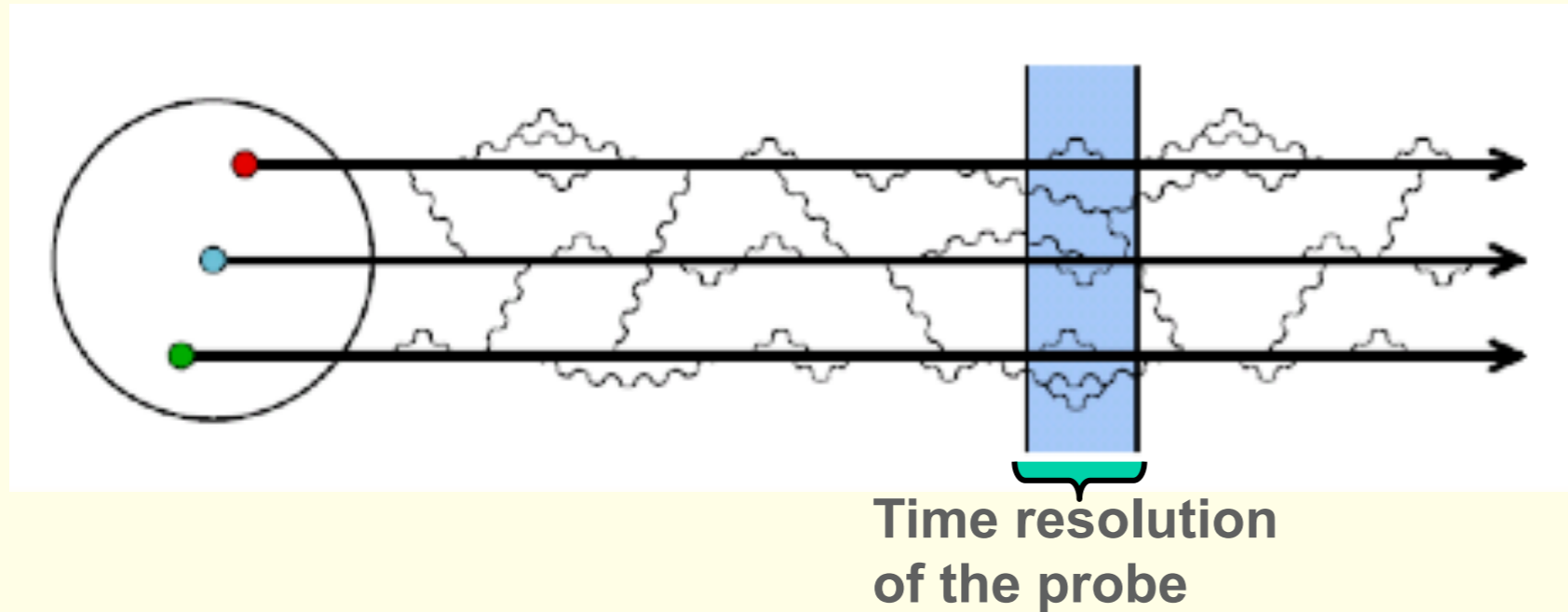
$$\frac{1}{p_T} \frac{dn_\pi}{dp_T} = A \cdot \frac{1}{p_T^n} \int_{x_T}^1 dz D_{q/\pi}(z) \cdot z^{n-2}$$

Integral depends only weakly on p_T since $x_T \approx 0$

**The pion p_T spectrum is also a power-law with the same power n .
This is called the Bjorken parent-child relationship.**

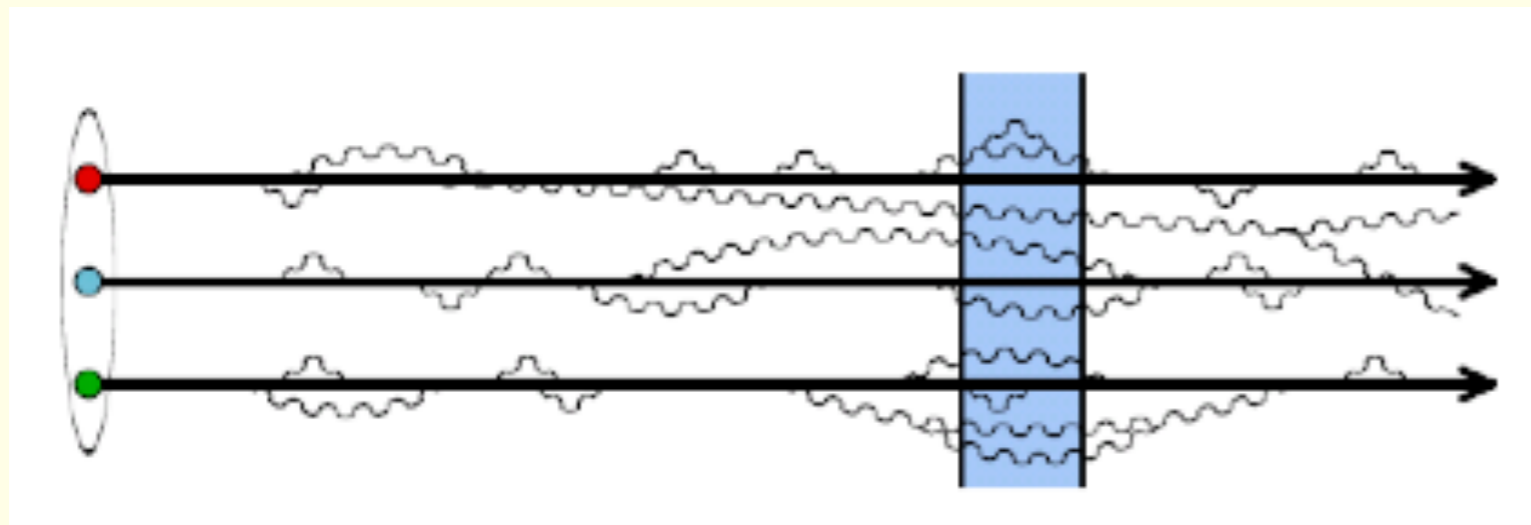
Interpretation of Scaling Violation (II)

Low energy proton



Fluctuations shorter than the resolution of the probe cannot be observed

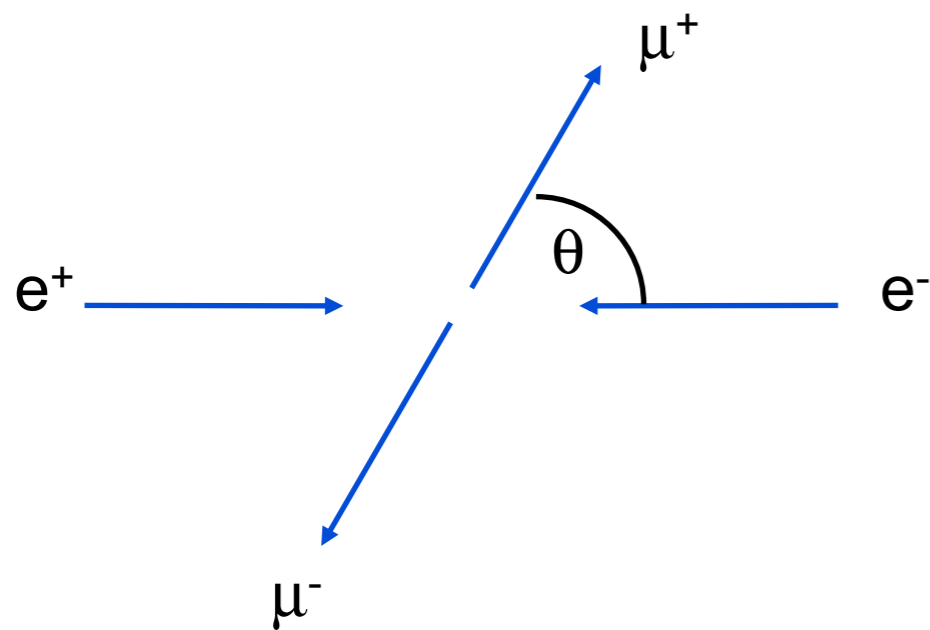
High-energy proton



Time dilation allows more fluctuations to be resolved by the probe

High energy proton appears to contain more gluons than low energy proton

Gelis, Lappi, Venugopalan: arXiv:0708.0047



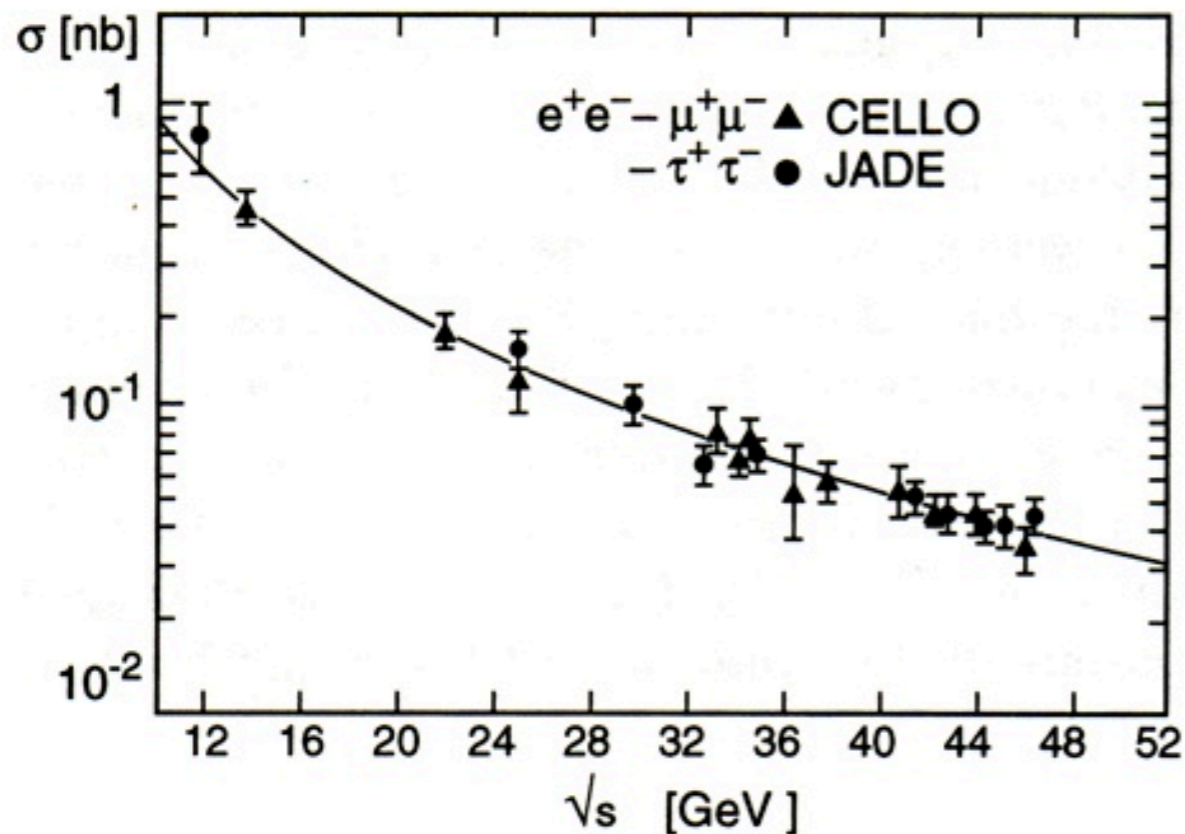
Differential cross section:

$$\frac{d\sigma}{d\Omega} = \frac{\alpha^2}{4s} (\hbar c)^2 (1 + \cos^2 \theta)$$

\sqrt{s} : center-of-mass energy

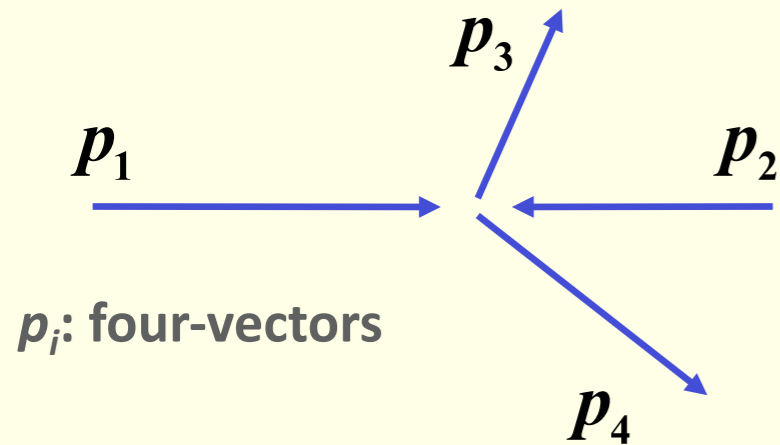
Total cross section:

$$\sigma = \frac{4\pi\alpha^2}{3s} (\hbar c)^2$$

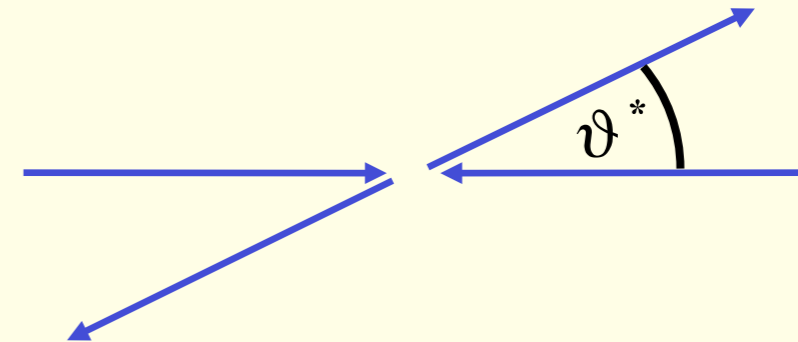


Parton Kinematics (I)

Laboratory reference frame



Center-of-mass system (CMS)



Parton 4-vectors conveniently represented as:

$$p^\mu = (E, p_x, p_y, p_z)$$

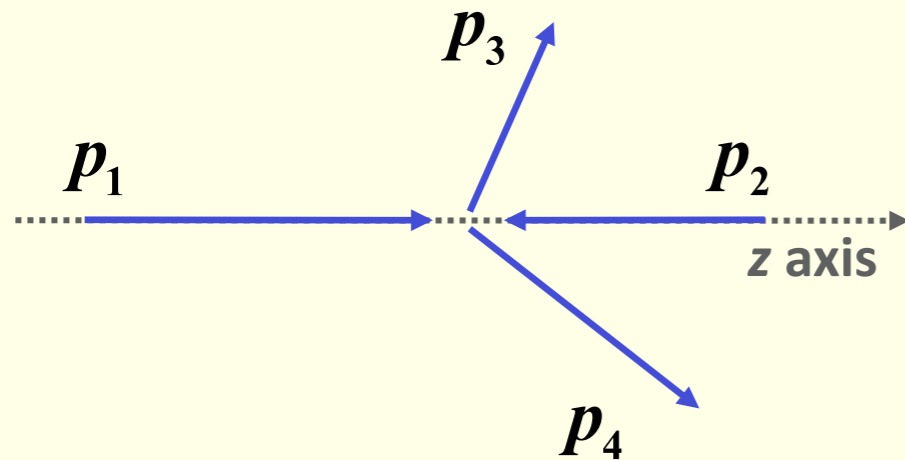
$$= (m_T \cosh y, p_T \cos \varphi, p_T \sin \varphi, m_T \sinh y)$$

with transverse mass $m_T = \sqrt{p_T^2 + m^2}$

and rapidity $y = \frac{1}{2} \ln \frac{E + p_z}{E - p_z}$

We will consider partons as massless so that $m_T = p_T$

Parton Kinematics (II)



$$p_{\text{beam}} \approx E_{\text{beam}} = \sqrt{s} / 2$$

Energy conservation:

Conservation of p_z :

This leads to:

$$x_1 = \frac{x_T}{2} (e^{y_3} + e^{y_4}) \quad x_2 = \frac{x_T}{2} (e^{-y_3} + e^{-y_4}) \quad \text{with} \quad x_T = \frac{2p_T}{\sqrt{s}}$$

four-vector of incoming proton 1

$$p_1 = x_1 P_1 = x_1 (\sqrt{s} / 2, 0, 0, \sqrt{s} / 2)$$

$$p_2 = x_2 P_2 = x_2 (\sqrt{s} / 2, 0, 0, -\sqrt{s} / 2)$$

$$p_3 = (p_{T,3} \cosh y_3, p_{T,3} \cos \varphi, p_{T,3} \sin \varphi, p_{T,3} \sinh y_3)$$

$$p_4 = (p_{T,4} \cosh y_4, p_{T,4} \cos \varphi, p_{T,4} \sin \varphi, p_{T,4} \sinh y_4)$$

$$(x_1 + x_2) \frac{\sqrt{s}}{2} = p_T (\cosh y_3 + \cosh y_4)$$

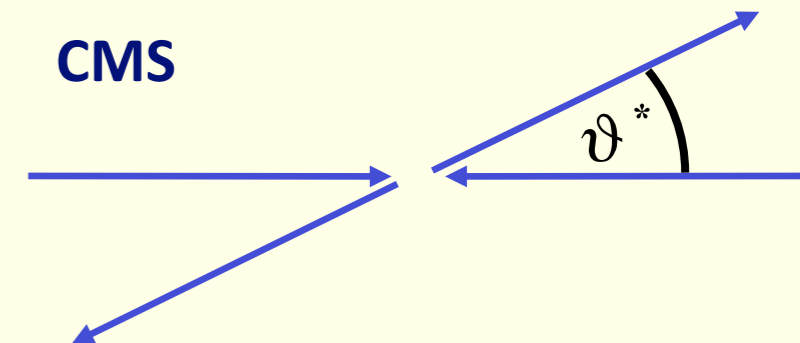
$$(x_1 - x_2) \frac{\sqrt{s}}{2} = p_T (\sinh y_3 + \sinh y_4)$$

Parton Kinematics (III)

√s of the parton system:

$$\hat{s} = (x_1 P_1 + x_2 P_2)^2 \approx x_1 x_2 s$$

CMS



Jet transv. momentum:

$$p_T = p_T^* = \frac{\sqrt{\hat{s}}}{2} \sin \vartheta^*$$

Energy-momentum vector of the two-jet system:

$$x_1 P_1 + x_2 P_2 = \frac{\sqrt{s}}{2} (x_1 + x_2, \mathbf{0}, \mathbf{0}, x_1 - x_2)$$

Rapidity of center-of-mass of the two-jet system:

$$y^{cm} = \frac{1}{2} \ln \frac{E + p_z}{E - p_z} = \frac{1}{2} \ln \frac{x_1}{x_2}$$

Rapidity y^* in the center-of-mass of the two-jet system:

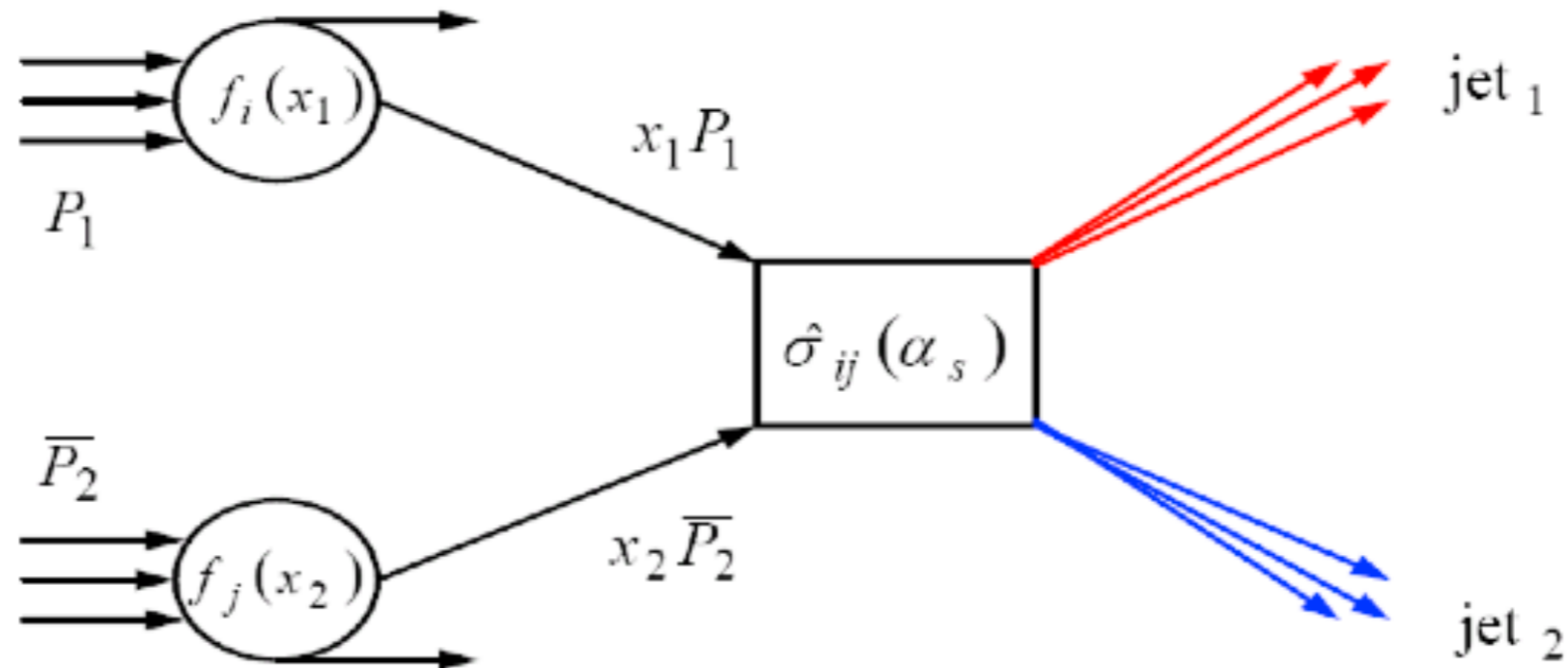
$$\left. \begin{aligned} y_3 &= y^{cm} + y^* \\ y_4 &= y^{cm} - y^* \end{aligned} \right\} y^{cm} = \frac{y_3 + y_4}{2}, \quad y^* = \frac{y_3 - y_4}{2}$$

Scattering angle:

$$\cos \vartheta^* = \frac{p_z^*}{E^*} = \frac{\sinh y^*}{\cosh y^*} = \tanh \frac{y_3 - y_4}{2}$$

Upshot: Fractional momenta x_1 , x_2 , and scattering angle in the CMS measurable

Calculation of Jet Cross Sections: Factorization



$$\sigma = \sum_{ij} \int dx_1 dx_2 f_i(x_1, \mu_F^2) f_j(x_2, \mu_F^2) \hat{\sigma}_{ij} \left(\alpha_s^m(\mu_R^2), x_1 P_1, x_2 P_2, \frac{Q^2}{\mu_F^2}, \frac{Q^2}{\mu_R^2} \right)$$

Sum over
initial states

Parton
Distributions

Factorization
Scale

Point Cross
Section

Order α_s^m

Renormalization
Scale

Jet Fragmentation (II)

Energy conservation:

$$\sum_h \int_0^1 z D_q^h(z) dz = 1$$

Average number of hadrons arising from quark q :

$$\int_{z_{\min}}^1 D_q^h(z) dz = \langle n_q^h \rangle$$

$$z_{\min} = \frac{m_h}{E_q} = \frac{2m_h}{\sqrt{s}}$$

Threshold energy for producing hadron with mass m_h

Fragmentation function often parameterized as:

$$D_q^h(z) = N \frac{(1-z)^n}{z}$$

$$\langle n_q^h \rangle \approx \int_{z_{\min}}^1 N \frac{1}{z} dz = -N \ln z_{\min} = N \ln \frac{E_q}{m_h}$$

Particle multiplicity grows logarithmically with parton energy

Jet Fragmentation (III)

Differential cross section:

$$\frac{d\sigma}{dz}(e^- + e^- \rightarrow h + X) = \sum_q \sigma(e^- + e^- \rightarrow q + \bar{q}) \left[D_q^h(z) + D_{\bar{q}}^h(z) \right]$$

Note that $\int \frac{d\sigma}{dz} dz = \langle n_h \rangle \cdot \sigma_{tot}$

Using

$$\sigma(e^+e^- \rightarrow q\bar{q}) = \frac{4\pi}{3} (\hbar c)^2 \cdot \frac{Q_q^2 \alpha^2}{s} \quad \sigma_{tot} := \sigma(e^+e^- \rightarrow h + X) = \sum_q \sigma(e^+e^- \rightarrow q\bar{q})$$

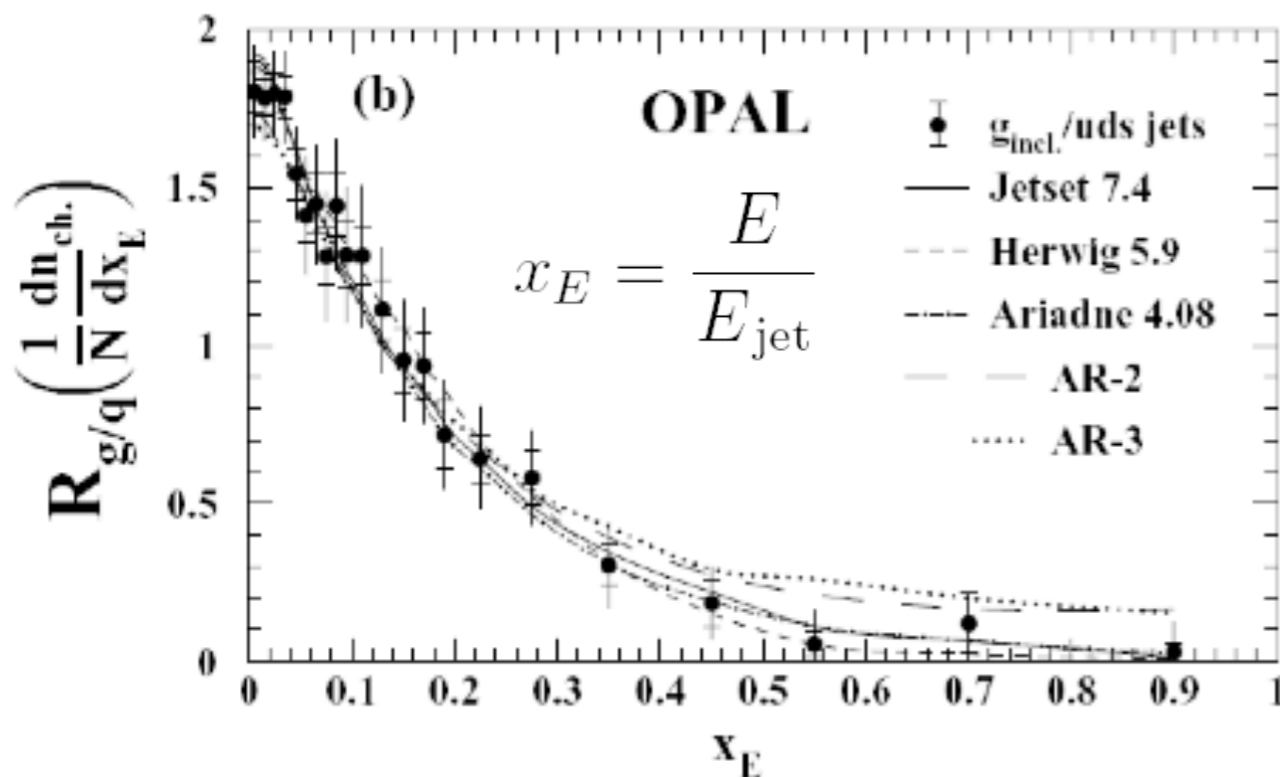
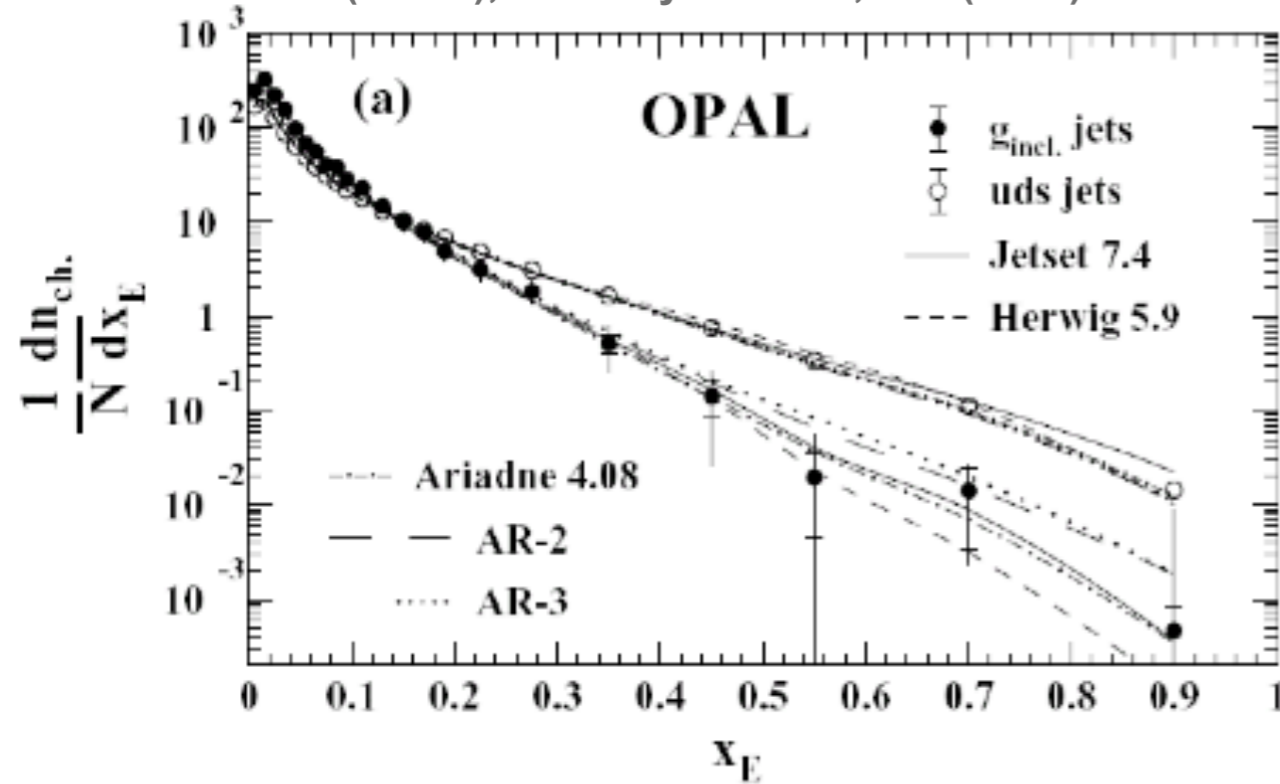
leads to

$$\frac{1}{\sigma_{tot}} \frac{d\sigma}{dz}(e^- + e^- \rightarrow h + X) = \frac{\sum_q Q_q^2 \left[D_q^h(z) + D_{\bar{q}}^h(z) \right]}{\sum_q Q_q^2} \equiv f(z)$$

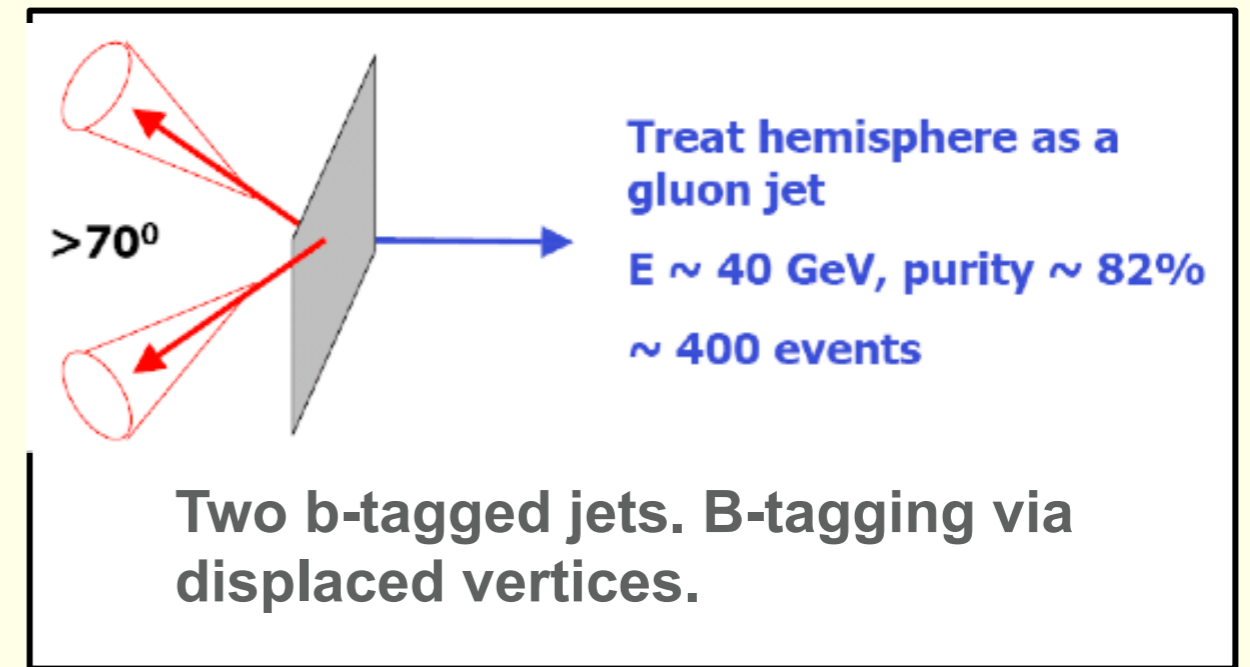
this cross section is expected to be a universal function, independent of \sqrt{s}

Quark vs. Gluon jet fragmentation (I)

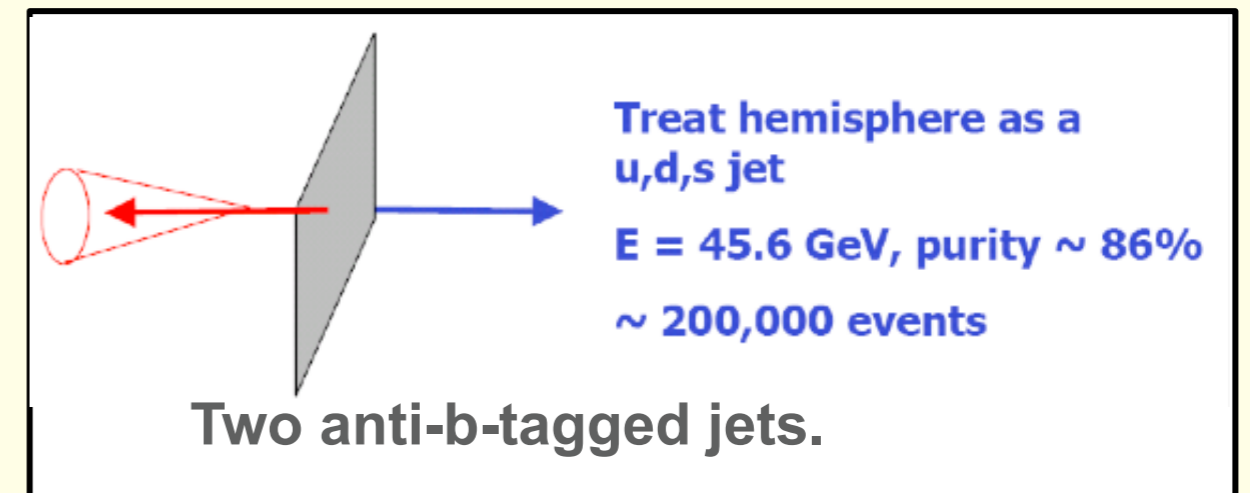
G. Abbiendi et al (OPAL), Eur. Phys. J. C11, 217 (1999)



Gluon jet:

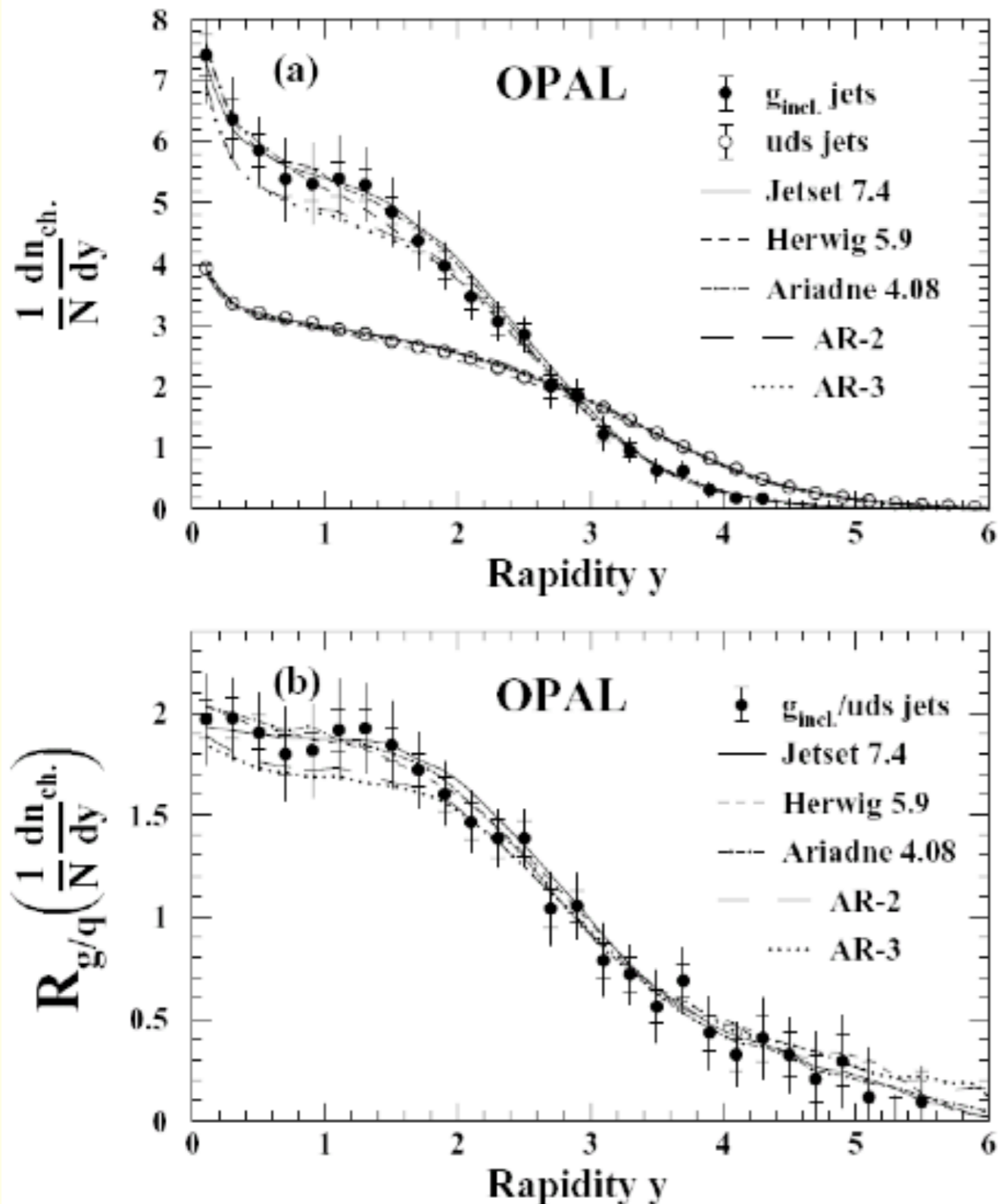


u,d,s jet:



Gluons fragment softer and broader than light quarks

Quark vs. gluon jet fragmentation (II): Charged Particle Multiplicity



Rapidity w.r.t. thrust axis \hat{r} :

$$y = \frac{1}{2} \ln \left(\frac{E + \vec{p} \cdot \hat{r}}{E - \vec{p} \cdot \hat{r}} \right)$$

Naively expect:

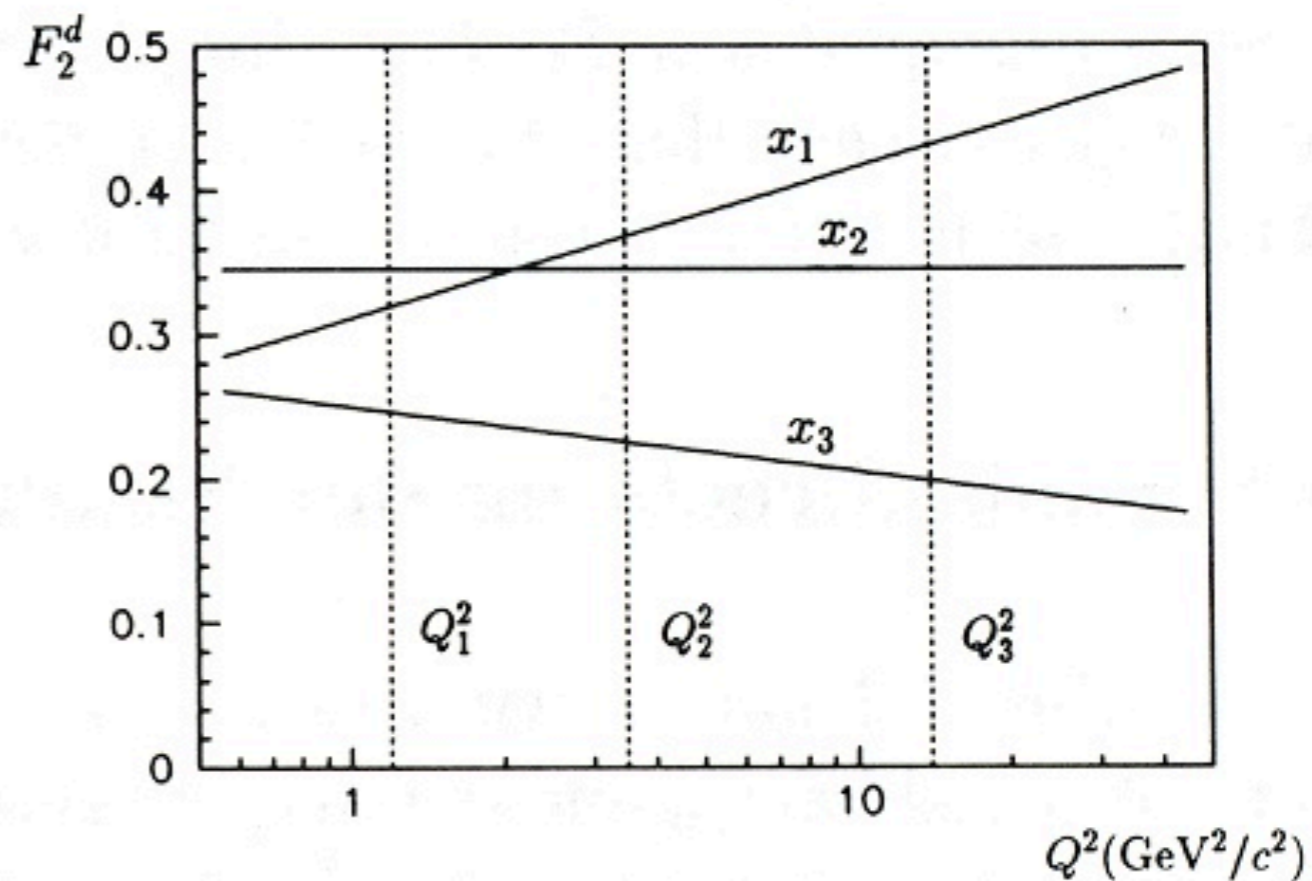
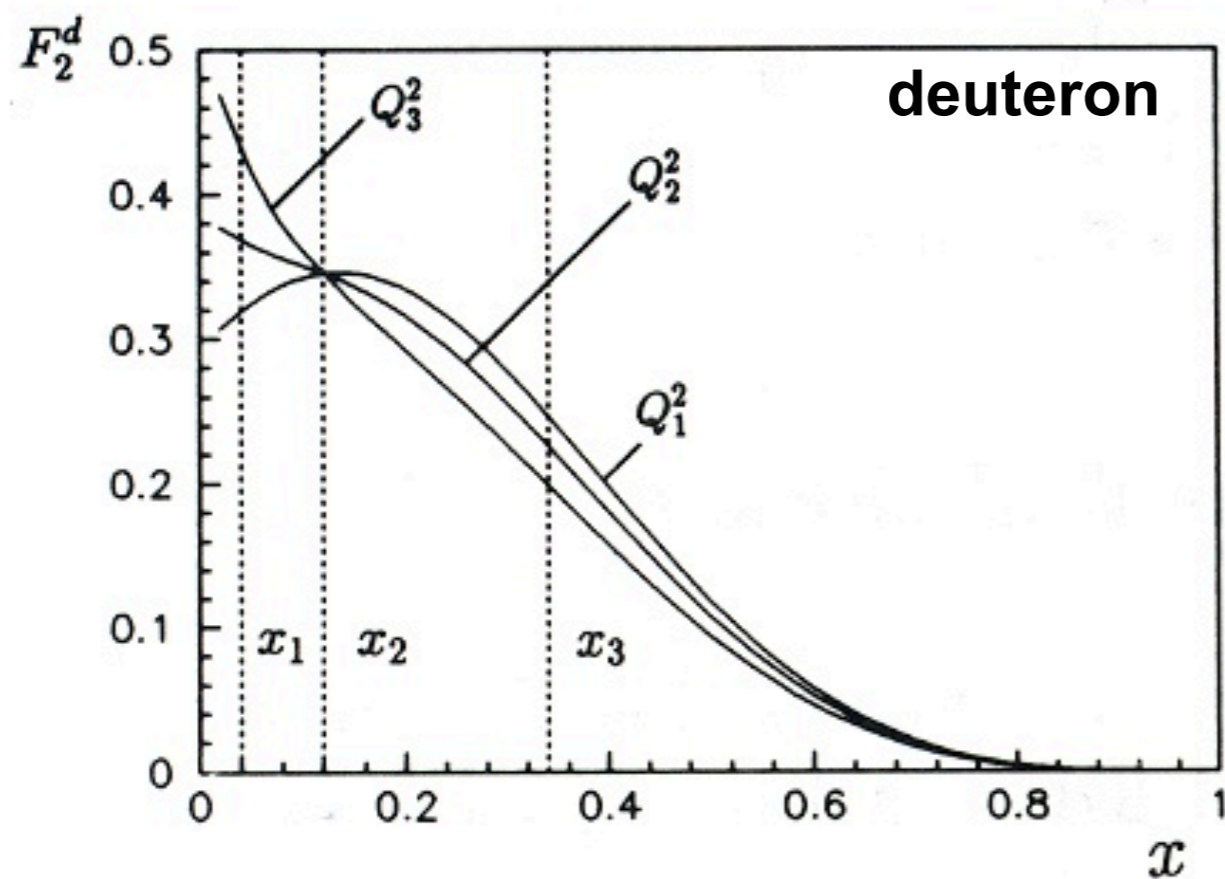
$$\left| \text{quark splitting} \right|^2 \sim C_F = 4/3$$

$$\left| \text{gluon splitting} \right|^2 \sim C_A = 3$$

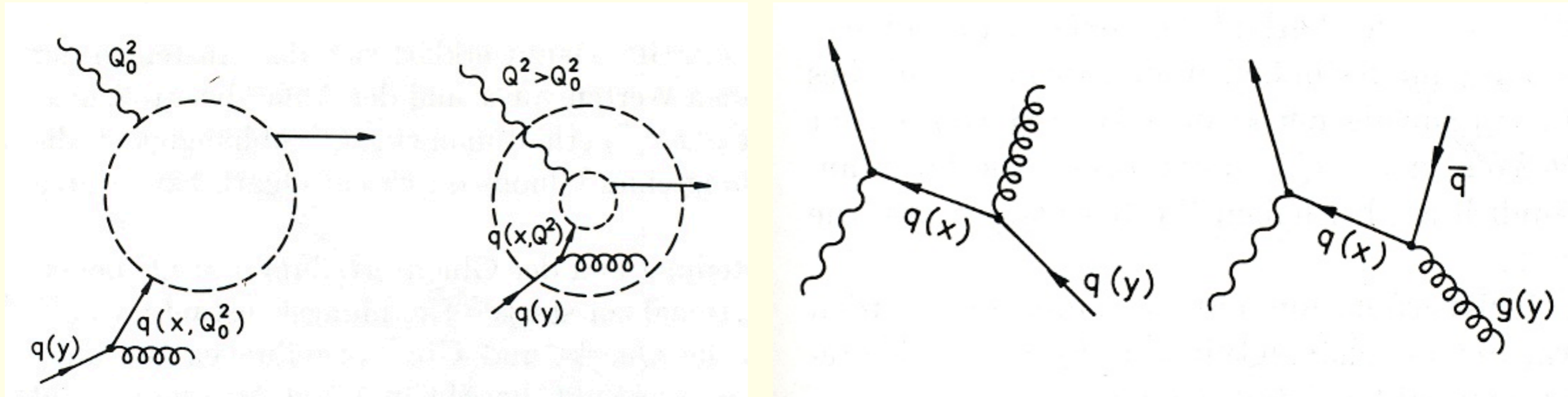
$$r \equiv \frac{\langle n_g \rangle}{\langle n_q \rangle} \equiv \frac{\langle \text{gluon jet multiplicity} \rangle}{\langle \text{quark jet multiplicity} \rangle} \sim \frac{C_A}{C_F} = \frac{9}{4}$$

Indeed approximately observed
at small rapidity

Scaling violations (II)



Interpretation of Scaling Violation (I)



Resolution of the virtual photon: $\lambda \approx \hbar / \sqrt{Q^2}$

- Momentum continuously redistributed among partons
- Increasing resolution of the virtual photon with rising Q^2 explains scaling violations
- This is quantitatively explained in QCD

Quark and Gluon distribution in the Proton as Function of x and Q^2

